The *In Vivo* and *In Vitro* Effects of 3,5,3'-Triiodothyronine (T3) on Control and mdx Muscle Cell Proliferation

by

Andrea Nichole Moor

A Thesis
Submitted to the Faculty of Graduate Studies
in Partial Fulfilment of the Requirements
for the Degree of

Doctor of Philosophy

Department of Human Anatomy
and Cell Science
Faculty of Medicine
University of Manitoba
Winnipeg, Manitoba

Canada

THE UNIVERSITY OF MANITOBA

FACULTY OF GRADUATE STUDIES

COPYRIGHT PERMISSION

THE IN VIVO AND IN VITRO EFFECTS OF 3,5,3'-TRIIODOTHYRONINE (T3) ON CONTROL AND MDX MUSCLE CELL PROLIFERATION

BY

ANDREA NICHOLE MOOR

A Thesis submitted to the Faculty of Graduate Studies of the University of Manitoba in partial fulfillment of the requirements of the degree of

DOCTOR OF PHILOSOPHY

Andrea Nichole Moor © 1997

Table of Contents

Abstract

The effects of excess thyroid hormone (T3) on *in vivo* and *in vitro* muscle regeneration in control and mdx muscles were examined. The mdx mouse is a genetic model of Duchenne muscular dystrophy (DMD), but unlike DMD, the course of the degenerative disease in this rodent stabilizes after most of its muscle tissue is successfully replaced with new muscle. The regenerative capabilities of control and mdx muscles were examined using *in vivo* histology and morphometric analyses, and *in vitro* cell cycle analyses. *In vivo* experiments showed that mdx muscle maintains a larger regenerative capacity than control muscle under hyperthyroid conditions. T3 differentially affected muscle repair and was deleterious only to controls. ^{3}H-thymidine incorporation and propidium iodide (PI) studies (*in vitro*) revealed that T3 primarily affected the control and mdx cell cycles during the G_0/G_1 and S-phases. More mdx myoblasts were observed in G_0/G_1 with T3 treatment compared to untreated mdx myoblasts. Results suggest that the large regenerative capability of mdx myoblasts may be a result of differential regulation of cell cycling. Distinct responses were observed in control and mdx fibroblasts with T3 treatment, and it was evident that myoblast and fibroblast interactions did occur *in vitro*. Bromodeoxyuridine (BrdU) and PI double-labelling experiments and MyoD staining showed differences in cycling activity between control and mdx myoblast cultures as they developed over time. Control myoblasts cycled less uniformly than mdx myoblasts. The proportions of myoblasts in early and late S-phases were higher in mdx cultures compared to control cultures and mdx cells appeared to cycle faster. T3 treatment only altered the cycling of control myoblasts, suggesting that these myoblasts may be more sensitive to the effects of T3 before MyoD expression during myogenic progression. Overall results suggest that T3 affects control muscle regeneration by reducing the growth of new myotubes *in vivo*, and that reduction in growth is a direct result of the effects of T3 on cycling behavior of control myoblasts and fibroblasts as shown *in vitro*. Surprizingly, this negative effect of T3 was not observed in mdx muscle, and has led us to question further the molecular mechanisms of this successful muscle regeneration.

Acknowledgements

List of Tables

List of Figures

List of Abbreviations

DMD	Duchenne muscular dystrophy
bFGF	basic fibroblast growth factor
BrdU	bromodeoxyuridine
CEE	chick embryo extract
Cdk	cyclin-dependent kinase
CTBP	cytosolic binding protein
devMHC	developmental myosin heavy chain
GH	growth hormone
HLH	helix-loop-helix
HRE	hormone response element
HS	horse serum
IGF-I	insulin-like growth factor I
MEM	minimal essential medium
MHC	myosin heavy chain
MLC	myosin light chain
mpc	muscle precursor cell
MRF	muscle regulatory factor
PDC	Percoll density centrifugation
PI	propidium iodide
Rb	retinoblastoma
rT3	reverse T3
RXR	retinoid-X-receptor
TA	tibialis anterior
TBG	thyronine binding globulins
TBPA	thyroxine binding prealbumins
TH	thyroid hormone
TR	thyroid hormone receptor
TRE	thyroid response element
T3	3,5,3'-triiodothyronine
T4	thyroxine

General Introduction

The mdx mouse, a genetic model of Duchenne muscular dystrophy (DMD), suffers from an X-linked muscle disease (Bulfield et al., 1984) as do patients with DMD, and the gene product dystrophin is absent from their skeletal and cardiac muscles (Koenig et al., 1987). The importance of the cytoskeletal proteins, specifically dystrophin and other associated proteins, in maintaining the integrity of muscle fibers is now well-established.

The successful recovery from dystrophy by compensatory regeneration in mdx muscle is in marked contrast to the deterioration and fiber death in muscle tissue in DMD. This contrast may be due to an altered control of myogenesis (development of muscle precursor cells (mpcs), their proliferation, fusion, and differentiation into myotubes), as was first suggested by autoradiographic studies in mdx regenerating muscle (Anderson et al., 1987). Additionally, the action of a key mitogen, basic fibroblast growth factor (bFGF: Gospodarowicz et al., 1987) which is present in large amounts in mdx but not DMD or most other human neuromuscular disease biopsy samples (Anderson et al., 1991, 1993) is likely important.

The influence of thyroid hormone, critical for the successful development of normal muscle (Ianuzzo et al., 1977; Izumo et al., 1986; Butler-Browne et al., 1990), on muscle disease and on muscle regeneration is less well understood. An excess of thyroid hormone *in vivo* reduces the contrast between DMD and mdx phenotypes: mdx dystrophy is worsened, in concert with lower levels of bFGF (Anderson et al., 1994a). Further study of thyroid hormone's effects on mdx and control myoblast (activated satellite cell) proliferation and fusion during regeneration both *in vivo* and *in vitro* may reveal some of the mechanism(s) that facilitate the unique regeneration from dystrophic and imposed injury in mdx muscles. These investigations are the subject of this thesis.

Chapter 1 - A Review of the Literature

1.0 Muscle Regeneration: Introduction and Brief History

The regeneration of muscle tissue has been investigated since the second half of the 18th century and can now be characterized by the following key events: revascularization, cellular infiltration, phagocytosis of necrotic damaged tissue, proliferation of mpcs (activated satellite cells) and their fusion (either into or with multinucleated myotubes or with the ends of damaged fibers), and reinnervation (Grounds, 1991).

Myogenesis is characterized by the following cytological events: (1) the mitotic expansion of a population of mononuclear mpc, termed myoblasts, capable of fusion, (2) the fusion of myoblasts to form multinucleate myotubes and (3) growth of the cytoplasm of myotubes and synthesis of proteins and organelles characteristic of mature skeletal muscle fibers (Partridge, 1982). It appears that the regeneration of muscle follows a similar, although not identical pattern to that seen with the formation of embryonic muscle tissue. However, the outcome of regeneration rarely leads to a histologically "normal" muscle (as indicated by centronucleation of fibers) since the environment is unlike that of fetal myogenesis (Schmalbruch, 1986). Fetal muscle fibers develop together with the connective tissue and capillary systems of muscle, whereas regenerating fibers must adapt to a pre-existing endomysial framework (Schmalbruch, 1986). Differential regulation of muscle regulatory factors (MRFs) between developing muscle and regenerating muscle has also recently suggested (Megeney et al., 1996, Anderson et al., 1997a, submitted).

The discovery of satellite cells in mature muscle fibers (Mauro, 1961) led to the original postulation that repair processes may follow the same cytological program as embryological myogenesis. Since the nuclei of myofibers are normally irreversibly post-mitotic they do not participate in the formation of new muscle fibers. Tissue culture studies in which individual muscle fibers were placed in

culture and allowed to become necrotic, revealed that the satellite cells on those fibers survived, proliferated and fused (Bischoff, 1975). Following injury that leads to myofiber necrosis, satellite cells on the dying fibers become "activated" from their relatively dormant state to proliferate, fuse and form new muscle fibers (Schultz, 1989). No new substantial evidence against the satellite cell concept (discussed more in section 1.4) has been presented during the most recent years, and it seems that satellite cells are the reserve population which provide myonuclei during the regeneration of muscle (Schmalbruch, 1986). However, one cannot rule out the possibility that other locally derived cells might also give rise to mpc *in vivo* (reviewed by Grounds, 1991), or that thymic myoid cells (which express dystrophin, MyoD, troponin and acetylcholine receptors among other proteins) may be involved since they appear to respond to muscle injury (Wong et al., submitted).

Impaired muscle regeneration and a progressive replacement by fat and connective tissue are features of myopathies such as Duchenne muscular dystrophy (DMD). This outcome of tissue repair is actually inadequate regeneration of muscle, and has been described as a failure of mpc (activated satellite cell) proliferation (reviewed by Grounds and Yablonka-Reuveni, 1993). Patients with DMD lack an important cytoskeletal protein called dystrophin, due to one of many mutations which disrupt the reading frame of the gene on the short arm of chromosome Xp21 (Hoffman et al., 1987). This results in the breakdown of the plasmalemma of the muscle fiber and subsequent necrosis of muscle tissue. The attempt at regeneration (proliferation of mpc and their fusion into new myotubes) cannot keep pace with the continued breakdown or degeneration and ultimately leads to the loss of skeletal, diaphragm, and cardiac muscle fibers.

The mdx mouse, a genetic model of DMD, is unique in that despite having the same gene mutation (Hoffman et al., 1987; Koenig et al., 1987; Bulfield et al., 1984), its limb muscles are capable of continued mpc proliferation in response to dystrophy and the disease is not lethal. However, more

similar to DMD muscles in humans, there is progressive degeneration of mdx mouse diaphragm muscles which are extensively replaced by fibrous tissue by one year of age (Stedman et al., 1991) or earlier (Dupont-Versteegden and McCarter, 1992; Anderson et al., 1997a, submitted) in this species. Most importantly, the mdx mouse does not appear to suffer any respiratory distress despite the obvious histopathological appearance of its diaphragm, which suggests that use of the mdx mutant for modelling DMD pathology, mechanisms or treatment must be carefully interpreted.

It will be important in future studies (from the stand point of designing treatment for DMD) to determine the mechanism(s) that allow for the continued mpc activation and successful regeneration of mdx muscle.

1.1 Summary of Skeletal Muscle Development

1.1.0 Early Stages - Proliferation and Fusion

The earliest events of muscle development include the formation of mesenchymal cells (undifferentiated precursor cells), which can differentiate into a variety of mesodermally-derived tissues, such as cartilage, blood, and connective tissue. These precursor cells undergo a restriction in their ability to express the total content of genetic information and eventually may become determined (see section 1.3) towards the muscle-forming line of cells termed myoblasts (reviewed in Carlson and Faulkner, 1983) which are spindle-shaped mononuclear cells.

The next phase in the development of the muscle cell lineage of cells is the proliferation and fusion of individual myoblasts. This occurs provided that proper regulatory factors, primarily within the local environment, are present. Myoblasts fuse with and into elongated multinucleated structures called myotubes (White and Esser, 1989) and become involved extensively in the synthesis and assembly of contractile proteins into regularly-arranged myofilamentous structures (Fischman, 1970).

Myotube formation only occurs during fetal development or after muscle damage, such that the

increase in the size of muscles after birth is due to hypertrophy rather than increased fiber number. In mammals, such as rats and mice, myogenesis and myotube formation occurs in two distinct phases: (1) primary myotubes are formed by the end-to-end fusion of myoblasts and (2) after a period of development in which no new myotubes are produced, secondary myotubes form, by the fusion of myoblasts, on the sides of primary myotubes (reviewed in McLennan, 1994) (see below).

The differentiation of myotubes into mature skeletal muscle fibers involves changes at many different levels. The nuclei of a myotube are long and contain prominent nucleoli, as would be expected of cells engaged in RNA and protein synthesis (Carlson et al., 1979). Once synthesized, contractile proteins of the myotube undergo a process of self-assembly into myofibrillar units, starting at the edges of the myotube (reviewed in Carlson and Faulkner, 1983). As the myotube matures, greater proportions of its volume become occupied by contractile proteins, the nuclei become more compact, the nucleoli lose their prominence, and the nuclei move from their central location to the periphery. These inherent changes, combined with influences of hormones and innervation give rise to a mature muscle fiber (White and Esser, 1989).

1.1.1 Primary and Secondary Myotube Formation

During primary myogenesis, muscles consist of independent myotubes or small numbers of cell aggregates which contain between one and several myotubes and some undifferentiated cells. Myotubes within these clusters are often irregular in shape with long thin cytoplasmic processes, contain high levels of glycogen and are of similar size and state of differentiation (reviewed in McLennan, 1994). During the period between primary and secondary myogenesis, primary myotubes elongate and the clusters of primary myotubes undergo disaggregation (Ontell and Kozeka, 1984a,b; Ontell et al., 1988a,b).

The production of secondary myotubes differs from that of the first-formed myotubes. Myoblasts (and probably satellite cells) proliferate on the surface of the primary myotubes and then fuse

to form secondary myotubes (reviewed in Bischoff, 1994). This generates small clusters of myotubes consisting of a large central primary myotube surrounded by undifferentiated cells and smaller secondary myotubes in various stages of development (reviewed in McLennan, 1994). Secondary myotubes are initially short and are connected to their associated primary myotubes by long pseudopod-like processes that interlaminate deep into the primary myotube. Primary and secondary myotubes are also electrically coupled through gap junctions. The secondary myotubes then elongate and become independent fibers as gap junctions disappear (Ontell, 1978; Ontell and Kozeka, 1984a,b; Ross et al., 1987; Ontell et al., 1988a,b). In fact, gap junction communication is a necessary requirement for development (Balogh et al., 1993; Proulx et al., 1997, in press).

It is important to note that the muscles in the above studies were small and derived from the limbs of small laboratory animals. It has been shown that there are qualitative and quantitative differences between the formation of small and large muscles (Draeger et al., 1987), and between fast and slow muscle fiber formation (Ontell and Kozeka, 1984a,b; Ontell et al., 1988a,b)

1.2 Skeletal Muscle Myosin

1.2.0 Myosin Isoforms in Skeletal Muscle

Myosin is the major contractile protein found in all differentiated muscle cells and is present in most non-muscle cells as well. The molecular structure of most myosins is very similar, consisting of 2 globular heads attached to an α-helical rod-like tail. The subunit structure of myosin consists of 2 heavy chains (MHC) of molecular weight 220kDa and 4 molecules (2 pairs) of light chains (MLC) of molecular weight 17 and 23kDa. *In vivo*, myosin assembles into bipolar filaments by interacting with the rod. In vertebrate striated muscle, these assemblies are part of a highly ordered stable structure, called the myofibril (reviewed in Schiaffino and Reggiani, 1994).

Our understanding of the complex nature of myosin diversity and of the functional importance

of MHC and MLC isoforms has progressed rapidly. Major advances in the study of mammalian skeletal muscle myosins include the recognition of a new fast MHC isoform that is widely distributed in most skeletal muscles. As well, the characterization of the developmental MHC transitions that lead to the emergence of the adult myosin isoform profile and the demonstration that both MHCs and MLCs influence the velocity of muscle shortening is reviewed in Schiaffino and Reggiani, 1994.

Muscle fibers in the mouse and most mammals can be divided into 4 types: one 1 slow type (I) and 3 fast types (IIa, IIx, and IIb) which were characterized according to the enzymatic and immunochemical characteristics of their myosin isoforms (Brooke and Kaiser, 1970; reviewed in Schiaffino and Reggiani, 1994). A mosaic of different fiber types contributes to most skeletal muscles in the body. Across a broad spectrum of vertebrate species, slow and fast skeletal muscles each contain multiple isoforms of myosin (D'Albis et al., 1985). This diversity is due to the polymorphic expression of MHC and MLC subunits that make up the myosin molecule (D'Albis et al., 1979). For example, adult skeletal muscle fibers are composed of at least 4 different MHCs (the slow or ßMHC and 3 fast isoforms IIa-, IIx-, and IIb-MHC) and 3 MLC isoforms (the slow MLC1s and the 2 fast MLC1f and MLC3f) (reviewed in Schiaffino and Reggiani, 1994).

Sarcomeric MHCs and MLCs are the product of 3 multigene families. They are all presumably derived from a single ancestral gene. The distribution of the various MHC and MLC isoforms is not always rigidly confined to specific muscle fibers or specific stages of development. For example, the embryonic and neonatal MHCs persist in adult extraocular muscles and in intrafusal nuclear chain fibers (within muscle spindles). Embryonic and neonatal MHCs and embryonic MLC1 are also re-expressed in regenerating and denervated muscle (Schiaffino et al., 1988; reviewed in Schiaffino and Reggiani, 1994).

1.2.1 Neuronal and Hormonal Influences on Myosin Composition of Skeletal Muscle

Multiple mechanisms, including myoblast predetermination, neuronal influences, and thyroid hormone are known to regulate muscle fiber diversity and myosin gene expression during development (reviewed in Gunning and Hardeman, 1991). It has been clearly shown that the type of motor innervation a muscle receives is a determining factor in differentiation of fiber type and MHC isoform expression. A great deal of supporting evidence from cross-innervation studies (Bárány and Close, 1971; Buller et al., 1960) and chronic electrical stimulation (Sréter et al., 1973) has been presented in the last 30 years. Cross-innervating a fast-twitch muscle with a nerve that originally innervated a slow muscle, causes the fast-twitch muscle to change its physiological, biochemical and ultrastructural properties to resemble those of slow muscles (Bárány and Close, 1971). Cross-innervation experiments in which a slow muscle was reinnervated with a fast motor nerve have yielded less clear cut results. It appears that fast myosin components can be induced, but slow myosin continues to be expressed during nerve-induced slow-to-fast switches (Bagust et al., 1981).

Some early studies suggested that innervation is the controlling stimulus during normal development (reviewed in Bandman, 1985). Muscle fibers in most newborn mammals are polyinnervated (i.e. supplied by more than 1 motor neuron), and it is only during the first few weeks that most muscle fibers become innervated by a single neuron and attain their adult characteristics. However, the denervation of newborn rat fast-twitch muscle delays but does not block the appearance of adult fast myosin (Butler-Browne et al., 1982). Thus, innervation per se does not appear to be an absolute requirement for the myosin isozyme transitions characteristic of fast-twitch fibers. In contrast, innervation is required for the maturation of slow-twitch muscles (reviewed in Bandman, 1985). If the rat soleus is denervated at birth, slow myosin synthesis progressively declines, slow isozymes are no longer detectable after 25 days and the fibers eventually contain only adult fast myosins (Gambke et al., 1983).

Thyroid hormone is known to be a key factor in normal muscle development. Studies in humans and in the neonate mouse revealed that hyperthyroidism significantly altered the MHC transition (resulting in a precocious accumulation of adult MHC and maturation of the muscle). These studies suggest that there may be a special role for thyroid hormones in directly regulating the appearance of adult types of myosins, and in modulating directly or indirectly the disappearance of the embryonic and neonatal types of myosins (D'Albis et al., 1987).

The expression of myosin genes can be further modulated in the adult stages by a variety of factors, such as innervation (see above), thyroid hormone, electrical stimulation, and mechanical factors. For example, IIx-MHC can be induced in the rat soleus, a muscle in which this isoform is normally absent, by either thyroid hormone treatment or electrical stimulation at high frequency. The MHC transitions appear to reflect an obligatory pathway of MHC gene expression in the order I→IIa→IIx→IIb (Schiaffino et al., 1990). Changes in the pattern of activity or in thyroid hormone levels can cause the transformation of the fiber phenotype to be pushed to the right or to the left along this sequence. This helps to explain the finding (Izumo et al., 1986) that the IIa-MHC gene is upregulated by thyroid hormone in the soleus muscle, which contains a majority of type I fibers, but is down-regulated in the extensor digitorum longus muscle, which is composed almost exclusively of type II fibers (reviewed in Schiaffino and Reggiani, 1994).

1.2.2 Regulatory DNA Sequences, Transcription Factors, and Fiber Type-Specific Myosin Gene Expression

It has been suggested (Hughes et al., 1993; Voytik et al., 1993) that the muscle regulatory factors (MRFs) MyoD and myogenin (discussed in detail in section 1.3), which play an important role in muscle cell differentiation during development (reviewed in Weintraub et al., 1991), may be implicated in changing muscle gene expression during differentiation. Hughes et al. (1993) suggest that MyoD mRNAs

are more abundant in type II muscle fibers, whereas myogenin mRNAs are more abundant in type I

fibers. It is also reported that transformation of fiber types induced by thyroid hormone or by cross-

reinnervation is accompanied by a corresponding alteration in the MyoD and myogenin mRNA levels

in a muscle. These results suggest that MRFs may have distinct roles in adult muscle [although others do

not report MRF gene expression in normal adult or mature muscle (Grounds et al., 1992; Garrett and

Anderson, 1995)]. At present there is no direct evidence of a specific role for MyoD and myogenin in the

differential regulation of myosin genes in adult skeletal muscle fibers (reviewed in Schiaffino and

Reggiani, 1994).

1.2.3 Myosin Isoform Transitions in Regenerating Muscle

Regenerating muscles in adult vertebrates transiently express embryonic and neonatal forms of

MHC (Matsuda et al., 1983). Muscle cell culture experiments are commonly used to model regeneration,

since the myogenic program during myogenesis *in vitro* is similar to that *in vivo*. Tissue culture studies

have shown that embryonic isoforms are initially synthesized following fusion of myoblasts derived from

embryonic muscle tissue (Whalen et al., 1979). In the chicken *in vitro* model, the embryonic phenotype

continues to be expressed (as in many other species), and no evidence of any MHC transitions is observed

for up to 6 months in culture (Bandman et al., 1982). Therefore, there are differences between *in vitro* and

in vivo myogenesis which depend on species, cell line and the precise questions under investigation.

It is difficult to draw any conclusions from cell culture as to what factors might be involved in

regulating myosin isozyme transitions. It is clear, however, that both *in vivo* and *in vitro*, newly formed

myotubes initially express only embryonic myosins. The inability of muscle cell cultures to continue the

normal sequence of myosin transitions during myogenesis suggests that isoform transitions are not simply

part of a rigid myogenic program. Rather the transitions may depend on external stimuli coming from

fibroblasts, satellite cells, or nerves in the *in vivo* sequence of myogenesis (reviewed in Bandman et al.,

1985).

1.3 Myogenic Cell Lineages and Muscle Regulatory Factors (MRFs) in Myogenesis

1.3.0 The Concept of Lineage

A number of studies have investigated the theory of a myogenic cell lineage in higher vertebrate development. These studies highlight the embryonic origins of myogenic precursor cells, the mechanisms of fiber type diversity and patterning, the distinction among myoblasts during myogenesis, and how a variety of factors both intrinsic and extrinsic to the myoblast determine the ultimate phenotype of a muscle fiber (reviewed in Stockdale, 1992).

1.3.1 Characterization of the Muscle Regulatory Factors (MRFs)

Skeletal muscle cell developement proceeds through several stages: commitment, which destines a cell to develop into a myoblast, proliferation to a defined number of generations, withdrawal from the cell cycle, and terminal differentiation, in which the cell becomes able to perform its specialized functions (Kelly, 1983). As each stage proceeds, groups of genes are activated to regulate and determine cell function (Hastings and Emerson, 1982). Recently, a family of genes was identified which encode skeletal muscle-specific transcription factors, the expression of which is each capable of converting mesodermal cells *in vitro* to stable myoblasts which ultimately can form myotubes (reviewed in Buckingham, 1992; Emerson, 1990; Olson, 1990; Weintraub et al., 1991; Rudnicki and Jaenisch, 1995). The gene family encodes four myogenic determination factors which include MyoD (Davis et al., 1987; Tapscott et al., 1988), myogenin (Edmondson and Olson, 1989; Wright et al., 1989), Myf-5 (Braun et al., 1990) and MRF4/herculin/Myf-6 (Rhodes and Konieczny, 1989; Minor and Wold, 1990; Braun et al., 1990). The MRFs represent four members of a gene family that show conservation in two structural motifs, the helix-loop-helix (HLH) domain involved in protein binding with other HLH proteins, and a basic c-myc-like binding domain presumably involved in DNA binding (reviewed in Sassoon, 1992). Except for one

published report (Grounds et al., 1992), and one work in preparation from this lab (Wong et al.), the

MRFs, myogenin in particular, are only and always expressed as specific muscle tissue markers.

Analysis of developing embryos using RT-PCR and in situ hybridization have shown that MRFs

are sequentially expressed in murine somites and limb buds (Bober et al, 1991; Hinterberger et al., 1991;

Ott et al., 1991; Hannon et al., 1992), but their specific roles in normal myogenesis in the developing

animal are not explicitly defined as yet (Smith et al., 1994). Myf-5 mRNA is first detected in the 8-day

somite and is down-regulated after day 14 (Ott et al., 1991). Myogenin mRNA appears on day 8.5 and

is expressed throughout fetal development (Sassoon et al., 1989). MRF4 mRNA appears transiently on

days 10 and 11, and is re-expressed at day 16 to become most abundant after birth (Bober et al., 1991).

Finally, MyoD mRNA appears around day 10.5, and is expressed from then on through development

(Sassoon et al., 1989). In the developing limb bud, Myf-5 mRNA is expressed transiently between days

10 and 12, myogenin and MyoD mRNAs are co-expressed after day 10.5 (Ott et al., 1991; Sassoon et al.,

1989), and MRF4 mRNA is expressed after day 16 (Bober et al., 1991). Tissue culture experiments

support the idea that myogenin acts downstream of MyoD and Myf-5. Most myoblasts in culture express

MyoD or Myf-5, but turn on myogenin only when induced to differentiate by removing growth-

promoting serum from the medium (reviewed in Weintraub, 1993; Yablonka-Reuveni and Rivera, 1994).

In culture, MyoD can activate its own transcription as well as that of myogenin; myogenin can activate

itself as well as MyoD; and Myf-5 can activate itself along with MyoD and myogenin (reviewed in

Weintraub, 1993). It is important to remember that the above autoregulatory loops reflect what can occur

in culture, and not necessarily what does occur in vivo.

Surprisingly, mice with homozygous gene-targeted mutations in either MyoD or Myf-5

expression (but not both) can produce fairly normal amounts of muscle (Rudnicki et al., 1992; Braun et

al., 1992), so there is some functional redundancy in the MRF gene family. This data begs one to ask

whether the MRFs are always a distinct requirement for normal muscle development. How are they "turned on" to result in production of normal amounts of functional muscle? A paradox exists here and implies that the MRFs are critical and muscle specific on one hand, but are redundant on the other!

This paradox has been resolved by 3 groups of experiments (reviewed in Weintraub, 1993; Megeney et al., 1996). In one, a genetic cross has shown that in the double homozygous mutants, lacking both MyoD and Myf-5, no muscle formation occurs, no muscle markers are present, and no myogenin is transcribed (Rudnicki et al., 1993). This study indicates that MyoD and Myf-5 share a redundant function which is itself absolutely required for generating or maintaining muscle cell identity and activating myogenin. A second study revealed that adult mice lacking MyoD showed marked deficits in satellite cell function during muscle regeneration (Megeney et al., 1996). Skeletal muscle regeneration in these MyoD(-/-) mice was impaired following an imposed injury to the tibialis anterior muscle. Although closer examination of these muscles revealed that the satellite cells present were morphologically normal, the number of myoblasts from primary cultures derived from the MyoD(-/-) mice was elevated, and paradoxically displayed reduced rates of proliferation once they became committed to the myogenic program and began expressing desmin (Megeney et al., 1996). A new report (McIntosh et al., 1997, submitted) confirms that idea since proliferation by myogenin-positive myoblasts but not Myf-5-positive myoblasts in muscle regeneration is altered by the lack of MyoD expression. These studies conclude that MyoD plays a unique and novel role in regulating satellite cell responses, and that Myf-5 does not substitute for MyoD in satellite cells (Megeney et al., 1996).

These latter observations help to confirm that MyoD is not only important for differentiation but also for proliferation, especially in adult skeletal muscle stem cells (satellite cells). In the third set of studies (Hasty et al., 1993; Nabeshima et al., 1993), mice with a homozygous targeted mutation of myogenin contain myoblasts since these embryos produce normal amounts of MyoD mRNA. However,

the myoblasts in the myogenin mutant mice fail to differentiate fully, which indicates that myogenin has a unique function that is required for the transition from a determined myoblast to a fully differentiated myotube.

It is now clear that the MRFs can promote the transcription of a number of muscle-specific genes such as the creatine kinase and myosin genes (Buskin and Hauschka, 1989; Wentworth et al., 1991; Hughes et al., 1993). They can also initiate transcription of their own genes and other MRF genes (Blau and Baltimore, 1991). The MRFs are believed to be negatively regulated by the Id (inhibitor of differentiation) HLH proteins, which lack a basic DNA binding domain (reviewed in Rudnicki and Jaenisch, 1995). These Id proteins inhibit MRF activity by heterodimerizing with E2-5 products (other HLH-containing proteins that form heterodimers with MyoD family members), and prevent their heterodimerization with MRFs and subsequent activation of skeletal muscle-specific genes (reviewed in Rudnicki and Jaenisch, 1995).

1.3.2 MRFs in Skeletal Muscle Regeneration

Little is known about the role of muscle-inducing genes like MyoD and myogenin during regeneration, and how the expression of these genes in regenerating muscle compares to their expression in embryonic development and *in vitro* (Füchtbauer and Westphal, 1992). These two MRFs have been found to be expressed in "activated" satellite cells *in vivo* after an injury (Grounds et al., 1992; Füchtbauer and Westphal, 1992). Smith et al. (1993) have described the presence of all four MRFs in cultured myogenic cells from newborn mice. Whether such myogenic cells, as Smith et al. used, are embryonic/neonatal myoblasts or activated "satellite cells" is not clear, and it is not resolved whether it would make a difference.

1.3.3 MRFs and Thyroid Hormone

Triiodothyronine (T3) treatment promotes terminal muscle differentiation and results in

increased MyoD gene transcription in myogenic cell lines; also MyoD and fast MHC gene expression are activated in slow-twitch muscle fibers (Carnac et al., 1992; Hughes et al., 1993). Hughes et al. (1993) observed in rat hindlimb, the selective accumulation of MyoD and myogenin in fast and slow muscles respectively. The T3 treatment studies suggest a possible role for the different MRFs in the determination of fast-versus-slow-fiber types. However, adult mice lacking MyoD do not exibit gross deficiencies in fast muscle, suggesting that Myf-5 can also substitute for MyoD in this regard (Rudnicki et al., 1992).

Muscat et al. (1994) suggest a molecular mechanism for the effects of T3 on myogenesis *in vitro*, the activation of MyoD gene expression in the slow-twitch fibers, and the cascade of myogenic events regulated by thyroid hormone. They identify a thyroid response element (TRE) in the mouse MyoD gene that directly interacts with the thyroid hormone-retinoid-X-receptor (RXR) heterodimer. The effects of thyroid hormones are mediated by the intracellular thyroid hormone receptors (TR), that are encoded by 2 distinct genes, c-erb Aα and c-erb Aβ (discussed in more detail in section 1.8.2.2). TRs bind to response elements containing tandom direct (and degenerate) repeats, of the AGGTCAN$_x$AGGTCA motif with spacings of 3 or 4 nucleotides and activate gene transcription (Kliewer et al., 1992; Mangelsdorf et al., 1991; Naar et al., 1991). TRs require accessory/auxiliary factors for high affinity binding to their cognate sequences (Darling et al., 1991; Glass et al., 1990; Murray and Towle, 1989). The RXR family is one of these accessory proteins and is activated by 9-cis retinoic acid. The RXRs heterodimerize with TRs and function to selectively target the high affinity binding of the receptors to their cognate elements (Mangelsdorf et al., 1991; Yu et al., 1991; Zhang et al., 1992; Leid et al., 1992). The sequences and motifs in the TRE that are necessary for an efficient DNA-receptor interaction were also characterized. The results showed that T3 directly controls the expression of the myogenic-specific HLH (MRF gene) proteins, and therefore outlined a mechanism for the changes in the contractile protein isoform profile observed in adult rodents exposed to T3. This information further supports the idea that

MRF gene expression is necessary for maintaining adult muscle characteristics (and adaptability) in addition to inducing differentiation in developing or regenerating muscle.

1.4 The Satellite Cell

1.4.0 Characterization of the Satellite Cell

In addition to embryonic myoblasts, the process of myogenesis gives rise to another mononuclear cell, the satellite cell, which is located outside of the muscle fiber plasma membrane but within the external (basal) lamina, thus defining the satellite position. In contrast, the true myonuclei are located inside the muscle fiber plasma membrane (sarcolemma). The satellite cell is characterized by an oval heterochromatic nucleus, relatively little cytoplasm, the usual organelles (Mauro, 1961) but lacks cell surface caveolae or plasmalemmal vesicles (reviewed in Schultz, 1976) and myofibrils (reviewed in Bischoff, 1994). Clear detection of satellite cells on myofibers, typically thought only to be made accurately using an electron microscope, can now be made using a light or a confocal microscope and commercially available antibodies to delineate the external lamina and plasmalemma of fibers (Zhang and McLennan, 1994).

Satellite cells are located in a depression in the myofiber, so the contour of the basal lamina covering both cells remains continuous. The gap between the plasmalemmae of the two cells is 15nm. Despite this small gap, no specialized junctional complexes of any type have been reported to occur between satellite cells in adult myofibers (reviewed in Bischoff, 1994), which suggests that this contact is specialized in a unique manner yet to be determined.

Satellite cells have been found in all vertebrate muscles examined. The frequency of these cells varies widely depending upon location, muscle type, age, and species. In studies of rat satellite cells, it has been shown that in fast-twitch muscle of adults, satellite cells comprise one to four percent of nuclei within the basal lamina, while slow-twitch muscle contains three to four times as many satellite cells. The

frequency and development of satellite cells appears to vary with fiber type. Therefore, it is possible that these cells can carry information specified by fiber type and that this may be passed on to myotubes formed *in vitro* (reviewed in Bischoff, 1994).

It has been shown using chicken and quail cells, that satellite cells are not uniform, but can be subdivided into populations which differ in their commitment to the types (fast or slow) of muscle fibers they form. In contrast, cultured rat satellite cells from fast or slow muscle make uniform myosin heavy and light chains as judged by biochemical and immunochemical analysis. These results indicate that there are differences between satellite cells of different origin in the absence of external influences (reviewed in Bischoff, 1994).

Satellite cells are most abundant during early postnatal development, when they contribute to muscle growth. Their number declines thereafter, relative to the number of myonuclei. True myonuclei (in myofibers) are incapable of mitosis soon after birth. It is the satellite cell that then supplies a normally growing postnatal fiber with additional nuclei (Moss and Leblond, 1971). During early development, satellite cells proliferate, withdraw from the cell cycle and become quiescent. In skeletal muscles of adults, satellite cells remain mitotically quiescent. However, satellite cells become active in response to mitogens released when fibers are damaged (Bischoff, 1986; DiMario and Strohman, 1988; Bischoff, 1990; Grounds et al., 1992).

Once isolated from adult muscle and placed in culture, satellite cells are generally no longer termed "satellite", but are called myoblasts or mpcs since they are no longer in the "satellite position". These cells can be released from adult muscle with the aid of enzymes, such as trypsin or pronase, which dissolve the basal lamina or by mechanical dissociation (as used for this study). Primary cultures are generally initiated in medium containing serum (and chick embryo extract (CEE) in some cases) to begin growth and later may be switched to serum-free medium (or stripped serum) while testing the effects of

various growth factors, steroids, or hormones. Because serum and CEE contain a variety of hormones and unspecified growth factors, the conditions needed to activate proliferation of isolated satellite cells *in vitro* are relatively unknown (reviewed in Bischoff, 1994), and there is some disagreement about whether it is possible to prepare adult mpcs for culture that are not already "activated" by the isolation procedure. Clearly that depends on the working definition of "activated".

1.4.1 Satellite Cells and Growth Factors

Many growth factors are small proteins of fewer than 200 amino acids and are active at very small concentrations. They appear to act locally within tissues following production by the target cells themselves (intracrine and autocrine stimulation) or by neighboring cells (paracrine stimulation). Growth factor signals are mediated by specific cell surface receptors. These receptors are tyrosine kinases that phosphorylate many intracellular substrates to pass on the growth factor signal to the nucleus or other target substrates (reviewed in Bischoff, 1994).

Satellite cells are thought to be activated and influenced by at least 2 different types of stimuli before they begin to proliferate: (1) the cell must become induced to enter the G_1 phase of the cell cycle by "competence factors" and then (2) stimulated to progress through the remainder of the cell cycle and undergo mitosis by "progression factors" (reviewed in Bischoff, 1994; Reddy, 1994). It has been reported that in cell types other than satellite cells, competence factors are needed only while the cell passes a critical point in G_1 (restriction point). On the other hand, progression factors are needed continuously to sustain proliferation. Two growth factors, fibroblast growth factor (FGF) and insulin-like growth factor I (IGF-I), have been tested on satellite cell cultures and found to be good candidates for a competence factor and a progression factor respectively (reviewed in Bischoff, 1994).

1.4.1.1 Fibroblast Growth Factors

FGFs are considered to be structurally-related, monomeric proteins (approximately 150 amino

acids in length) that are encoded by at least 6 separate genes. There are acidic and basic classes due to differences in isoelectric points. All FGFs stimulate the proliferation of fibroblasts, and all bind to heparin (reviewed in Bischoff, 1994). Gospodarowicz (1975) and Gospodarowicz et al., (1975) first isolated FGF from the brain and pituitary. It is also present in CEE (Kimura et al., 1989) which can be used in addition to serum to promote the proliferation of satellite cells (as in this study).

FGF stimulates the proliferation of cultured myoblasts from a variety of species and can inhibit their differentiation. FGF also has the ability to stimulate the proliferation of myoblasts in serum-free medium, while rat myoblasts produce their own FGF in culture. Receptors for FGF have been detected on myoblasts of several myogenic cell lines (Olwin and Hauschka, 1988), but adult satellite cells have not been tested for FGF receptors (reviewed in Bischoff, 1994).

FGF does not appear to have a signal sequence; it is not secreted from cells by defined exocytotic routes and its mechanism of release is unknown. However, evidence exists that FGF is bound to heparin sulfate proteoglycan components in the extracellular space, and FGF may be able to enter that space following cell injury. Disruption of heparin sulfate metabolism in myoblasts appears to interfere with the action of FGF. This disrupted metabolism may prevent the binding of FGF to its receptor (Rapraeger et al., 1991). Satellite cells on single isolated myofibers remain quiescent when grown in serum-containing medium. It has been shown that FGF is the only defined substance that will induce their proliferation (reviewed in Bischoff, 1994). Recently, hepatocyte growth factor was demonstrated to stimulate proliferation as well (Allen, personal communication).

FGF is present *in vivo*, and its level varies with physiological changes in the muscle (reviewed in Bischoff, 1994). Immunohistochemistry studies reveal that FGF is localized to the basal lamina of normal adult mouse muscle, and the amount is elevated in mdx dystrophic mouse muscle (in myoblasts, fibroblasts, and new myotubes), in which there is active ongoing regeneration (DiMario et al., 1989;

Yamada et al., 1989; Anderson et al., 1991, 1993, 1995). FGF mRNA is expressed in many mononuclear myogenic precursors and also in new myotubes *in vivo* in regenerating mdx muscle, so it is not accurate to say that FGF inhibits differentiation per se (Garrett and Anderson, 1995). Basic FGF (bFGF) is expressed in dividing, MRF-positive (myogenic) cells *in vivo* as well (Anderson et al., 1997a, submitted).

1.4.1.2 FGF and Thyroid Hormone Interaction

Studies that examined the role of thyroid hormone in regulating bFGF levels in the heart (Liu et al., 1993) indicated that elevated levels of bFGF could be observed in cardiac ventricles in either physiological or experimentally induced hypothyroidism. These results led to the conclusion that thyroid hormone may, directly or indirectly, down-regulate accumulation of higher molecular mass forms of bFGF in the heart (Liu et al., 1993). Another study (Anderson et al., 1994a) showed a general reduction in bFGF immunostaining in mdx skeletal muscle under hyperthyroid conditions. Both of these studies clearly indicate that interactions between hormone and growth factor pathways do occur.

1.4.1.3 Insulin-like Growth Factors

IGFs are highly conserved proteins (about 70 amino acids in length) and are related to insulin. IGFs are secreted by many tissues and are carried in the circulation by specific binding proteins that compete with cellular IGF receptors and thus modulate growth factor activity. IGFs stimulate the proliferation of cultured satellite cells in serum-free medium and also promote their differentiation. The mitogenic effects of IGFs are much less pronounced than is the enhancement of differentiation. High levels of proliferation are only obtained with a combination of IGF and FGF (reviewed in Bischoff, 1994).

IGF action is mediated by 2 different cell surface receptors: (1) the type I receptor is a multi-unit structure closely related to the insulin receptor, while (2) the type II receptor is a monomeric protein identical to the mannose-6-phosphate receptor. In rodent satellite cell cultures, the effects of IGFs are

mediated by the type I receptor in both mpcs (activated satellite cells) and myotubes. Quiescent satellite cells on single myofibers *in vitro* do not proliferate in response to IGF or high concentrations of insulin, but satellite cells can be activated by exposure to muscle growth factor or FGF (as mentioned above). However, these satellite cells are dependent upon serum for continued proliferation, and that serum requirement can be replaced by IGF. It appears that IGF stimulates satellite cell proliferation, but only if the cells have already been activated (reviewed in Bischoff, 1994).

Successful regeneration requires a number of processes (see section 1.0) and it would certainly be advantageous (from the stand point of designing treatments to increase myogenesis) for a single multifunctional molecule, such as FGF, to regulate some of these events. There is evidence that growth factors are made by activated satellite cells themselves, and this may provide an autocrine mechanism for magnifying the effect of injury (reviewed in Bischoff, 1994). However, to date no single growth factor can ensure effective muscle regeneration, and the best treatment will likely be complex.

1.5 The Cell Cycle

1.5.0 Cell Cycle Dynamics and Ploidy

The following text on the cell cycle is paraphrased from a book by Longobardi-Givan, 1992, *in: Flow Cytometry*, Chapter 7. The amount of DNA in the nucleus of a cell, called the 2N or diploid amount of DNA, is species specific (for example, human cells contain about 6pg of DNA per nucleus). With 2 major exceptions, all normal cells within a given organism contain the same amount of DNA. These 2 exceptions are: (1) cells that have undergone meiosis in preparation for sexual reproduction and therefore contain the 1N or haploid amount of DNA and (2) cells that are synthesizing DNA in preparation for mitosis and therefore contain between the 2N amount of DNA and twice that amount, 4N or tetraploid (Longobardi-Givan, 1992).

The cell cycle has been divided into phases (Fig. 1.1 - note that all figures and tables discussed

in a particular chapter can be found at the end of that chapter). Cells designated as being in the G_o phase are not cycling or are quiescent. Cells in G_1 are either just recovering from division or preparing for entry into S-phase. Cells are said to be in S phase when they are actually in the process of DNA replication. Cells in the G_2 phase are those that have finished DNA synthesis and therefore possess twice the normal amount of DNA. Cells in M phase are undergoing chromosome condensation and karyokinesis which occurs immediately prior to cytokinesis. Normal division results in the formation of two daughter cells, each with the 2N amount of DNA (Longobardi-Given, 1992).

1.5.1 Cell Cycle Analysis

The distribution of cells throughout the cell cycle may be determined by staining the cells of interest with a fluorescent dye which binds to DNA on a stoichiometric basis. One dye which is commonly used for this purpose is propidium iodide (PI). Following staining, the cells are analyzed by flow cytometry and the relative fluorescence (DNA content) of each cell is determined. Figure 1.2A presents a theoretical histogram expected from a population of nomally cycling cells. The distribution of different kinds of nuclei present at a particular moment can be shown. If the DNA content of cells that are dividing is examined, there will be some cells with the 2N amount of DNA (either G_o or G_1 cells), other cells with the 4N amount of DNA (G_2 or M cells), and finally some cells with different amounts of DNA that span the range between these 2N and 4N populations. Figure 1.2B illustrates a typical DNA cell cycle histogram obtained from the analysis of stimulated lymphocytes (Logobardi-Given, 1992). Typically, 5,000 - 10,000 cells are analysed. Computer algorithms are readily available to compartmentalize and calculate the percentage of cells in each phase of the cell cycle.

The traditional method for analyzing cell division involves measuring the amount of DNA being synthesized in a culture by counting the radioactivity incorporated into DNA during exposure to a pulse with ^{3}H-thymidine. A DNA histogram resulting from flow cytometric analysis is a powerful alternative

to this technique, since cells with the 2N, 4N, and amounts of DNA in between 2N and 4N (synthesizing DNA) can be calculated. Cells in S-phase, i.e. those distributed between the 2 peak regions should in some way correlate with the values obtained for DNA synthesis based on the uptake of ^{3}H-thymidine. The values are not directly convertible one to the other; the radioactive method measures the total amount of DNA being synthesized and will give higher values when more cells are present, whereas the flow method measures the percentage of cells that are in the process of making DNA and that distribution is not dependent on the total number of cells analyzed. It should be noted that the radioactive method will give higher values if there is a significant amount of DNA repair occurring. The flow method will give higher values if a proportion of cells are blocked in S phase (Longobardi-Given, 1992).

The use of bromodeoxyuridine (BrdU) and flow cytometry provides a more direct way to measure DNA synthesis. This method is similar to the method of measuring the incorporation of ^{3}H-thymidine, but with BrdU serving as a thymidine analogue. When cells are pulsed with BrdU, this analogue will be incorporated into the cellular DNA in the place of thymidine. Following limited DNA denaturation to expose the BrdU within the double helix, FITC-conjugated anti-BrdU antibody is added. Cells that have incorporated BrdU during the pulse will become FITC-positive. The resulting flow cytometric analysis of cells stained with this protocol is a two-color contour plot (Fig. 1.2C) in which the red fluorescence of PI (proportional to total DNA content) is plotted versus the green flourescence of the FITC antibody. As expected, the cells in the middle region of the PI distribution have all incorporated BrdU, as well as the cells at either end of the PI distribution (early and late S). Operationally, this method permits a more difinitive quantification of the cells in S-phase when compared to that obtained with PI staining by itself (Longobardi-Given, 1992).

Additionally, BrdU can provide information about the kinetics of the cell cycle. In cells pulsed

briefly with a small amount of BrdU, killed immediately and stained with both PI and anti-BrdU antibody, the FITC label should stain equally in all cells in S phase. If there is a lag between labelling and killing the cells (and if the BrdU has been used up very quickly), then the cells that have incorporated BrdU (all the cells that were in S phase at the time of the pulse) will have synthesized more DNA and some of those cells will have progressed into the G_2 or M phase of the cell cycle (or even cycled back to G_1). Some new cells will have started to make DNA after the BrdU had been used up, and these cells will now be in S phase but will have DNA that did not incorporate BrdU. Thus, the rate of movement of the BrdU-containing cells through S phase and into the G_2 peak can be estimated by assuming that they are evenly distributed throughout S phase at the time of pulsing and that they each incorporate BrdU at the same rate. Then the samples are stained at one subsequent time. The rate of increase in PI intensity of the FITC-positive nuclei is equivalent to the rate of DNA synthesis, and therefore provides information about the cycle time of actively dividing cells (Longobardi-Given, 1992).

1.5.2 Cyclins, Cyclin-Dependent Kinases (Cdks), and Cell Cycle Progression

The following background (in this section and in section 1.5.4) on cell cycle progression is paraphrased from chapter 17 of Alberts, Bray, Lewis, Raff, Roberts and Watson, 1994 *in Molecular Biology of the Cell*, 3rd edition (Murray et al. as contributors). The "cell cycle control system" consists of many interacting proteins that influence and coordinate the downstream events that duplicate and divide the cell's contents. In the cell cycle, this control system is regulated by "brakes" that can stop the cycle at specific "checkpoints" (see section 1.5.3). At these points, feedback signals from downstream processes can influence the control system itself, so as to prevent it from invoking the next downstream process before the previous one has finished. The checkpoint brakes also allow the control system to be regulated by signals from the environment. Such signals generally act on the control system at either of two major checkpoints in its cycle: (1) in G_1, just before entry into S phase and (2) in G_2, at the entry to

mitosis. In higher eukaryotic cells, signals that arrest the cycle usually act at the G_1 check point (Murray et al., 1994).

The "control system" is based on two key families of proteins: (1) the cyclin-dependent protein kinases (Cdks), which stimulate downstream processes by phosphorylating particular proteins on serines and threonines, and (2) the cyclins, specialized activating proteins that bind to Cdk molecules and control their ability to phosphorylate the correct target proteins. The cyclic assembly, activation and disassembly of cyclin-Cdk complexes are fundamental events driving the cell cycle. G_1 cyclins bind to Cdk molecules during G_1 and are required for entry into S phase. Mitotic cyclins bind to Cdk molecules during G_2 and are required for entry into mitosis (Murray et al., 1994).

In budding yeast, G_1 cyclins (CLN1, CLN2, and CLN3) drive cells through G_1 by activating the kinase CDC28 (a homolog of fission yeast cdc2). Distinct cyclins also promote S phase (CLB5 and CLB6) and mitosis (CLB1 and CLB4) (reviewed in King et al., 1996). Higher animals also have multiple cyclins: at least six types have been found, namely cyclins A, B, C, D, E, and F (Murray et al., 1994). The cyclins with known roles in cell cycle control include: A-, B-, D-, and E-types along with their kinase partners Cdk1, Cdk2, Cdk4, or Cdk6. The D-type cyclins in complexes with Cdk4 or Cdk6 regulate progression through the G_1 phase of the cell cycle, while cyclin E-Cdk2 regulates entry into S phase. Cyclin A-Cdk2 regulates progression through S phase, while cyclins A and B in association with Cdk1 regulate entry into M phase (reviewed in Edgar and Lehner, 1996).

1.5.3 Cell Cycle Checkpoints

The controlling events of the cell cycle of most organisms appear to be ordered into dependent pathways in which the initiation of late events is dependent on the completion of earlier events (reviewed in Hartwell and Weinert, 1989). New reports propose that this interdependence may be established by positive or negative regulatory circuits. The regulatory circuits are referred to as surveillance mechanisms

that check for completion of critical cell cycle events and permit further cell cycle transitions. One circuit acts in each cell cycle to order events, while another circuit acts only when a defect is found. Loss of these circuits can lead to the reduced proficiency of cells to detect errors in cell cycle events such as chromosome duplication and segregation. Checkpoint is the term given to these surveillance circuits. This term should only be used to refer to the biochemical pathways that control movement into and out of phases of the cell cycle, and should not be used synonymously with the term transition. To give an example: the DNA-damage checkpoint is the mechanism that detects damaged DNA and generates a signal that arrests cells in the G_1 phase of the cell cycle, slows down S phase, arrests cells in G_2 phase, and induces the transcription of repair genes (reviewed in Elledge, 1996).

In mammals, only the G_1 DNA-damage checkpoint is understood in any detail. There is also a spindle assembly checkpoint and a DNA-replication checkpoint. Three genes control the DNA damage: ATM (mutated in ataxia telangiectasia), p53, and p21. Ataxia telangiectasia is a disorder were cells do not show a decrease in the rate of DNA synthesis and delay of mitosis in response to damaged DNA. p53 is a tumor suppressor gene (see section 1.6.3.2 for more on p53) and encodes a transcription factor that is activated in response to DNA damage. Cells that do not have a operative p53 gene cannot arrest in G_1 in response to τ-irradiation and show decreased apoptosis. p53 arrests cells in G_1 by the activation of p21 transcription. p21 is an inhibitor of cyclin dependent kinases (Cdks) that control entry into S phase (reviewed in Elledge, 1996). When treated with DNA-damaging drugs, cells lacking p21 appear to undergo repeated S phases (reviewed in Sherr, 1996).

To summarize this section, there is a distinction between cell cycle phase transitions and the above surveillance mechanisms. Most importantly, the role of checkpoints is to stop the cell cycle when the cell's DNA becomes stressed or damaged.

1.5.4 The G_0 State, Early and Late Response Genes, and an Introduction to the Retinoblastoma Gene

Proliferating cells, specifically cells already in S-phase, that are transfered to culture medium that does not contain serum will stop growing and only pass through the next cell cycle phase (G_2/M) to reach the G_0/G_1 phase. Upon reaching G_0/G_1, they will remain in a quiescent non-proliferative state termed the G_0 resting state, in which the rate of protein synthesis is reduced to as little as 20% of its value in proliferating cells. The absence of appropriate growth factors such as FGFs in serum-deficient medium sends cells into a state where the cell cycle control system inhibits progression past the G_1 checkpoint. G_0 cells are severely depleted in one or more types of Cdk protein and in all of the G_1 cyclins. Therefore, the G_0 cells have suspended their cell cycle control system. After serum is added to the medium there is a lag of several hours during which the Cdk and G_1 cyclins are returned to their normal cycling levels. This explains the delay observed before the cells resume their normal cycling behavior (Murray et al., 1994).

Two classes of genes that growth factors induce are the early-response genes (such as c-jun and c-fos) and the delayed-response genes. Early-response genes are induced within 15 minutes of growth factor treatment and their induction does not require protein synthesis. Delayed-response genes are not induced until at least 1 hour after growth factor treatment and this induction requires protein synthesis. Delayed-response genes are also induced by the products of the early-reponse genes and are not made in G_0 (Murray et al., 1994).

The products of the delayed-response genes include Cdk proteins and several cyclins. Because of the timing of their expression, they are suspected to be involved with Cdk proteins in driving cells past the G_1 checkpoint and in initiating S phase. In order for the expression of these early and delayed-response genes and the production of their protein products to take place, specific inhibitory devices must be overcome. These devices ensure that the cell doesn't proliferate in the absence of a positive signal to

proliferate. One of these inhibitory devices is the tumor supressor gene termed the retinoblastoma (Rb) gene (Murray et al., 1994).

Mutations in the Rb gene causes a rare cancer that occurs in the eyes of children. Loss of both copies of the gene leads to increased proliferation of cells in the immature retina, suggesting that Rb normally keeps proliferation in check. Rb protein binds to many other proteins, and its binding depends on its state of phosphorylation. When Rb is dephosphorylated, it binds a set of regulatory proteins that favour cell proliferation. Phosphorylation of Rb makes it release those proteins, allowing them to act (see section 1.6.3.1). Rb is present in all normal cells and whether the cells are in G_0 or cycling, only its state of phosphorylation changes. When cells are in G_0 they contain little amounts of phosphate and this appears to prevent the transcription of the early-response genes that are required for proliferation. Growth factors can alleviate the inhibition exerted by Rb by causing the protein to become phosphorylated on multiple serine and threonine residues. The cells can then express Cdk protein and pass the G_1 checkpoint (Murray et al., 1994) (see section 1.6 for more about Rb function during the G_1-S phase transition).

1.6 The G_1 to S Phase Transition

1.6.0 Control of the G_1 to S Phase Transition by the E2F Gene Family

The E2F gene family can control viral and cellular gene expression, and is also thought to play a role in growth regulatory processes such as the G_1 to S phase transition. In 1986 a cellular-protein activity was identified that was required for the transactivation of the adenovirus E2 promoter by the E1A oncoprotein; this cellular DNA-binding activity was termed E2F. Further studies indicated that transcriptional activation by E1A results from the release of E2F from complexes with other cellular proteins. Free E2F then interacts with the viral E4 protein which mediates cooperative protein binding at two E2F sites in the E2 promoter. Many viruses can break up E2F-protein complexes. The same parts

of the viral oncoproteins that break down E2F complexes also trigger viral transformation. Thus, increasing the amount of free E2F in the cell is thought to be essential for neoplastic transformation by viruses such as adenovirus, papilloma virus, and simian virus 40 (SV40) (reviewed in Slansky and Farnham, 1996).

Information on how disruption of E2F complexes leads to the formation of tumours was provided by studies with the Rb tumor suppressor protein. Rb negatively regulates cell growth (see section 1.5.4) and, is suggested to be a target of some viral oncogenes (reviewed by Slansky and Farnham, 1996). Rb was discovered to be one of several proteins that is bound by the adenoviral E1A protein. Since it was known that E1A releases E2F from protein complexes, it was hypothesized that E2F-mediated transcription was activated through the removal of Rb by E1A. Evidence came in 1991 when investigators showed that Rb, when bound to a column, could associate with cellular proteins that interacted with an E2F-binding site. The association of Rb with E2F was confirmed by gel mobility shift assays. Rb negatively regulates progression through G_1 into S. It is now believed that when viral oncoproteins disrupt E2F/Rb interactions, E2F is released to activate genes that are essential for progression through G_1 into S phase. (reviewed in Slansky and Farnham, 1996).

1.6.1 How the Different E2F and DP Family Members were Discovered

Based on the hypothesis that E2F and Rb interacted directly, Rb protein was used to probe human cDNA expression libraries. Several investigations proposed the existence of more than one family member, and the first clone was named E2F1. Two additional E2F members were isolated by screening human cDNA libraries with an E2F1 probe and were called E2F2 and E2F3 (reviewed in Slansky and Farnham, 1996).

Different cellular complexes can bind to E2F sites. This indicated that proteins similar to, but distinct from, Rb could also interact with E2F (reviewed in Cobrinik, 1996). p107, a cellular protein that

has homology to Rb, was observed in E2F-specific gel shift complexes. Also, an E2F protein distinct from E2F1 was immunoprecipitaed using p107-specific antibodies. Knowing this information allowed others to screen cDNA expression libraries using p107, instead of Rb, as a probe and this resulted in the isolation of E2F4. E2F5, which binds specifically to another Rb-related protein, p130, has also been cloned (reviewed in Slansky and Farnham, 1996).

In studies of the E2 promoter, it was discovered that an activity that binds to E2F sites was abundant in F9 embryonal carcinoma cells, but only after the cells were induced to terminally differentiate. The activity was named differentiation-regulated transcription factor 1 (DRTF1). Protein sequences obtained from purified DRTF1 led to the cloning of a partial cDNA with some homology to the human E2F1 DNA-binding domain, and the encoded protein could bind to E2F sites. However, the cDNA was different from other E2Fs and was named DP1 (DRTF protein 1). An antibody specific to DP1 supershifted the majority of the protein species that bound to an E2F site, suggesting that most E2F cellular complexes also contain DP1. Using the probe, human DP1 and a highly related protein, DP2, were obtained (reviewed in Slansky and Farnham, 1996).

To summarize, the protein sequences of four different mammalian E2Fs and two different mammalian DPs have been reported. At least one other mammalian E2F gene, E2F5, has been cloned. E2F activity has been identified in other species that include: *Drosophila* (Ohtani and Nevins, 1994), *S. cerevisiae* (Mai and Lipp, 1993), *S. pombe* (Malhotra et al., 1993) and *Xenopus* (Philpott and Friend, 1994).

1.6.2 E2F and Cellular Promoters

Several viruses have evolved ways to increase E2F activity, but only adenovirus contains E2F-regulated promoters, suggesting that the key targets of E2F transcription factors may be cellular promoters. Reports in 1989 showed that E2F sites were important for the activity of two cellular

promoters, dihydrofolate reductase (dhfr) and c-myc. E2F sites in these promoters are also required for activation by viral oncogenes. We now know that cellular promoters whose E2F sites contribute to transcriptional regulation include many genes required for DNA synthesis (dhfr, thymidine kinase, DNA polymerase-α), transcriptional regulators of cell growth (N-myc, Rb, cdc2, E2F1, and b-myb), and growth factors (IGF-I) (reviewed in Slansky and Farnham, 1996).

Therefore, E2F sites appear to be necessary, but they are not the only factors important for growth regulation. Other transcription factors work together with E2F to stipulate growth-regulated transcription (Sp1 and CCAAT factors) (reviewed in Slansky and Farnham, 1996).

1.6.3 E2F Multiprotein Complexes

The binding of DNA tumor virus oncoproteins to Rb overcomes Rb's tumour suppressing ability causing cells to become transformed. The inability of DNA tumour virus oncoproteins to bind to mutant inactive forms of Rb in retinoblastoma or other tumour cells suggests that these oncoproteins bind to a region of Rb, termed a pocket, that is critical to Rb's growth-inhibiting capability. It was proposed that to overcome Rb's growth-inhibition, growth-promoting proteins had to be removed from the Rb pocket. It is now realized that E2Fs, when removed from the pocket regions of Rb as well as Rb-related proteins, disrupts cell growth (reviewed in Cobrinik, 1996).

1.6.3.1 Cell Cycle Dependent Regulation of the Rb:E2F Complex

Rb is phosphorylated in a cell cycle dependent manner, becomes hyperphosphorylated as cells pass from G_1 into S phase and later becomes dephosphorylated to a basal state as cells leave mitosis. Rb is phosphorylated at amino acid residues that fall within concensus target sites for the Cdk family and evidence suggests that Rb is phosphorylated by at least one and possibly by a series of these kinases. Currently, the best Rb kinase candidates are cyclin D/Cdk4 and cyclin E/Cdk2 (reviewed in Cobrinik, 1996) (Fig 1.3).

E2F binds only to the hypophosphorylated form of Rb, and free E2F can be released from Rb:E2F complexes upon Rb phosphorylation by the cyclin E/Cdk2 or the cyclin D/Cdk4 kinases in vitro. These observations suggest that hyperphosphorylation of Rb by cyclin-dependent kinases releases free E2F from the complex, just as cells commit themselves to enter into the late G_1 and early S phases of the cell cycle. Phosphorylation of E2F1 on specific serine residues has also been reported to prevent the interaction of E2F1 with Rb (reviewed in Cobrinik, 1996).

How do the free E2F and cyclin E become inactivated when most E2F-dependent genes are shut off as the cell enters S phase? The rapid turnover of cyclin E is mediated by ubiquitin-dependent proteolysis. Phosphorylation by its own catalytic partner, Cdk2, signals cyclin E destruction (reviewed in Sherr, 1996). There are many proteolytic processes inside and outside of cells, but the ones known to be important for cell cycle progression rely on the assembly of a ubiquitin chain on the substrate, which targets it for degradation by the 26S proteosome (reviewed in King et al., 1996). *In vitro*, cyclin A/Cdk2 phosphorylation of DP1 abolishes DNA binding by E2F-DP1 heterodimers and stops E2F-dependent transactivation. These same events may occur *in vivo*. DP1 is phosphorylated in S phase, at the time of the activation of cyclin A/Cdk2 kinase. These findings suggest that E2F1 acts as a go-between in directing the cyclin A kinase to phosphorylate DP1 and cause E2F1-DP1 heterodimers to be released from their promoter DNA binding sites in S phase. E2F2 and 3 are probably shut off in the same way. The E2F1 cyclin A-binding region is conserved in E2F2 and 3, and these E2Fs also stably associate with cyclin A/Cdk2 (reviewed in Cobrinik, 1996).

1.6.3.2 Cdk Inhibition

Cyclin D-, E-, and A-dependent kinases are negatively regulated by Cdk inhibitors that include at least three proteins: p21, p27, and p57 (reviewed in Sherr, 1996). An interesting feature in relation to cancer is the inducibility of the p21 gene by p53 (see section 1.5.3). These genes also respond to many

other types of stimuli during terminal differentiation (see section 1.7.0). p53 can induce apoptosis when it is overexpressed, and initiating this program does not depend on p21. p53 may directly activate death genes, such as BAX, or down-regulate survival genes, such as BCL-2. Thus, G_1 arrest and apoptosis appear to be alternative p53-induced outcomes.(reviewed in Sherr, 1996).

To summarize, E2Fs appear to promote cell cycle progression through their activation of growth-promoting genes, while the binding of Rb to E2F represses the expression of such genes. The phosphorylation of Rb by Cdks represents a critical link between the central cell cycle control machinery and the expression of E2F-responsive genes involved in cell cycle progression. Rb is not the only such link though, since E2Fs are also bound and are apparently regulated by other members of the pRb family (p107 and p130) (reviewed in Cobrinik, 1996).

Interestingly, the phenotype of Rb$^{-/-}$ mice does not support the hypothesis that Rb mediates cell cycle exit. These mice die young, but most of their cells proliferate and arrest normally. Rb$^-$ cells also contribute normally to many tissues in chimeric mice (animals partially composed of Rb-deficient cells, but not heterozygous for the Rb mutation). These mice have cataracts, hyperplasia of the adrenal medulla, and enlarged cells in the cerebellum and liver (Williams et al., 1994). These chimeras also get tumours of the intermediate lobe of the pituitary and exhibit an increased rate of pituitary tumourigenesis (Williams et al., 1994). However, the lack of major proliferation defects in Rb$^-$ cells *in vivo* could result from functional overlap with other members of this gene family. Many mouse knock-out experiments seem consistent with the paradigms generated *in vitro*, but recent reports describing the phenotypes of E2F-1 mutants has revealed problems in clarifying results when using these *in vitro* models. It was expected that E2F$^-$ mice would lack tissues because it was presumed that there would be no cell proliferation. In fact, these mice develop normally, only to suffer a wide range of tumors later on in life (reviewed in Edgar and Lehner, 1996). These experiments demonstrate once again how important it is

to compare *in vitro* versus *in vivo* results.

1.7 Myoblast Cell Cycle Progression

Proliferating myoblasts do not express the differentiated phenotype. In response to differentiation signals, they permanently withdraw from the cell cycle, fuse into multinucleated myotubes and express muscle-specific gene products (Martelli et al., 1994). MyoD is a MRF involved in the complex control of myogenesis. Negative regulation of MyoD function by growth signals occurs in proliferating myoblasts, while withdrawal of exogenous growth factors triggers MyoD to arrest cell growth and initiate the differentiation program (Martelli et al., 1994).

It is thought that growth factors repress MyoD function by: (1) inducing phosphorylation of the MRFs (Li et al., 1992a), and (2) by stimulating expression of early-response genes which have been shown to repress MyoD transactivation (Li et al., 1992b; Bengal et al., 1992). In addition to activating myogenesis, MyoD induces growth inhibition during G_1 in the cell cycle (Martelli et al., 1994).

The mechanism(s) involved in the MyoD mediated growth arrest include functional interaction with cell cycle regulatory proteins (Martelli et al., 1994). MyoD can interact with the product of the Rb gene and this interaction may be required for the cell cycle arrest produced by MyoD (Gu et al., 1993) (Fig 1.3).

As mentioned (section 1.5.4), the product of the Rb gene suppresses cell growth (Goodrich and Lee, 1993) and is a nuclear protein, the phosphorylation of which is regulated during the cell cycle and during cell differentiation. The growth-suppressing effects of Rb are exerted in the G_0/G_1 phase of the cell cycle and are inactivated by phosphorylation or by binding viral oncoproteins such as (SV40) (see section 1.6). One interpretation of the above evidence is that the effects of Rb on cell growth may be mediated by its physical and functional interaction with important cell cycle regulatory molecules (Martelli et al., 1994).

Gu et al. (1993) have demonstrated that Rb plays an important role in the process of terminal differentiation of muscle cells, and its function or the function of an Rb-related gene product is required for the myogenic activity of MyoD (Caruso et al., 1993). Martelli et al. (1994) have described a novel regulatory interaction between MyoD and Rb1. They demonstrate that MyoD induces high level Rb1 gene expression in differentiating C2 cells (a murine muscle cell line) by activating the Rb1 gene promoter. They also show that MyoD can activate the human Rb1 gene promoter in transient assays by a mechanism independent of direct binding to promoter sequences. Another group (Halevy et al., 1995) reported a mechanism that keeps Rb functionally active in muscle cells (see below). Rb family members are functionally regulated by Cdks and their associated cyclins (Sherr, 1993). One way by which these molecules regulate the transition from the G_1 phase to the S-phase of the cell cycle is through the phosphorylation of Rb. This relieves repression of cellular transcription factor complexes such as E2F-DP, resulting in activation of genes important for the initiation of DNA synthesis (Nevins, 1992) (see section 1.6).

1.7.0 Cdk Inhibitors and MyoD

Molecules that inhibit the activity of Cdks have been identified: p21 (El-Deiry, 1993) and p27 (Polyak et al., 1994) (see section 1.6.3.2). Because Cdk inhibitors activate negative regulators of Rb, these molecules may positively regulate Rb function. Halevy et al., (1995) proposed that myogenic factors (such as MyoD) might indirectly regulate Rb function by inducing the expression of Cdk inhibitory proteins (such as p21) (Fig 1.3). They also propose that p21 activates a positive regulatory loop to keep MyoD functionally active in differentiated myotubes in the presence of growth factors to ensure they remain terminally withdrawn from the cell cycle. These studies were performed on cultured cells, and, although MyoD is sufficient to arrest the cell cycle and induce muscle differentiation, neither MyoD nor myogenin is required for p21 regulation *in vivo*.

Thus, in spite of the accumulating evidence, the link between p21 and terminal differentiation is not tight, as seen by conflicting cell culture and *in vivo* results. It is possible that Myf-5 takes over MyoD's role *in vivo* (Parker et al., 1995), although it has been shown that Myf-5 does not substitute for MyoD in satellite cells during proliferation (Megeney et al., 1996). According to Marx, (1995) if p21 is turned on as cells differentiate, it does not neccessarily mean that it plays the postulated role in linking differentiation to growth cessation. Continued work in this area will lead to the mechanisms involved in regulating muscle cell passage through the complex cell cycle.

1.8 Hormonal Regulation of Skeletal Muscle Development and Regeneration

1.8.0 A Review of Thyroid Hormone Circulation and Biosynthesis

The iodinated thyroid hormones are major regulators of metabolic rate, food intake and the differentiation and maturation of numerous cell types. Normal human adult blood contains approximately 8000 (4000-11,000)ng/dl of thyroxine (T4) and 120 (80-180)ng/dl of triiodothyronine (T3). T4 binds with high affinity to plasma proteins with an estimated 2ng/dl (0.03%) present in the active form. T3 associates more loosely with plasma proteins, and 0.4ng/dl (0.3%) is readily available for entry into cells. Three types of plasma proteins function as reservoirs and buffers. They protect the hormones against rapid degradation and excretion, contribute to control of target cell uptake, and may facilitate hormone transport through the bloodstream.

Seventy-five to seventy-seven percent of the circulating T4 is associated with neuraminic acid-rich α-glycoproteins with molecular weights of approximately 60,000. These proteins were at first collectively known as thyroxine binding globulins. They are now called thyronine binding globulins (TBGs) as it had been demonstrated that there were interactions between T3 and some other T4 metabolites (reviewed in Martin, 1985). Each protein molecule bears one hormone attachment site, but normally only 30% of the sites are occupied. The total TBG concentration is 1.5-2.0mg/dl. Thyroxine binding prealbumins (TBPAs)

are tetrameric proteins with molecular weights of around 54,000 that bind an additional 15% of T4 but have little affinity for T3. Usually more than 99% of the T4 attachment sites remain unoccupied and plasma concentrations are approximately 30ng/dl. Plasma albumins are proteins that bind T4 with low affinity but high capacity due to their abundance. Each molecule has several attachment sites for T4, one with much higher affinity than the others. The properties of the protein facilitate rapid association with the hormone when T4 levels rise, but also rapid transfer to target cells. Albumins have molecular weights of near 69,000 and are present in 3500-5500 µg/ml concentrations. They usually bind approximately 8% of the circulating T4 (reviewed in Martin, 1985).

Normal human thyroid glands secrete approximately 90µg of hormone daily, most of it as T4. Eighty percent of the secreted T4 undergoes deiodinations that result in the formation of a variety of metabolites. Two of these metabolites include T3 and reverse T3 (rT3). Thirty-five percent of the total T4 is converted to T3 and around 40% to rT3. The liver is the major site for deiodination and it releases a great quantity of the products to the bloodstream. Kidneys also deiodinate T4, but at a lower activity level than in the liver, and therefore they also contribute to the plasma T3 levels. Both T3 and rT3 undergo successive deiodinations that lead to the formation of diiodo and monoiodothyronines and finally to thyronine (reviewed in Martin, 1985).

1.8.1 Thyroid Hormone Receptors and Signalling Pathways

Thyroid hormones can bind to: (1) the plasma membrane, (2) cytoplasmic proteins, (3) the mitochondria, and (4) to the nucleus (reviewed in Soboll, 1993). The function of nuclear binding sites as nuclear receptors is well-established (Oppenheimer, 1979), whereas the roles of the other binding sites are less clear.

Binding proteins have been characterized in rat liver plasma membranes, rat kidney, rat thymocytes, erythrocytes, beef liver and in mouse fibroblasts. High and low-affinity types have been

identified. Additionally, evidence has been presented for the uptake of thyroid hormone into hepatocytes, mouse fibroblasts, rat adipocytes and erythrocytes and human red cell ghosts. Due to their similarity with amino acids, it has often been theorized that thyroid hormones may be taken up by one of the amino-acid carriers in the plasma membrane (reviewed in Soboll, 1993).

Interestingly, in rat skeletal myoblasts T3 uptake is decreased in the presence of inhibitors of cell integrity and endocytosis, such as vinblastine, cytochalasine, and cochicine, suggesting that endocytosis (as T3-protein complex) may be a possible uptake mechanism for thyroid hormones. The presence of thyroid (thyronine) binding globulin (TBG) in human breast adipose tissue and serum pre-albumin in rat hepatocytes, and the observation that thyroid hormones are co-transported with serum protein are supportive of endocytotic uptake of TH (reviewed in Soboll, 1993).

The binding of T3 and T4 to cytosolic proteins (CTBPs) is described for liver, heart, brain, lung and kidney (reviewed in Soboll, 1993). The physiological function of CTBPs is not clear. Ichikawa and Hashizume (1991) suggest that, beside their role as a reservoir for thyroid hormones, they may be required for the intracellular transport of hormones to mitochondria and nuclei. From uptake and intracellular binding kinetics, Oppenheimer et al. (1972) concluded that CTBPs function as transport proteins for T3 between the plasma membrane and the nucleus.

Mitochondrial binding sites for thyroid hormones have been demonstrated as early as 1975 (Sterling and Milch, 1975). They were found to be high-affinity binding sites, apparent in electron-microscopic autoradiographs 30 minutes after administration of $[^{125}I]T3$ to hepatocytes (Sterling et al., 1984a) and localized to the inner mitochondrial membrane (Sterling et al., 1984b), although the specificity of these binding sites has been questioned (Greif and Sloane, 1978). Specific binding sites for T3 were also identified in the outer mitochondrial membrane (Hashizume et al., 1984). The physiological significance of this outer mitochondrial membrane receptor is unclear.

Nuclear receptors are the longest known and best-characterized cellular thyroid hormone receptors (reviewed in Soboll, 1993). Oppenheimer et al. (1972) discovered high-affinity thyroid hormone binding proteins in the cell nucleus of rat liver and kidney. Ichikawa and Hasizume (1991) have cloned and purified the labile receptor protein. The nuclear thyroid hormone receptor is an acidic non-histone protein with a molecular weight of 47-57 kDa. It binds tightly to chromatin, DNA and histones, and distributes preferably in transcriptionally-active chromatin. The structure of the receptor is widely conserved among species. It is most abundant in the pituitary gland, followed by liver, kidney, heart, brain, spleen and testis. Molecular biology techniques revealed that the nuclear thyroid hormone receptor belongs to the c-erb A superfamily (reviewed in Soboll, 1993).

Thyroid hormone receptors (TRs) are ligand-dependent transcription factors and there are two major isoforms, TRα and TRß encoded on separate genes (Evans, 1988; Lazar and Chin, 1990). There are two TRß isoforms, TRß1 and TRß2, which differ in their amino termini but are both ligand-dependent transcriptional enhancers (Zhang et al., 1991). At least three distinct isoforms have been isolated from the human and rat TRα genes (Benbrook and Pfahl, 1987; Koenig et al., 1988), but only TRα1 is a ligand-dependent activator of transcription. These TR isoforms bind to thyroid hormone response elements (TREs) in the promoter region of target genes as monomers and homodimers (Halloway et al., 1990; Forman et al., 1992; Lazar et al., 1991; Yen et al., 1992) (Fig.1.3). TRs heterodimerize with nuclear proteins [T3-receptor auxiliary proteins (TRAPs)] such as the retinoid-X-receptors (RXRs) (Zhang et al., 1992). Heterodimerization with RXRs enhances overall TR binding to TREs and also appears to augment ligand-regulated transcriptional activity with T3 alone (Yu et al., 1991).

The long-term action of thyroid hormones is mediated in higher organisms by regulation of nuclear transcription (Oppenheimer, 1979; also reviewed in Martin, 1985). This regulation of

transcription involves: (1) binding of T3 to the nuclear receptor followed by a direct or indirect effect on transcription, (2) a change in polymerase II activity followed by a change in cytosolic mRNA, (3) changes in translation products, and finally (4) metabolic and clinical effects (reviewed in Soboll, 1993).

Thyroid hormones exercise their main effect on tissues and cells by regulating the transcription of proteins, but recent evidence suggests that thyroid hormones may also act through extranuclear pathways (reviewed in Soboll, 1993). The possible existence of mitochondrial receptors was cited earlier. T3 can also rapidly activate Ca^{2+}-ATPases, and the targets include fully differentiated (non-nucleated) erythrocytes (Davis et al., 1982). Zhang et al. (1991) carried out a series of transfection experiments and *in vitro* DNA binding assays that showed the existence of a novel pathway by which TRs, at physiological levels, can regulate the activity of oncogenes and the tumor promoter tetradecanoyl phorbol acetate (TPA). Growth factors, TPA, ras and many other oncogenes function via a signal transduction pathway that leads to activation of c-jun/c-fos genes (early response genes that are components of the transcription factor AP-1, which mediates mitogenic signals) (Karin, 1990; Ransone and Verma, 1990). Their findings that TRs can interfere with the expression of genes regulated through this signal transduction pathway may represent a major regulatory pathway of TR action. They also found that TR activity can be regulated by c-jun/c-fos and also by the ras oncogene product (cited as unpublished data). The mutual inhibition between TR and the AP-1 complex provides another example that the membrane-signaling pathway and nuclear receptor signaling pathway can "cross-talk" to regulate gene transcription in response to extracellular stimuli (Zhang et al., 1991). These interactions may play a crucial role in controlling cell growth and differentiation.

1.8.2 Influences of Thyroid Hormones on Muscle Tissue and Muscle-Specific Gene Expression

As previously mentioned, myofibers are grouped into functionally co-operative units, which are sensitive to hormones, mechanical activity and motor innervation (Olson, 1992, 1993). In culture, the

differentiation of activated satellite cells is regulated through a suppression mechanism mediated by oncogene products and growth factors, which prevent cell cycle arrest and repress trans-activation of myogenic gene expression. Hormonal stimulation and growth factor deprivation induce proliferating myoblasts to exit the cell cycle and fuse into post-mitotic multinucleated myotubes that express muscle-specific phenotypic markers (reviewed in Muscat et al., 1995).

1.8.2.1 Regulation of Myogenesis by Thyroid Hormone

Thyroid hormone action in muscle involves its transport across the plasma membrane and nuclear membrane into the nucleus. In the 1950's it was demonstrated that thyroid hormone played a significant role in the formation of skeletal muscle. During the 1960's and 1970's, correlations between the velocity of shortening and ATPase activity were made. Studies also established that the thyroid status of animals affected the myosin isoform profile in skeletal muscle. In the 1980's it was demonstrated that alterations in circulating thyroid hormone affected muscle phenotype and contractile properties, in the presence and absence of motor neuron activity. Generally, hyperthyroidism results in slow-to-fast transitions and a common observation is that slow muscle is considered to be more sensitive than fast muscle to dysthyroidism, probably due to differential T3 uptake (reviewed in Muscat et al., 1995).

During the development of skeletal muscle, the normal transition of embryonic to adult MHC isoforms was shown to be accelerated by hyperthyroidism, independent of motor innervation and growth hormone. Later studies revealed that thyroid hormone was involved in the steady-state regulation of many different contractile protein mRNAs and that thyroid hormone treatment could activate or repress gene expression in a fiber-type-specific manner in adult rodents (reviewed in Muscat et al., 1995).

Hyperthyroidism worsens a number of human myopathies, including myasthenia gravis and myotonic dystrophy (Nicol et al., 1981) and can change the muscle phenotype of mdx dystrophin-deficient mice to more resemble that of DMD (increased areas of dystrophic foci in muscles) than is

typical in the mdx mutant (Anderson et al., 1994a).

1.8.2.2 Genetics and Mechanism of Thyroid Hormone Action

TRs bind to response elements containing tandem direct and degenerate repeats of the AGGTCA N_x AGGTCA motif with spacings of 3 or 4 nucleotides, and are known to activate gene transcription. Without ligand, TRs act as transcriptional silencers by a mechanism which is dependent on interactions with the basal transcription factor called TF IIB. TRs can function as homodimers, but they normally require accessory/auxiliary factors for high-affinity binding to their cognate sequences (see sections 1.3.3 and 1.8.1.4). Again, TRs are encoded by 2 distinct genes, c-erbAα and c-erbAβ. The c-erbAα gene is alternatively spliced into α1 and α2 (hormone and non-hormone binding) isoforms. The c-erbAβ gene is alternatively spliced into β1 and β2 isoforms. The c-erbAα locus has been shown to contain an overlapping transcription unit that utilizes coding information on the opposite strand (rev-erbAα) (reviewed in Muscat et al., 1995).

1.8.2.3 Orphan Receptors and their Modulation of Thyroid Hormone Action

Orphan receptors are members of the steroid and thyroid receptor superfamily. Their ligand is unknown, but they can be activated by covalent modificaton/phosphorylation. The Chicken Ovalbumin Upstream Promoter-Transcription Factors (COUP-TFs) are orphan receptors, and genes for 2 species have been cloned, COUP-TFI and II. COUP-TF II isoforms are ubiquitously expressed. However abundant levels have been observed in human skeletal muscle, cardiac tissue and proliferating skeletal myoblasts (reviewed in Muscat et al., 1995). COUP-TF II isoforms bind to oligonucleotides containing both direct repeats and palindromes with different spacing (0-12 nucleotides) of the A/GGGTCA motifs. COUP-TFs can repress hormonal induction of target genes by the vitamin D_3, thyroid hormone and retinoic acid receptors. COUP-TFs bind a variety of hormone response elememnts (HREs) as homodimers and may compete against other receptors for HRE occupancy (reviewed in Muscat et al.,

1995).

1.8.2.4 Regulation of Myogenic Transcription by Thyroid Hormone

Presented here are important studies that reveal interactions of thyroid hormones and muscle at the molecular level. In the first study, thyroid hormone treatment of the myogenic cell line C2.7, promoted terminal muscle differentiation, increased MyoD gene transcription and resulted in the precocious expression of myogenin and contractile protein mRNAs (Carnac et al., 1992). In a second study, TR and RXRs were observed to be involved in the T3-influenced induction of MyoD mRNA in rodent muscle and myogenic cell lines (reviewed in Muscat et al., 1995). The next studies showed that thyroid response elements (TREs) were identified in the mouse myogenin (Downes et al., 1993), MyoD (Muscat et al., 1994) (Fig.1.3), and skeletal α-actin genes (Muscat et al., 1993). Combined, these studies suggest that thyroid hormone (T3 specifically), mediated by TRs and RXRs, targets the MyoD gene family and the contractile protein genes in skeletal muscle (reviewed in Muscat et al., 1995).

To conclude, it is now known that thyroid hormones can induce the expression of the MyoD family and promote withdrawal of C2 cells from the cell cycle (reviewed in Muscat et al., 1995). It is not known if thyroid hormones and TRs play more direct roles in the expression or repression of other genes (cyclins and/or Cdks) directly related to the cycling behavior of activated satellite cells or myoblasts, or exactly how TH might effect proliferation of these cells during muscle regeneration. The present studies were undertaken to examine three specific related hypotheses (see chapter 2) concerning the effects of thyroid hormone on myoblast proliferation and cell cycle activity during control and mdx muscle regeneration.

Fig. 1.1. The four successive phases of a standard eucaryotic cell cycle. Interphase is the time period in which the cell grows continuously; cell division occurs during M phase or mitosis. The replication of DNA is confined to that part of interphase known as S phase. G_1 and G_2 are the gaps in between M and S phases and in between S and M phases respectively (modified after Fig. 17-3, Murray et al., 1994).

Division

24 hours

Interphase

G₂

G₁

M

S
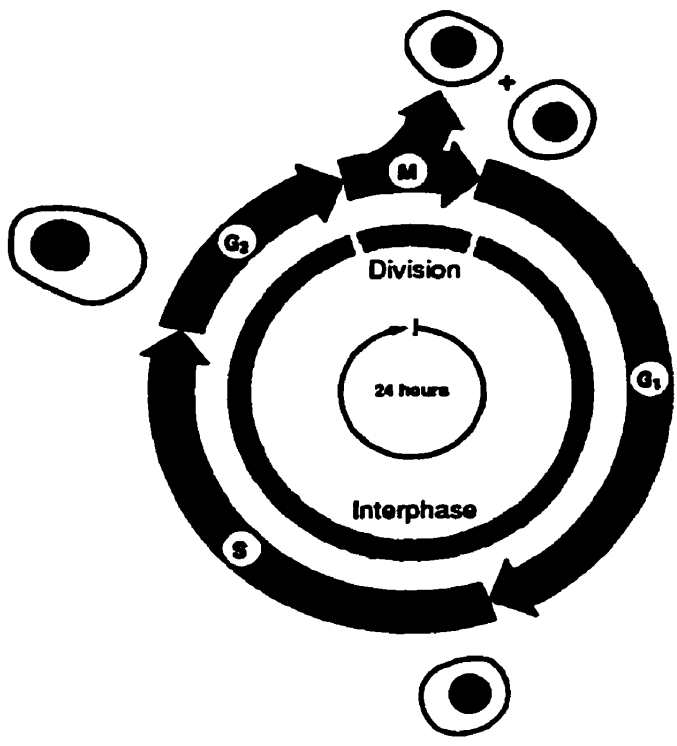
Fig. 1.2. (A) Shows a theoretical histogram expected from the sampling of a population of cycling cells

(modified after Fig. 7.6, Longobardi-Given, 1992). The first peak is the G0/G1 peak, followed by S phase

cells, and a second smaller peak called the G2/M peak. These peaks are clearly visible in (B). (B) A typical

DNA histogram obtained from the analysis of cells (lymphocytes) stimulated to divide and then stained

with propidium iodide (PI) (modified after Fig. 7.7, Longobardi-Given, 1992). (C) Two-colour correlated

contour plot of cultured human keratinocytes, pulsed with BrdU, and subsequently stained with FITC-

conjugated anti-BrdU antibodies and PI. The cells in S-phase are clearly identified (modified after Fig.

7.9, Longobardi-Given, 1992).

A

Number of Cells

Channel Number

G0/G1

S-PHASE

N/2D

B

Number of Cells

2N

4N

PI Fluorescence

C

FITC-Anti-BrdU

S-Phase Nuclei (BrdU-Positive)

Propidium Iodide

48
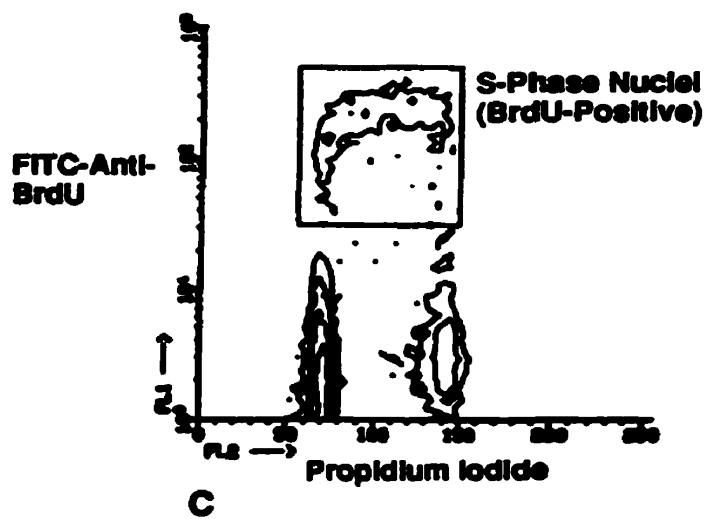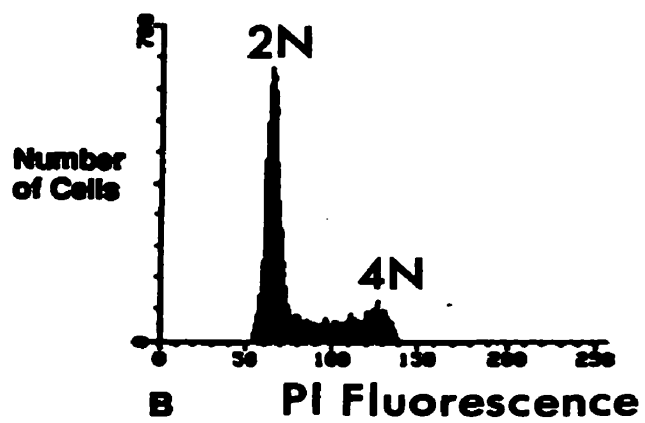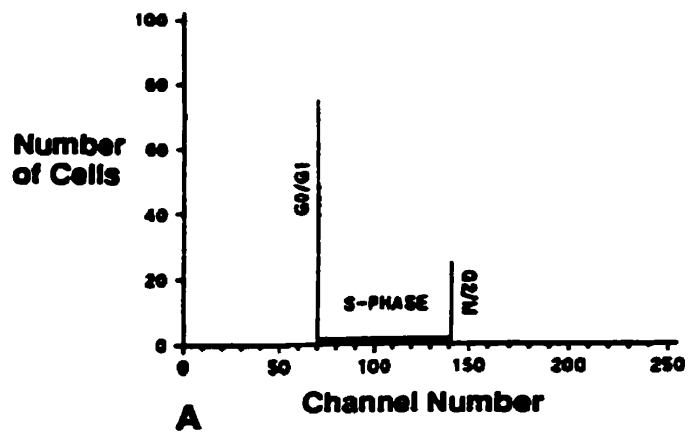
Fig.1.3. A diagram summarizing the events of thyroid hormone binding to its receptor (top), and the

binding of the thyroid hormone receptor complex to thyroid hormone response elements (TREs) on two

muscle regulatory factor (MRF) genes (MyoD and myogenin). Specific interactions between MyoD, p21

(a Cdk inhibitor) and Rb that might prevent myoblasts from making the G_1-S-phase transition are shown

in the middle of this schematic. Rb phosphorylation by specific cyclins and their Cdk partners results in

the successful transition of myoblasts through S-phase and is depicted in the bottom portion of this

diagram.

Thyroid
Hormone

hsp90

Inactive Receptor
Complex w/hsp90

Active Receptor Complex
w/T3

NUCLEUS

MyoD (TRE)
Myogenin (TRE)

[p21]

Transcription
(Muscat et al.)

Inhibits cyclin D/cdks
(Halevy et al.)

Rb Dephosphorylated
Interact w/ Rb
(Martelli et al.)

M

G2

CELL CYCLE

G0/G1

S

Rb Phosphorylation by
cdk4/cyclin D
cdk2/cyclin E
(Cobrinik 1996)
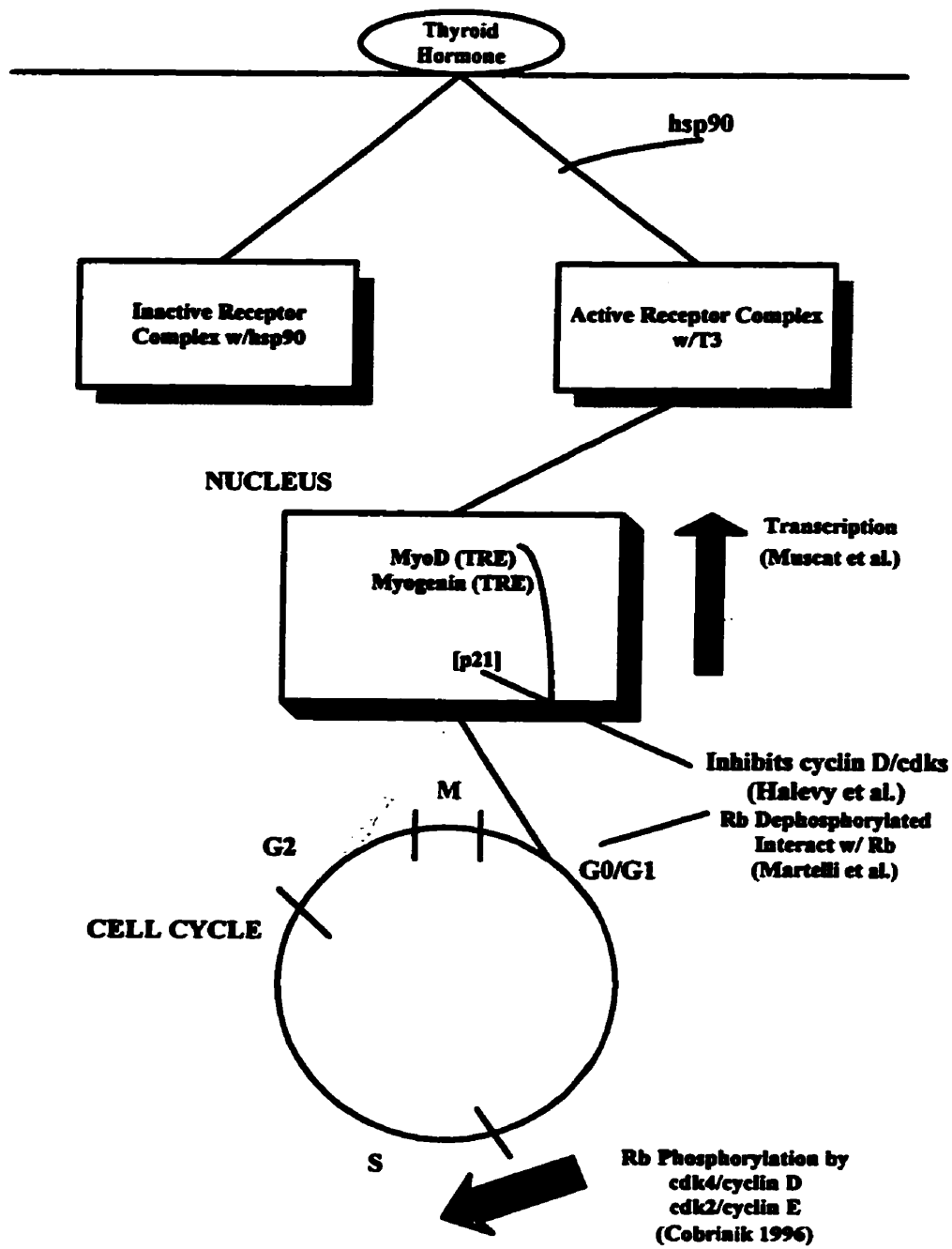
Chapter 2 - Thesis Hypotheses and Specific Objectives

2.0 Hypotheses

In initial *in vivo* studies, it was (A) hypothesized that hyperthyroidism would impair the growth of new myotubes in regenerating control and mdx muscle, either by reducing myoblast proliferation and/or affecting myoblast differentiation. Further studies, *in vitro*, tested the (B) hypothesis that proliferation is greater in mdx than control myoblasts, and may be differentially affected by T3 in the two strains. Finally, experiments tested the last (C) hypothesis that T3 would slow down or stop those muscle cells in S-phase from passing through the next late S - G_2/M and G_0/G_1 - early S transitions of the cell cycle. We also tested whether this passage through each transition might be differentially affected by T3 in the control and mdx muscle cells.

2.1 Specific Objectives For Each Hypothesis A, B, and C

(A) The incorporation of myoblast nuclei into myotubes and parameters of myotube growth were examined in muscle during the synchronous regeneration resulting from a crush injury (Grounds and McGeachie, 1989). Control and mdx, untreated and T3-treated muscles were compared. The presence of developmental myosin heavy chain (devMHC), transiently and specifically expressed by new myotubes in regenerating muscle *in vitro* (Sartore et al., 1982) and *in vivo* (Marini et al., 1991; Davis et al., 1991), was used as a marker for new myotube formation. Finally, autoradiography was used to localize myotube nuclei produced by myoblast division and fusion in the 24hr period prior to sacrifice. These studies were undertaken to determine the effects of T3 treatment on myoblast proliferation, fusion, myotube formation and growth *in vivo*.

(B) Control and mdx myoblasts and fibroblasts were cultured together, subsequently arrested and then stimulated to determine the optimal interval for detecting initial changes in S phase after a stimulus.

Further experiments were done to separate myoblasts and fibroblasts using Percoll density centrifugation and flow cytometry. The incorporation of ^{3}H-thymidine into DNA in S-phase cells (as an indicator of cell proliferation) and the cell cycle distribution of cultures (analyzed by PI staining and flow cytometry) from control and mdx, untreated and T3-treated, myoblast and fibroblast cell populations were compared. These experiments were undertaken to determine the effects of T3 on myoblast and fibroblast proliferation and cell cycling *in vitro*, as counterparts to the *in vivo* experiments in **(A)**. These same myoblast and fibroblast populations were compared to myoblasts and fibroblasts recombined in a 1:1 ratio to test whether cell-cell interactions promote proliferation, since *in vivo* regeneration certainly includes intercellular communication.

(C) To approach the two questions in the final hypothesis, a preliminary experiment was designed to determine the best pulse time for labelling muscle cells in S-phase with bromodeoxyuridine (BrdU). A second experiment determined the optimal density of cell cultures which would allow for the clear separation of all of the phases of the cell cycle (early S, late S, G_2/M, and G_0/G_1) by 2-colour fluorescence (BrdU/PI) analysis using flow cytometry. Finally, the G_0/G_1 - early S and the late S - G_2/M transitions were examined under the influence of T3 in cycling control and mdx muscle cell cultures.

Chapter 3

Hyperthyroidism Impairs Early Repair in Normal but not Dystrophic mdx Mouse

Tibialis Anterior Muscle. An *In Vivo* Study

This chapter describes work published in 1996. The paper is appended to this thesis.

(see Appendix #1)

3.0 Introduction

The mdx mouse model for X-linked Duchenne muscular dystrophy (DMD) (Bulfield et al., 1984) is invaluable for the study of regeneration in dystrophin-deficient (Hoffman et al., 1987) muscle. It has been suggested that mdx muscle responds to segmental fiber damage by a larger than normal proliferative response (Anderson et al., 1987) which compensates for ongoing dystrophy. This proliferation may be due in part to an altered control of myogenesis in view of the large amount of a key mitogen, basic fibroblast growth factor (bFGF) (Gospodarowicz et al., 1976) observed in mdx muscles (Anderson et al., 1991). bFGF is much lower in DMD or other human muscle biopsy samples from neuromuscular disease biopsy samples (Anderson et al., 1993), and it is co-expressed with muscle regulatory genes like myogenin in regenerating mdx muscles (Garrett and Anderson, 1995).

It is known that DMD myoblasts do not proliferate as well *in vitro* as normal human myoblasts (Webster and Blau, 1990). However, mdx myoblast proliferation *in vivo* (Anderson et al., 1987; Zacharias and Anderson, 1991; McIntosh and Anderson, 1995) can compensate for substantial fiber damage due to dystrophy and/or crush injury. If the difference in regenerative capacity between DMD and mdx muscle involves myoblast cycling, then alteration of proliferation may help to elucidate that distinction.

Hyperthyroidism was shown to increase regions of fiber damage in the soleus and cardiac (but not fast-twitch) muscles of mdx mice, possibly in relation to a slow-to-fast transition in myosin heavy chains (MHC) expressed by the soleus (Izumo et al., 1986), increased cardiac work and cardiomyocyte hypertrophy (Anderson et al., 1994a). As well, the relative tissue bFGF content was lower in hyperthyroid muscle. However, it was not determined if hyperthyroidism had a specific effect on muscle regeneration. Since bFGF expression is down-regulated by excess thyroid hormone (TH) (Liu et al., 1993) and the expression of two muscle regulatory genes, MyoD and myogenin (Muscat et al., 1994; Downes et al., 1993) are stimulated by TH, this hormone was used as a treatment that might alter proliferation

and differentiation in regenerating mdx and control muscle.

As outlined in section 2.0 (A), it was hypothesized that hyperthyroidism would impair the growth of new myotubes in regenerating control and mdx muscle, either by reducing myoblast proliferation and/or affecting myoblast differentiation.

3.1 Materials and Methods

3.1.0 Animals and Treatment

Mdx dystrophic (C57BL10/ScSn mdx) and control (C57BL10/ScSn) mice were made hyperthyroid by triiodothyronine (T3) injections (subcutaneous) at a dose of 2μg/g body weight/day (Anderson et al., 1994a) for 4 weeks beginning at 5.5 weeks-of-age, after the maximum period of mdx fiber damage and repair (Anderson et al., 1987, 1988). Non-dystrophic control and mdx littermate mice were untreated for the same period; mice were housed according to the Canadian Council on Animal Care. Multiple experiments were performed in order to examine histology, myotube density, myotube and myofiber diameter, devMHC localization, and to quantify myoblast proliferation and fusion into myotubes. Sections were omitted if they were not in the required orientation (see below) for assessing different parameters, which accounts for the reported variation in group size (control untreated, n=2-5; control T3-treated, n=2-7; mdx untreated, n=3-8; mdx T3-treated, n=4-8).

After 3.5 weeks of treatment, mice were anesthetized (ketamine:xylazine 1:1, 0.01cc/10g body weight) and subjected to a crush injury (Grounds and McGeachie, 1989) of the right or both tibialis anterior (TA) muscles. Three days later, mice received ^{3}H-thymidine (Amersham Inc., Oakville, ON) (2μCi/g, intraperitoneal injection) to label DNA synthesis. One day later (4 days after the crush injury) and under ether anesthesia, the TA muscles were removed rapidly from mice, oriented in Tissue Tek O.C.T. compound (uncrushed TA in cross-section, and crushed TA longitudinally) and frozen for cryosectioning (8μm). Soleus and gastrocnemius muscles were dissected from both limbs and weighed

to document T3 effects on muscle mass. Alternate serial sections were coded and stained with hematoxylin and eosin (H&E) for morphometric studies, immunostained to localize devMHC (Davis et al. 1991) or prepared for autoradiography.

3.1.1 Morphometry of Uncrushed Muscles

In the uncrushed TA muscles, one set of H&E-stained cross-sections was used to determine myofiber diameter using a calibrated computerized graphics tablet and the SigmaScan program (Jandel Scientific, Corte Madera, CA) as previously reported (Anderson et al., 1994a). Mdx uncrushed TA muscles were also examined for the proportionate area of active dystrophy (area of fiber disruption and inflammation as a proportion of muscle cross-sectional area) and the number of foci of active dystrophy per cross section (normalized to area). The proportion of fibers with central nuclei (centronucleation), an index of previous fiber regeneration from dystrophy (Karpati et al., 1988), was also determined. The mean and standard error (SEM) were determined for each parameter, and the frequency distribution of fiber diameter in each group was plotted. Sections were viewed and photographed using an Olympus photomicroscope and TMAX400 B&W film (Kodak).

3.1.2 Morphometry of Crushed Muscles

H&E-stained sections were used to examine the extent of regeneration in pre-defined zones of injured muscle. Data for each zone were averaged from all myotubes observed in microscope fields in the necrotic crushed muscle (crush zone, 2 fields), the adjacent area of mononuclear cells and new myotube formation (adjacent zone, 4 fields), and the surviving muscle furthest from the crush site (surviving zone, 3 fields) exactly as reported (McIntosh et al., 1994, after Mitchell et al., 1992). The crush, adjacent and surviving zones of injured TA were examined in 200X fields, corresponding to 4.4×10^5 μm^2 of tissue area. Selected fields were strictly examined at pre-set distances from the geometric centre of the necrotic crush zone as follows. The crush zone was sampled in 2 fields in a horizontal row across the muscle.

Fields in the adjacent zone were sampled at a width of 1 field diameter either proximal (toward the knee, 3 fields) or distal (toward the ankle, 1 field) from the crush zone. Fields in the surviving zone were sampled either 1 field diameter proximal (2 fields) or 1.5 field diameters distal (1 field) to the adjacent zone. Sampling was carried out systematically to standardize analysis, taking into account the architecture of the TA muscle.

The area of the central necrotic portion of the crushed muscle, surrounded by many mononuclear cells, was measured using SigmaScan. In addition, the mean ($\pm$ SEM) density of small myotubes in each zone (the number of myotubes per field averaged over the fields in that zone), and myotube diameter (and frequency distribution) in the adjacent zone were determined.

3.1.3 Immunostaining

A separate set of sections was blocked with a solution of 10% horse serum and 1% bovine serum albumin in phosphate-buffered saline (0.01M) for 1hr, and incubated overnight with a monoclonal antibody against developmental MHC (devMHC) (diluted 1:5), a gift from Dr. L.V.B. Anderson (née Nicholson), or 1:250 dilution of the same antibody (Novocastra Inc, Newcastle UK). According to standard methods (Anderson et al., 1991), antibody binding was detected using biotinylated goat anti-mouse antibody (1:100) and Texas Red-streptavidin (Amersham Inc., Oakville ON). Negative controls for immunostaining included the omission of primary or secondary antibodies in each staining experiment. Fluorescence for devMHC was viewed along with phase contrast to examine myotube structure.

3.1.4 Autoradiography

One set of crushed mdx TA muscle sections (from untreated and T3-treated mice) were prepared for autoradiography as previously reported (McIntosh and Anderson, 1995). The incorporated ^{3}H-thymidine was allowed to expose the emulsion in darkness for 6wks at 4°C. Autoradiograms were

developed, fixed and stained with modified Gomori's trichrome. In coded sections, counts were made of

the number of nuclei in new myotubes within the adjacent zone as follows. The above sampling method

of fields and zones (McIntosh et al., 1994) was modified to examine 400X fields using an ocular grid (3.53

X 10^4 μm^2 in area at 400X). Two rows of 3 fields each were sampled in the adjacent zone proximal from

the crush, and two rows of 3 fields each were sampled distal to the crush. The proportion of labelled

(more than five grains per nucleus) myotube nuclei and the mean ($\pm$ SEM) number of nuclei per field

were counted as an indicator of myoblast fusion which had occurred over 4 days of muscle regeneration.

3.1.5 Statistics

Differences in data (mean $\pm$ SEM) from each group or time point were tested using 2-way

analysis of variance (ANOVA) to study the effects of strain (mdx versus control), T3 treatment, and the

interaction between strain and T3. Duncan's test was used post hoc where appropriate to compare

individual group means. A Student t-test (unpaired) was used to compare mdx treated and untreated

groups where appropriate. Chi-square statistics were used to assess differences in the frequency

distribution of the diameter of myofibers or myotubes between groups. In all cases, a probability of

$p < 0.05$ was used to accept a difference as significant.

3.2 Contributions by Others

During the course of these experiments LM McIntosh kindly helped to perform the T3

injections, and assisted with the crush-injury surgeries, and post-surgical tissue collection.

3.3 Results

3.3.0 Uncrushed Muscles

Gastrocnemius mass was greater in mdx than treatment-matched control mice (Table 3.1.1), and

was reduced after T3 treatment in both strains ($p < 0.01$). Soleus mass was also lower ($p < 0.01$) after T3

treatment in mdx but not control mice. TA muscle weight was previously reported to decrease in

hyperthyroid control and mdx mice (Anderson et al., 1994a).

Fiber diameter did not differ between control and mdx TA muscle. However, fiber diameter was lower in control TA muscle after T3 treatment, according to changes in the mean ($p<0.01$, Table 3.1.2) and frequency distribution ($p<0.05$, df=118, Chi-squared, Fig. 3.1A). In comparison, the mean and distribution of fiber diameter in mdx TA muscles were not changed by T3 treatment (Fig. 3.1B, Table 3.1.2).

In mdx mice, the area of active dystrophy (as a proportion of muscle area) was significantly decreased (by half) after T3 ($p<0.05$, Table 3.1.3), although the number of foci of damage per section was not changed. As expected, T3 treatment did not change fiber centronucleation, an index of previous fiber repair (Table 3.1.4), likely due to the use of older mice (5.5wk) with relatively advanced dystrophy and regeneration at the start of treatment.

3.3.1 Crushed Muscles

In regenerating TA muscle, the area of the crush zone did not differ between control and mdx muscles, and was not affected significantly by T3 treatment (Table 3.2.1). Myotubes in the adjacent zone had greater diameter ($p<0.01$) in mdx than control TA muscle, regardless of treatment (Figs. 3.1, 3.2a,c). Myotube density in the proximal surviving zone of control TA muscle was lower after T3 treatment ($p<0.05$) (Table 3.2.2), although it was not changed in adjacent zone fields (Table 3.2.2). However, myotube diameter in control TA muscle was significantly reduced by T3 treatment (mean, Table 3.2.3; distribution, $p<0.001$, Chi-square, Figs. 3.1C, 3.2b). mdx myotube diameter was not affected by T3 (Figs. 3.1D, 3.2d).

Immunofluorescence for devMHC was absent from sections where either a primary or secondary antibody was omitted (not shown). In stained sections, small myotubes were seen as elongated cells with brightly-fluorescent sarcoplasm containing multiple non-fluorescent central nuclei. Surviving fibers in

muscle of control and mdx mice did not fluoresce (Fig. 3.3a-d). In the larger (typically mdx not control) devMHC-positive myotubes, fluorescence was oriented in narrow longitudinal bands that often had sarcomeric periodicity (Fig. 3.3d) around many closely-packed nuclei. The identification of multinucleated myotubes with early sarcomere formation was confirmed in phase contrast observations of the same sections, and in H&E-stained serial sections of the same region.

In addition, both control and mdx crushed TA demonstrated a small number of ovoid or fusiform mononuclear cells, ranging from 10-25μm in diameter, that also contained devMHC-positive cytoplasm (Fig. 3.3a,d). The devMHC-positive mononuclear cells had a nucleus-to-cytoplasm ratio of about 1:1. The cells were distinguished from endothelial cells around small capillaries and fibroblasts by their shape and location between or near devMHC-positive myotubes. Fewer of the devMHC-positive mononuclear cells were present in the surviving than in the adjacent zone, and there they were closely juxtaposed with devMHC-negative surviving fibers (Fig. 3.3b,d). Where direct close contact was apparent, the sarcoplasm of a devMHC-positive mononuclear cell and a surviving fiber were clearly delineated by the distinct absence of devMHC fluorescence from the sarcoplasm of the older fiber (Fig. 3.3b). Often the fluorescent mononuclear cells were elongated, apparently extending toward a new myotube (Fig. 3.3b,d). Muscle spindle fibers also contained devMHC fluorescence (not shown).

In the adjacent zone of crushed muscles (Table 3.2.4, Fig. 3.4a,c), the proportion of labelled myotube nuclei was lower in the distal zone (p<0.01, 2-way ANOVA, df=1,136) in mdx than control crushed TA muscle. However, the proportion of labelled myotube nuclei in the proximal zone was not different between control and mdx regenerating muscles. That proportion was also unaffected by T3 in either strain (Fig. 3.4b,d). Comparison of fields proximal or distal to the crush suggested that the difference in the proportion of labelled myotube nuclei between control and mdx TA was likely due to differences in the distal fields, as in a previous report (McIntosh and Anderson, 1995). The number of

myotube nuclei per adjacent zone field did not differ between control and mdx regenerating muscle. However, there were fewer nuclei in control myotubes after T3 treatment (p=0.02 interaction, df=1,137), but increased numbers of nuclei in mdx myotubes in hyperthyroidism (Fig. 3.4b,d).

3.4 Discussion

The present results show that regeneration in crushed mdx muscle after 4 days was more advanced than in control crushed muscle: specifically, regenerating mdx myotubes have a larger diameter with similar numbers of myotube nuclei compared to control myotubes in untreated mice after the same interval of recovery. Hyperthyroidism interfered with muscle repair by different means in control and mdx mice. In control regenerating TA muscle, myotube density was decreased in the surviving zone, where repair is stimulated at a distance from the primary site of injury (McIntosh and Anderson, 1995). As well, myotube growth (diameter), and the number of nuclei in those myotubes were significantly lower in hyperthyroid than in untreated control muscles. Those changes were not observed in mdx regenerating muscle after T3 treatment. Recent myoblast proliferation and fusion in control muscle were not significantly affected by T3 treatment. In mdx TA muscle by contrast, T3 treatment actually increased the number of nuclei in myotubes, without effects on myotube diameter, myotube density, or myoblast proliferation and fusion (labelled nuclei) in the 4th day of regeneration. It is possible that in untreated control muscle, both daughter cells of a myoblast in S-phase since the ^{3}H-thymidine injection had fused while in untreated mdx muscle only 1 of the daughter cells from dividing myoblasts fused, leaving more proliferative myoblasts to contribute to myotubes. This might explain why T3-treated control muscle contains myotubes with fewer nuclei and why T3-treated mdx myotubes have many more nuclei. The results suggest that mdx myoblasts have a greater resistence to a treatment that is deleterious to control muscle repair. T3 treatment may reduce control myoblast proliferation but does not impair fusion *per se*, and has the general consequence of reducing myotube growth. Thus, although lower myoblast

proliferation in a regenerative response may be expected to result in the formation of fewer myotubes, the effect of T3 in this study decreased myotube diameter in the area of most intense repair in control muscle, and only reduced myotube density in a zone distant from the original injury.

Hyperthyroid-induced fiber atrophy may play a role in decreasing myotube growth, since muscle mass and fiber diameter in uncrushed muscles were reduced with T3 treatment (Anderson et al. 1994a, this study). In hyperthyroid control TA, there was a decreased density of new myotubes in the surviving zone. However in mdx muscle, myotube growth was not decreased by hyperthyroidism. These results differ from the changes noted in muscle repair under hypothyroid conditions, where myotube density was lower in the distal adjacent zone particularly in mdx TA muscle (McIntosh et al., 1994). Hypothyroidism resulted in prolonged and increased mdx myoblast proliferation, and delayed myotube formation in both normal and dystrophic TA muscle (McIntosh and Anderson 1995). Indeed, the presence of new (devMHC-positive) myotubes *per se* in surviving control fields is interesting, since new myotubes would not typically be expected in surviving non-dystrophic muscle. Again, the observation (McIntosh and Anderson, 1995) suggests that the effect of an injury to stimulate myoblast proliferation and fusion, can be quite far removed from the primary insult to muscle fibers. The decreased myotube density from the distant impact of injury was the only obvious (ie. myotubes versus none) effect of excess T3 on control muscles, despite the net reduction in myoblast proliferation and fusion in the adjacent zone (fewer myotube nuclei per field). In control regenerating TA muscles, it is clear that the reduction in new myotube diameter and lower accumulated incorporation of nuclei within myotubes support the idea that myoblast proliferation and fusion during the early phase of repair (prior to 3 days when ^{3}H-thymidine was injected) may be impaired in hyperthyroidism.

Significant differences in the histology of tissue repair were found between mdx and control strains in this study. New myotubes in the adjacent zone of crushed muscles are easily distinguished from

larger myofibers and previously-regenerated myotubes in the surviving zone using anti-devMHC immunostaining. That new myotube diameter was always greater in regenerating mdx than control TA, regardless of treatment. There may be more favourable growth conditions, or faster mitotic cycling and fusion of myoblasts in mdx than control muscles (Anderson et al., 1988). The apparently superior mdx response to injury is consistent with previous reports of repair under a variety of conditions (DiMario et al., 1989; Anderson et al., 1991; Zacharias and Anderson, 1991; McIntosh et al., 1994), and may derive in part from the action of mitogens including bFGF (DiMario et al. 1989; Anderson et al. 1991, 1993; Anderson et al. 1995). The limited effects of T3 on cellular parameters of mdx muscle repair after injury are also consistent with the strain differences in bFGF content (DiMario et al., 1989; Anderson et al., 1991) particularly in new myotubes (Anderson et al., 1991). The down-regulation of bFGF by excess T3 (Gospodarowicz et al., 1987; Liu et al., 1993) might have a smaller or more transient effect on myoblast proliferation and differentiation in mdx than control regenerating muscle, consistent with the positive relation between relative bFGF content and muscle repair capacity in two other mouse strains (Anderson et al., 1995).

Thyroid and growth hormone (GH) are both required for normal muscle development and growth, and thyroid hormone also influences the GH-insulin-like growth factor I (IGF-I) axis (Rodriques-Arnao et al., 1993; Thomas et al., 1993). Ullman and Oldfers (1991) demonstrated that GH is required for muscle repair in young rats and for normal skeletal muscle growth *in vivo*. GH also promotes differentiation of myoblasts transfected from 10T1/2 cells *in vitro* (Nixon and Green, 1984). T3 negatively influences GH gene expression in rats (Cattini et al., 1986) and humans (Morin et al., 1990), so excess T3 could impact on muscle repair via GH. GH-mediated effects, which may contribute to fiber hypertrophy and repair in mdx mice (Anderson et al., 1994b), are compounded by influences on IGF-I (Daughaday and Rotwein, 1989), a mitogen that promotes differentiation (Florini et al., 1986; Rodriques-

Arnao et al., 1993). Indeed, since the area of active dystrophy was reduced by half in hyperthyroid mdx TA, as opposed to an increase in hyperthyroid mdx soleus and cardiac muscle (Anderson et al., 1994a), there may be a fiber-type specific influence of metabolism on myoblast responses to fiber injury.

New myotube formation by myoblast fusion is clearly critical in determining the effectiveness of muscle repair, and the magnitude of the response was easily observed by immunostaining for devMHC. Although the identity of the mononuclear cells which also contained devMHC is not certain, the cells are very likely myogenic since they contain a muscle-specific sarcomeric protein as reported for "differentiating myoblasts" (Robertson et al., 1990). The close juxtaposition with new myotubes, morphological features, and the observation that some devMHC-positive mononuclear cells are elongated and appear about to fuse with new myotubes or surviving fibers, further suggests that devMHC-positive mononuclear cells may be presumed to be differentiated myoblasts. Recent evidence showed that small numbers of mononuclear cells in mdx muscle *in vivo* that are positive for myogenin mRNA by in situ hybridization, also contain the same devMHC (Garrett and Anderson, 1995). That evidence supports the idea that myoblasts may be devMHC-positive just before fusion into myotubes or myofibers. It is not known whether such differentiated myoblasts can still proliferate before contributing to myotube formation and segmental fiber repair.

The present results demonstrate that mdx TA muscle maintains a larger regenerative capacity than control muscle under hyperthyroid conditions. The effects of T3 treatment on repair may be related partly to a larger than normal number of myoblasts in non-injured mdx muscle as a consequence of dystrophy and repair (Zacharias and Anderson, 1991), similar to previous comparisons between Duchenne and normal human muscle (Wakayama, 1976). We made mdx muscle more similar to DMD (more dystrophy) by T3 treatment (Anderson et al., 1994a) and expected that a change in myoblast numbers would be exhibited as reduced myotube number and growth in mdx muscle regenerating from

a crush injury. However, those effects were only observed in control regenerating muscles. Therefore, if

differences in myogenesis do account for the differences between DMD and mdx dystrophy, it is early

during the myoblast proliferation or cell cycling phase, not at the later phase of myoblast fusion and

myotube differentiation where the differences will be apparent. The differences may originate early in

muscle regulatory gene expression (eg. MyoD and Myf-5) or possibly in the proportion of myoblasts that

co-express those muscle regulatory genes and bFGF (Garret and Anderson, 1995) or other mitogens.

TABLE 3.1: Morphometry data for uncrushed TA, soleus and gastrocnemius muscles in control and mdx groups with and without 4 weeks treatment with T3.

	Control Untreated	Control T3-Treated	Mdx Untreated	Mdx T3-Treated
1.muscle mass (mg)				
soleus	8.0 ± 0.6ª(10)	10.5 ± 1.0 (13)	8.1 ± 0.5 (16)	4.6 ± 0.6*♦ (24)
gastrocnemius	126.5 ± 3.8 (10)	114.2 ± 3.3* (13)	152.0 ± 5.5♦ (16)	127.7 ± 4.5*♦ (24)
2.fiber diameter (μm) [# measured]	42.1 ± 2.2 (3) [213]	31.5 ± 3.5* (3) [193]	43.1 ± 1.8 (4) [256]	45.5 ± 2.6♦ (7) [509]
3.dystrophy (%area)	--	--	2.17 ± 0.6 (6)	1.00 ± 0.3* (6)
no. of foci (#/section)	--	--	6.14 ± 1.11 (7)	5.67 ± 1.72 (6)
4.centronucleation (% CN/total)	0.6 ± 0.2 (5)	0.7 ± 0.3 (3)	75.8 ± 3.2♦ (7)	73.2 ± 2.2♦ (9)

a:data are mean ± SEM (n=number of animals)

*:indicates significant difference from untreated group of same strain (p<0.05)

♦:indicates significant difference from control group with same treatment (p<0.05)

TABLE 3.2: Morphometry and autoradiography data for crushed TA muscles in control and mdx groups with and without 4 weeks treatment with T3.

	Control Untreated	Control T3-Treated	Mdx Untreated	Mdx T3-Treated
1. area of crush ($X10^3$ μm^2)	67.6 ± 22.4ᵃ (6)	38.9 ± 12.9 (6)	51.5 ± 13.1 (10)	27.2 ± 10.0 (8)
2. myotube density [#/field]				
crush zone:				
adjacent zone:	5.0 ± 1.0 (3)	7.0 ± 3.0 (2)	7.8 ± 3.1 (6)	5.0 ± 1.5 (3)
proximal	12.0 ± 2.1 (3)	18.0 ± 5.0 (2)	17.0 ± 3.6 (6)	13.0 ± 7.2 (3)
distal	17.7 ± 7.6 (3)	12.5 ± 3.5 (2)	21.3 ± 6.9 (6)	11.7 ± 8.0 (3)
surviving zone:				
proximal	5.0 ± 2.6 (3)	0* (2)	3.5 ± 1.2 (6)	2.0 ± 0.6φ (3)
distal	14.0 ± 3.0 (2)	9.0 ± 5.0 (2)	12.5 ± 2.9 (6)	11.7 ± 9.7 (3)
3. myotube diameter (μm)	12.8 ± 1.0 (4)	8.5 ± 0.7* (4)	14.8 ± 0.8φ (8)	13.9 ± 0.4φ (6)
4. labelled myotube nuclei				
total (%/field)	44.0 ± 3.6 (27)	40.8 ± 3.4 (22)	32.5 ± 2.5φ (71)	34.9 ± 3.9 (21)
proximal	40.3 ± 4.5 (16)	35.5 ± 4.8 (9)	33.5 ± 3.7 (37)	33.9 ± 5.0 (10)
distal	48.9 ± 6.6 (9)	44.4 ± 4.8 (12)	31.9 ± 3.7φ (34)	35.8 ± 6.3 (11)
5. number of myotube nuclei (#/field)	15.7 ± 1.2 (26)	12.1 ± 1.7* (22)	14.3 ± 0.9 (69)	18.3 ± 2.2φ (21)

a:data are mean ± SEM (n=number of animals for 2.1, 2.2 & 2.3; n=number of fields for 2.4, 2.5)

*:indicates significant difference from untreated group of same strain (p<0.05)

φ:indicates significant difference from control group with same treatment (p<0.05)

Fig. 3.1. The frequency distributions of myofiber diameters from control and mdx uncrushed TA muscle (top row), and of myotube diameter from control and mdx crushed TA muscle (bottom row). Untreated (black bars) and T3-treated (cross-hatched bars) groups are indicated. There was a significant shift toward smaller fibers in control myofiber (A) and myotube (C) diameter with T3-treatment in controls, whereas T3 had no effect on the diameter of mdx uncrushed myofibers (B) or myotubes (D). The numbers of myofibers and myotubes measured in each group are given in Tables 3.1 and 3.2 respectively.

control uncrushed
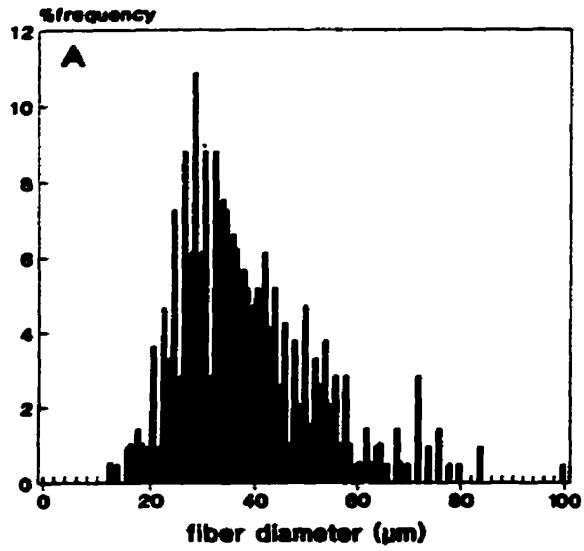
mdx uncrushed
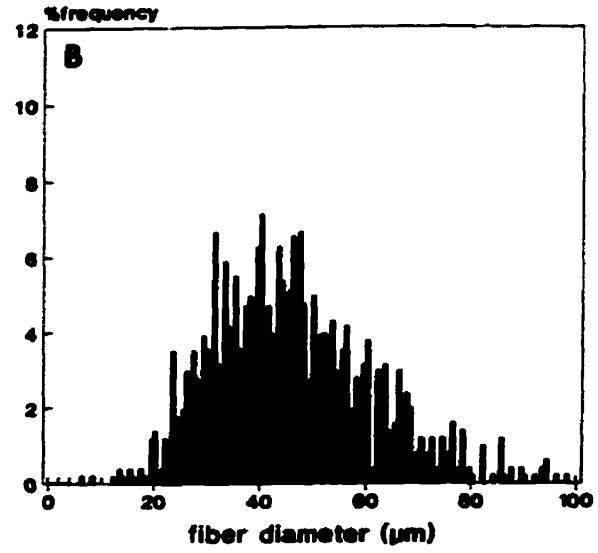
control crushed
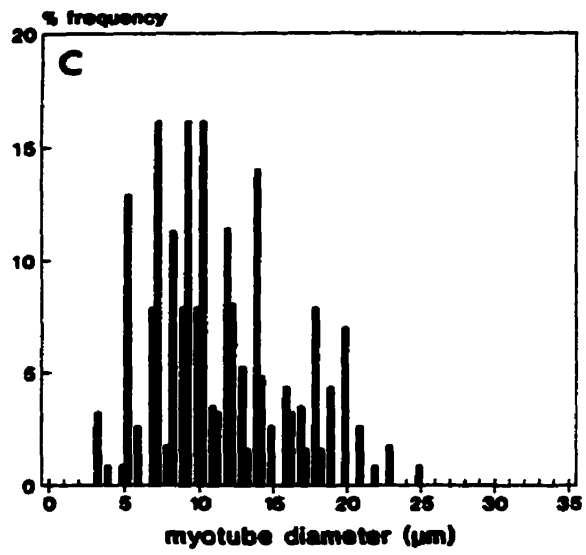
mdx crushed
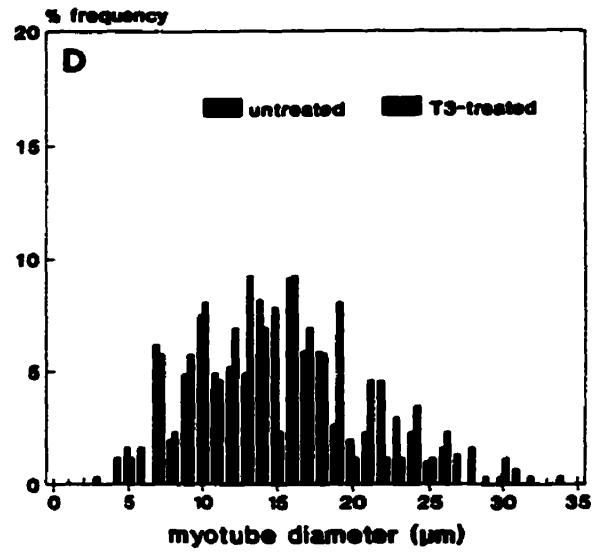
Fig. 3.2. Myotubes in adjacent zones of crushed TA, 4 days post-injury. Myotubes (large arrow) are present in the adjacent zone of an untreated control TA (a). Myotubes regenerating in an untreated mdx crushed TA (c) are larger in diameter, and have more sarcoplasm than control myotubes (a). The mdx myotubes also contain many more nuclei than control myotubes after the same recovery period. A mononuclear cell with a round nucleus (small arrow) is seen close to the border of one myotube (c). (b) and (d) show myotubes (arrows) from T3-treated control and T3-treated mdx TA respectively. H&E stain, bar=20μm, X475.

Fig. 3.3. Micrographs of developmental MHC immunostaining in crushed TA showing representative stages of myotube development. Mononuclear cells (similar to the mononuclear cell in Figure 2c) that are presumed to be myoblasts (mb), and small myotubes (mt) in an untreated control TA (a) are brightly stained with anti-devMHC, while a surviving fiber (S) does not fluoresce. In a control T3-treated crushed TA (b), a very small devMHC-positive myotube (mt) is well-delineated from the directly juxtaposed, unstained surviving myofiber (S). Other small myotubes in the same field are not attached to surviving fibers. A differentiating myotube from an untreated mdx TA (c) demonstrates early myofibril formation (arrow), around multiple internal nuclei (short arrows) that do not contain devMHC. Sarcomeric striations (short arrows) are present in a more differentiated myotube between two surviving fibers (S) in a T3-treated mdx TA (d). Two dev-MHC-positive mononuclear cells (mb) are indicated; one appears to be extending towards a small diameter myotube. Bar=20μm, X460.
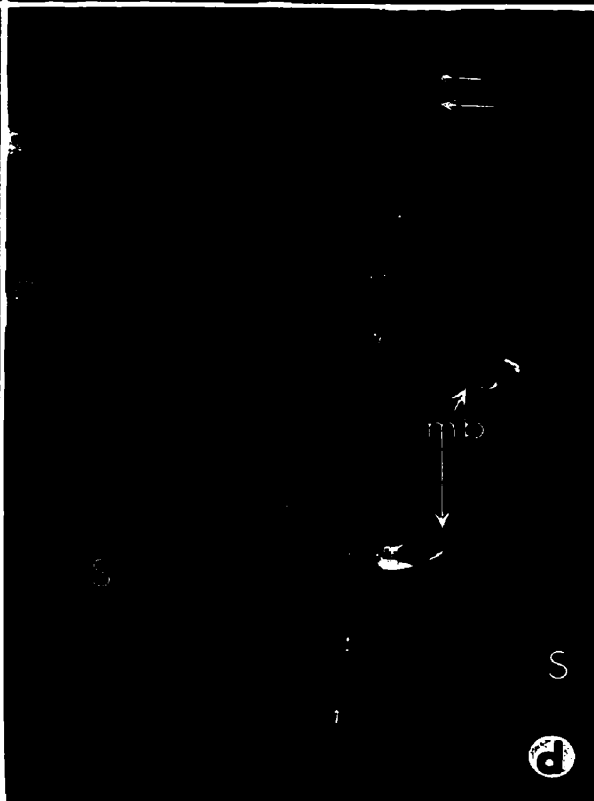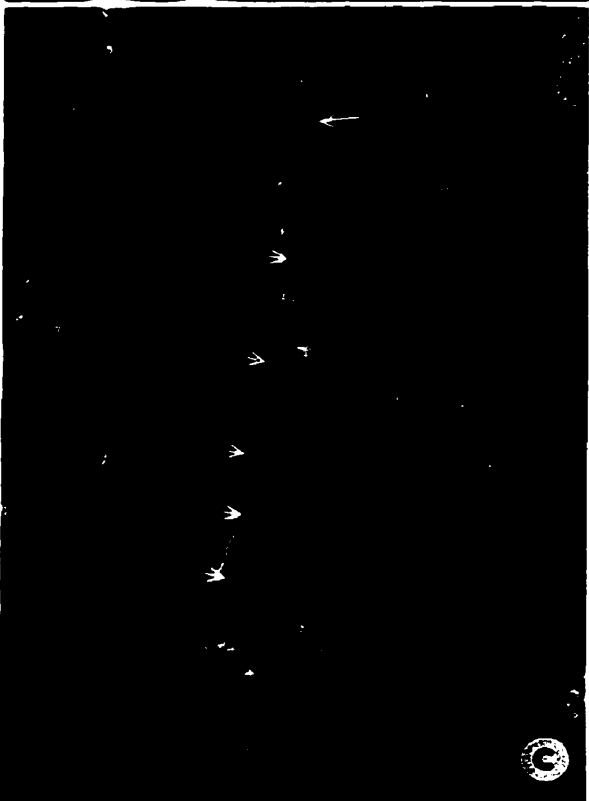
Fig. 3.4. Autoradiographs of the adjacent zone of TA 4 days after crush-injury. In the untreated control

TA (a), most myotube nuclei (large arrows) are labelled by silver grains, as are some large, round (short

arrow) and other smaller mononuclear cells. Mdx untreated crushed muscle (c) contains large myotubes

with many unlabelled (arrowheads) and some labelled (long arrow) nuclei. Some mononuclear cells are

also labelled (small arrows). (b) shows control T3-treated myotubes with fewer nuclei (arrowhead), while

(d) shows mdx T3-treated myotubes with many nuclei (arrowhead). A polymorphonuclear leukocyte is

also indicated (small arrow). Note that the grains are in focus, and lie above the tissue. Gomori trichrome

stain, bar=20μm, X500.

Chapter 4

Differential Effects of 3,5,3'-Triiodothyronine (T3) on Control and mdx

Myoblasts and Fibroblasts: Analysis by Flow Cytometry

This chapter contains work published in 1996. This paper is appended to this thesis.

(see Appendix #2).

4.0 Introduction

Thyroid hormone (TH) is known to be critical for the normal growth and metabolism of skeletal muscle (Baldwin et al., 1978; Simonides and van Hardeveld, 1989). THs, mainly 3,5,3'-triiodothyronine (T3), exert their effects via intranuclear receptors (Samuaels and Tsai, 1973). T3 treatment promotes terminal muscle differentiation and results in increased MyoD gene transcription in myogenic cell lines (Carnac et al., 1992). Furthermore, MyoD and fast myosin heavy chain gene expression are both activated in rodent slow-twitch muscle fibers after T3 treatment (Carnac et al., 1992; Hughes et al., 1993). Recent studies indicate that T3 directly controls the expression of MRFs (Muscat et al., 1994), and suggest that thyroid response elements (TREs) on muscle genes are the mechanism underlying changes in the contractile protein isoform profile observed in adult rodents exposed to T3 (Izumo et al., 1986). Thus, the expression of MRF genes is likely necessary to maintain adult muscle characteristics (and adaptability) in addition to its role in inducing differentiation in developing or regenerating muscle (Hughes et al., 1993).

The dystrophic mdx mouse demonstrates X-linked dystrophin myopathy and fiber necrosis (Bulfield et al, 1984; Koenig et al., 1987), but shows effective ongoing limb muscle repair (Anderson et al., 1987; Anderson et al., 1988). As discussed (Pernitsky et al., (1996) and chapter three), T3 treatment appeared to speed the transition from proliferation to fusion in regenerating mdx and control mouse myoblasts (activated satellite cells) in muscle regenerating from a crush injury. However, T3 treatment reduced overall repair only in control muscle, suggesting that in comparison to control myoblasts, mdx myoblasts have a large enough proliferative capacity to accomodate a T3-induced shift from proliferation toward fusion. That capacity may permit the very effective recovery of mdx muscle from an imposed injury compared to control muscle. Other reports from this laboratory (McIntosh et al., 1994; McIntosh and Anderson, 1995) show the opposite trend occurs under hypothyroid conditions, that of slowed

myoblast proliferation and fusion, which delays repair in regenerating mdx muscle. Since we know that mdx mice are euthyroid (Anderson et al., 1994b), the alteration of various features of muscle repair in mdx mice under both hypothyroid and hyperthyroid conditions suggests that there may be a differential response to T3 by regenerating control and mdx muscle tissue and possibly in myoblasts isolated from those two strains.

To date there are few studies which report differences in myoblast proliferation in regenerating mdx versus control muscle. However, it has been suggested that growth factor-induced cell proliferation *in vitro* appeared to be greater in mdx myoblasts (satellite-derived cells) compared with mdx fibroblasts, or myoblasts of other strains (DiMario and Strohman, 1988). As outlined in section 2.0 **(B)**, it was hypothesized that proliferation would be greater in mdx than control myoblasts, and would be differentially affected by T3 in the two strains.

4.1 Materials and Methods

4.1.0 Animals and Cell Culture

Adult (seven-to-ten-week-old) control (C57BL10/ScSn) and mdx dystrophic mice were used in these experiments. On day 0, 4 mice from each strain and for each experiment were anesthetized (ethyl ether) and sacrificed by cervical dislocation (according to Canadian Council on Animal Care guidelines). Muscles were dissected from the hindlimb, forelimb, and back using aseptic technique. Muscle pieces were further dissected to remove tendons and fat, and chopped into a sludge using a sterile razor blade. The sludge was placed into $25cm^2$ (50ml) flasks (Falcon, Lincoln Park, NJ) with warm minimal essential medium (MEM) (Gibco BRL, Grand Island, NY) supplemented with 15% horse serum (HS) (Hyclone Laboratories Inc., Logan, Utah) and 2% chick embryo extract (CEE) (containing < 0.3 nmols/L T3 by commercial assay) (Gibco) and incubated at $37°C$ in 5% O_2 and 95% CO_2 for 72 hours. This technique increases cell yield by maximal activation of quiescent satellite cells in non-dystrophic (control) muscle,

and homogeneously activates satellite cells in dystrophic (mdx) muscle.

4.1.1 Percoll Density Centrifugation

After 3 days, the flask contents were emptied into 50ml centrifuge tubes (Falcon), vortexed for 1 minute and filtered 2X through gauze (Nitex) to remove larger pieces of debris. Filtered contents were centrifuged at 1200 rpm for 10 minutes at 4°C (Heraeus Sepatech Varifuge RF, Baxter Inc.), resuspended in 1ml of warm MEM (supplemented with 15% carbon-stripped HS) and pooled by strain (usually 2 samples). The final sample (brought to 2ml) was layered onto 25ml of 20% Percoll (Pharmacia, Uppsala, Sweden) on a cushion of 5ml of 60% Percoll, centrifuged at 10,000 rpm (IEC B-20A, Damon/IEC Division), using a fixed-angle rotor (brakes off) for 5 minutes at 8°C. Heavier debris was observed at the 20/60 interface between the 2 Percoll fractions. The fraction just above the interface contained most of the cells of interest (myoblasts and fibroblasts) (modified after Yablonka-Reuveni and Nameroff, 1987) and was collected. This fraction was diluted with MEM, supplemented with 15% carbon-stripped HS, pelleted by centrifugation at 1200rpm for 10 minutes at 4°C, resuspended in 10ml of warm MEM supplemented with 15% HS and 2% CEE, and plated into 10, 60 X 15mm Primaria (Falcon) culture dishes each containing 3ml of the same warm MEM supplemented as above. Cells were fed once a day until semi-confluent.

To determine the length of time required for cells to pass through the cell cycle, semi-confluent control and mdx cells were subcultured and plated at equal densities. After 2-3 days, cells were arrested in metaphase using colchicine alkaloid (0.1µg/ml) (Inland Alkaloid, Inc., Tipton, Indiana) in MEM supplemented with 15% carbon-stripped HS. After 42 hours, cells were stimulated with MEM supplemented with 15% carbon-stripped HS and 4% CEE, and were incubated with ^{3}H-thymidine (2µCi/ml, specific activity = 92.0Ci/mmol) (Amersham Life Science). Duplicate samples of cells from both strains were taken over 36 hours as follows: every 2 hours for 12 hours, then every hour for 12

hours, then every 2 hours for the final 12 hours of the experiment. Cells were removed from culture dishes by treatment with warmed 0.05% trypsin-EDTA (Gibco) (1-3mins) and enzyme action was halted with 2X the amount of HS. Cells were counted, centrifuged as above and resuspended in 5mls of 100% methanol to precipitate DNA. Following 24 hours in methanol at 4°C, DNA was pelleted (6000 rpm at 4°C) and resolubilized in 1ml of 2% Triton X100 (J.T. Baker Chemical Co., Phillipsburg, NJ) and 2% lauryl sulfate (SDS) (Sigma Chemical Co., St. Louis, MO) overnight at 4°C (after Smith et al., 1980). Aliquots of soluble DNA were placed in 5ml scintillation vials (Kimble Glass, Vineland, NJ) followed by addition of 5mls of scintillation cocktail (Ready Safe, Beckman Instruments, Inc., Fullerton, CA). Vials were counted for 5mins on a Beckman LS 6500 scintillation counter (Beckman Instruments, Inc., Fullerton, CA). DPM were corrected for cold thymidine in the carbon-stripped HS (unstripped HS contained < 0.43µM cold thymidine and carbon-stripping removed 80% of radioactive thymidine in a triplicate test experiment).

Serum was carbon-stripped (modified after Tanswell et al., 1983). Briefly, to 75ml of HS was added 6.0g of activated carbon (Fisher Scientific, Nepean, Ontario). This mixture was stirred at 4°C for 22 hours and then centrifuged at 10,000rpm for 90 minutes at 4°C. The supernatant was passed through a 0.20µM filter unit (Nalge Sybron Co., Rochester, NY) and then added to MEM and stored at 4°C prior to use. This treatment removes thyroid hormones, cortisol and a number of other steroid hormones, yet the serum appears to retain growth promoting properties (Tanswell et al., 1983). In the present experiments, carbon-stripping of HS removed 75% of T3 (as analyzed by a commercial T3 assay).

4.1.2 Flow Cytometry

Semi-confluent cells were removed from culture dishes by treatment with warmed 0.05% trypsin-EDTA (Gibco) (1-3mins) and enzyme action was halted with equal amounts of HS. Cells were pelleted and resuspended in 2ml of HEPES-buffered MEM (no serum) and analyzed by a flow cytometer (Model

EPICS 753, Coulter Electronics Inc.) equipped with an argon-ion laser operating at 500mW (488nm). Forward angle scatter (linear) was first gated to remove debris and dead cells. Ninety degree light scatter (also linear) was used to gate cells based on their cytoplasmic granularity (Yablonka-Reuveni, 1988). The cell suspension was sorted under sterile conditions (using saline as sheath fluid) into two populations based on "low" and "high" cytoplasmic granularity. Cells were sorted into tubes containing 2mls of sterile HEPES-buffered MEM and subsequently plated into 100 X 20mm Primaria culture dishes with MEM supplemented with 15% HS and 2% CEE. The cultures were allowed to proliferate until semi-confluent.

Populations were further subcultured into 5 100 X 20mm Primaria dishes each and then 2-3 days later were subcultured into 6 100 X 20mm dishes (6 low and 6 high for each strain) with an additional 6 dishes plated with a 1:1 ratio of mixed low and high cells for each strain. Before plating, cells were counted using a hemacytometer (Sigma Chemical Co., St. Louis, MO) and cell suspensions were diluted to allow for the equal plating of cells for each population (low, high and mixed). Cell populations were grown for 3 days in MEM supplemented with 15% HS and 2% CEE.

4.1.3 Immunocytochemistry

To characterize the populations, mdx low and mdx high sorted cells were grown on sterile coverslips until they began to differentiate, were fixed for 5 minutes at room temperature in methanol/acetone (1:1), and then rinsed in 0.01M PBS twice. Cells were blocked for 1 hour with 10% horse serum (HS) and 1% bovine serum albumin (BSA) in PBS. Following a 60 minute incubation at 37°C with rabbit anti-skeletal muscle myosin (Sigma Chemical Co., St. Louis, MO) monoclonal antibody (diluted 1:100 in PBS plus 10% HS and 1% BSA), coverslips were rinsed twice in PBS, and incubated for 1 hour at 37°C with an anti-rabbit Ig, Texas Red-linked whole antibody (Amersham Inc. Mississauga, Ont.) (diluted 1/200). Coverslips were rinsed, incubated in 1μM bisbenzimide in PBS for 4 minutes at room temperature to stain nuclei, rinsed, and mounted with Immumount (Lipshaw

Immunon, Pittsburgh, PA). Cells were photographed with black and white film (TMAX400, Kodak) on

a BHT-2 Olympus photomicroscope equipped with epifluoresence optics.

4.1.4 T3 Treatment and Propidium Iodide Staining for Flow Cytometry

After 3 days in MEM supplemented with 15% HS and 2% CEE, cells were switched to MEM

containing 15% carbon-stripped HS and 4% CEE and allowed to adapt for 24 hours. Cells were once

again fed with the above MEM and supplements. At this time, T3 (Sigma Chemical Co., St. Louis, MO)

(10^{-9}M in 0.05M NaOH vehicle) was added to 3 of the 6 plates in each group (control and mdx; low, high

and mixed cells). Nineteen hours later, one hour before sampling, ^{3}H-thymidine (2μCi/mL, specific

activity = 92.0Ci/mmol) was added to 2 of the 6 plates (one T3-treated plate and one untreated plate from

each group) for 1 hour. These cells were collected and cell DNA was prepared for scintillation counting

using the method described above (Smith et al., 1980). Data were collected as ^{3}H-thymidine uptake per

cell for mdx and control strains, and low, high and mixed cells, with T3 or without T3. At the same time

that these cells were collected, the remaining 4 plates of cells from each group were dealt with by trypsin-

EDTA treatment as above (the two T3-treated plates were pooled and the two untreated plates were

pooled from each group), centrifuged at 1200rpm for 10 minutes at 4°C, resuspended in 3ml 0.05M PBS,

counted, centrifuged at 1200 rpm for 7 minutes at 4°C and resuspended in 500μL of sterile 0.9% NaCl

on ice. Cells from each group were then added to 5mls of ice-cold 70% EtOH while vortexing and

incubated on ice for 30 minutes. Cells were centrifuged as above, resuspended in 0.05M PBS, centrifuged

again and resuspended (in the dark) in 500μL of 10μg/ml propidium iodide (PI) (Molecular Probes Inc.,

Eugene, OR) and 50μg/ml RNAse (ICN Biochemicals Inc., Cleaveland, Ohio) solution.

Flow cytometry analysis was performed on a Coulter Electronics, Inc. EPICS 753 cell sorter with

laser excitation set at 488 (500mW). Forward versus side light scatter histograms were used to gate on

intact cells and eliminate debris, while peak versus integrated PI derived fluorescence signals were used

for doublet discrimination gating. PI fluorescence was detected through a 610 nm long pass filter.

Fluorescence histograms of 256 channel resolution were based on 5000 cells satisfying the light scatter

and doublet discrimination gating criteria. Cell cycle determinations were performed using the PARA

1 analysis program (Coulter Electronics Inc., Hialeah, FL).

4.1.5 Statistics

Data (mean ± SEM) were tested using a 3-way ANOVA to compare different cell types (low and

high light scatter), T3 treatment effects, strain differences, and interactions (NWA Statpak, NW

Analytical INC., Portland, OR). A probability of $p<0.05$ was used to accept a difference as significant.

Chi-squared contingency tests were used to analyse the frequency distributions of cells in different phases

of the cell cycle, comparing cell populations and treatment effects (Stats Plus, Human Systems Dynamics,

Northridge, CA).

4.2 Results

**4.2.0 Isolation and Characterization of Myoblasts and Fibroblasts by Percoll Density
Centrifugation, Flow Cytometry, and Immunocytochemistry**

The use of Percoll density centrifugation (PDC) allowed cells of interest to be separated from

larger debris and erythrocytes. Many cells were present in the low density (20%) Percoll fraction in all

control and mdx experiments, and were harvested from the gradient for culture. Within 6 days, cells were

abundant enough to collect for analysis and sorting using flow cytometry. The use of flow cytometry

allowed a mixed population of cells to be separated (from both strains) into two populations based on

side scatter (cytoplasmic granularity) and forward angle light scatter (size). A gate of between 10 and 60

units (arbitrary) was selected for the cells of interest (modified after Yablonka-Reuveni, 1988). Cells that

had a cytoplasm with very little or no granularity were sorted into the low light scatter category, and cells

that had a very high cytoplasmic granularity were sorted into the high light scatter category (Fig. 4.1).

Similar contour plots of cell size versus granularity were revealed in the sorts for mdx and control cells, which also yielded the same cell populations by identical low and high gatings.

The low and high populations were characterized using antibodies to skeletal muscle myosin. Cultures of mdx low cells (Fig. 4.2) allowed to differentiate for a short period (1-2 days) contained many cells which expressed small amounts of skeletal muscle myosin (Fig. 4.2B), indicating that the low cultures contained a large majority of myoblasts. In contrast, cultures of mdx high cells contained very few myosin-positive cells (Fig. 4.2D). Control and mdx low and high cell isolates had very similar proportions of cells with myosin staining.

4.2.1 Determination of Cell Cycle Length in Control and mdx Unsorted Cells

After release from cell cycle arrest by stimulation (time 0 in Fig. 4.3), both control and mdx cells showed an extended lag period approximately 6-10 hours in length between stimulation and the initial observation of cytokinesis. After this, cells proceeded through the remaining phases of mitosis and moved into G_1 (at about 12 hours, judging by the general end of cytokinesis). This phase lasted for approximately 8-10 hours for both strains. Cells then proceeded through the G_1 checkpoint into S-phase, as indicated by the rise in ^{3}H-thymidine uptake per cell by cells of both strains (beginning at 19-20 hours). The ^{3}H-thymidine incorporation continued for the remaining hours of the experiment prior to mitosis. Thus, eliminating the initial lag period for the release from the arrested state (6-10 hours), the optimal interval for detecting changes in DNA replication during S-phase in cycling cells begins between 19-20 hours after stimulation. Although cells in this experiment did not complete the G_2/M phase (which would be observed as a drop in ^{3}H-thymidine incorporation per cell), data suggest that the approximate length of the cell cycle for the unsorted cells under the current conditions is 26-28 hours.

4.2.2 Analysis of ^{3}H-Thymidine Uptake into DNA in Control and mdx Sorted Cells

As an estimation of cell proliferation, the incorporation of ^{3}H-thymidine into DNA (during the

hour before sampling) by sorted low and high cells and mixed cell populations was examined after 24 hours adaptation to MEM supplemented with 15% carbon-stripped HS and 4% CEE, plus an additional 20 hours with or without T3 treatment. Figure 4.4 represents the mean uptake per cell ($\pm$ SEM) of duplicate samples (2 DPM readings for each strain, cell type and treatment group). Analysis of variance determined a significant effect of strain on proliferation ($p<0.0001$), since overall mdx cells had greater uptake per cell than control cell populations. There were significant differences in uptake by low, high and mixed populations ($p<0.0001$) and significant interaction between strain and cell type populations ($p<0.0001$). Those two effects are observed as a lower uptake per cell in control high cells compared to control low or mixed cells, while uptake by mdx mixed cells was greater than in mdx low or high populations.

While there was no significant general effect of T3 treatment on uptake per cell ($p=0.63$), T3 treatment had differential effects on cell proliferation, observed as significant interaction between strain and T3 treatment ($p<0.05$) and between cell type and T3 treatment ($p<0.0001$). The interactions are observed in low cells, where T3 decreased uptake per cell in both control and mdx populations. T3 treatment affected only the mdx high cells (not controls), increasing their uptake per cell. Mixed control cell populations showed increased uptake after T3 (approximating an additive effect of the uptake by separated low and high T3-treated cells). Mdx mixed cells showed additive uptake in untreated conditions, but a significant decrease in uptake per cell was observed after T3 treatment. These results suggest that the mdx low cells are stimulated to proliferate by the presence of the high cells (i.e. in the untreated mdx mixed group), and that mdx low cell uptake is inhibited by T3 in the presence of high cells in the mixed population. In this experiment, the variation in uptake within groups was low, likely since the low, high and mixed populations were all derived from the same animals, and were processed together. Therefore, data show there were significant interaction effects of T3 treatment with strain and

cell types which support the possibility of differential effects of T3 on control and mdx myoblast populations.

4.2.3 Analysis of Proliferation in Control and mdx Sorted Cells by Propidium Iodide

The precise origin of the changes in uptake per cell in the above analysis (Fig. 4.4) are not certain, since the estimation of proliferation by ^{3}H-thymidine uptake per cell over 1 hour is only a rough indicator of population dynamics. In order to examine more closely the proliferative phase in cycling cells, the frequency distribution of cells in the cell cycle was determined by PI staining and flow cytometric analysis. Figure 4.5 shows the plotted histograms of DNA content (2N in G_0/G_1 phase, 2N to 4N in S-phase and 4N in G_2/M phase) versus cell number from each of the 12 populations (control and mdx; untreated and T3-treated; and low, high and mixed cells). The proportion of cell populations in G_0/G_1, S, and G_2/M phases are indicated, as calculated by the algorithm. The proportions of cells in each phase were converted to frequencies and were used in a Chi-squared statistical comparison of populations by cell type (differences down the columns of Figure 4.5), by treatment group (differences across the rows of Figure 4.5) or by phase (testing G_0/G_1, S, and G_2/M phases separately). The separate comparisons allowed for the origin of the significant differences in Chi-squared to be determined.

In comparing distributions within each cell type (columns), there were significant differences between treatment distributions only in the low cell category (Chi-squared = 34.9, p<0.001, df=6), most of which originated in the proportions in G_0/G_1 (partitioned Chi-squared =17, or approximately 50%), with smaller contributions from changes in the distribution in S-phase (partitioned Chi-squared = 9.5, or approximately 27%).

The comparison between cell types for each treatment group (rows) showed significant differences between the frequency distribution of cell type populations for untreated controls (Chi-

squared = 14.9, p=0.005, df=4), T3-treated controls (Chi-squared = 9.3, p=0.05, df=4) and untreated mdx cells (Chi-squared = 10.4, p=0.03, df=4). Again the G_0/G_1 phase contributed significantly to the differences (20-30% of Chi-squared), with S-phase contributing in control untreated and T3-treated groups (50% and 55% of Chi-squared respectively). The G_2/M phase contributed 50% of Chi-squared changes from expected frequencies only in untreated mdx cells.

In comparing within phases as a confirmation of the comparisons by cell type or treatment, Chi-squared tests were significant only in G_0/G_1 phase (Chi-squared = 15.6, p=0.02, df=6), with contributions by untreated low cells (35% of Chi-squared) and T3-treated high cells (25% of Chi-squared).

Therefore, the three Chi-squared partitioning studies (of the same data) suggest that there are consistent differences in how the different populations cycle. Those differences originate from G_0/G_1 in three categories: a) in untreated low cells, with more mdx low cells in G_0/G_1 than control low cells, b) in mdx T3-treated high cells, with fewer in G_0/G_1 than mdx low cells (untreated and T3-treated) and c) in control T3-treated high cells, with more in G_0/G_1 than in control low cells (untreated and T3-treated). S-phase contributed to significant changes in Chi-squared in control untreated low cells (more in S-phase than in mdx untreated or T3-treated low cells) and in mdx T3-treated low populations (fewer in S-phase than in mdx untreated low cells).

Note that data reported in Figures 4.4 and 4.5 are from one large experiment. One plate per group was used to estimate proliferative populations by recording radioisotope uptake per cell, while 2 other plates per group were used to study cell cycle phase distributions by PI staining and flow cytometry.

4.3 Discussion

The results of the these experiments show that control and mdx dystrophic muscle cells demonstrate different changes in proliferation and cell cycling when treated with T3. Those differences are also specific to certain cell types (myoblasts, fibroblasts, or mixed myoblast and fibroblast

populations). There were significant differences between treatment groups, cell types and strains in G_0/G_1 and S as analyzed by flow cytometry and PI staining. The results also show a differential response to T3 between control and mdx myoblasts (low cells stained by anti-skeletal muscle myosin) by significant interactions between T3 treatment, cell type and strain. Results thus confirm and extend earlier work *in vivo* (chapter 3 of this thesis) on the effects of hyperthyroidism and hypothyroidism on muscle regeneration (McIntosh et al., 1994; McIntosh and Anderson, 1995). The results suggest that the regenerative capability of mdx myoblasts compared to that in control muscle may be a result of differential regulation of cell cycling between the two strains. That differential may involve distinct muscle regulatory gene sensitivity to T3, and endogenous production of basic fibroblast growth factor (bFGF) (Garrett and Anderson, 1995), or expression of bFGF or T3 receptors and their signal transduction pathways controlling the cell cycle.

It was previously shown that mdx muscle contains more bFGF, a potent mitogen, compared to normal mouse muscle (Anderson et al., 1991), Duchenne muscular dystrophy or other human biopsy samples (Anderson et al., 1993). Since myoblasts produce bFGF during repair (Garrett and Anderson, 1995), it is possible that the mdx myoblasts and fibroblasts may express more of that mitogen than the control myoblasts and fibroblasts *in vitro*. This would subsequently lead to a greater early proliferation or more sustained proliferation in mdx cultures. While the experiment made to time the initiation of DNA synthesis after stimulation does not suggest a difference in proliferation rate compared to control populations, the idea requires further testing. However, there were some multinucleated cells observed in those particular cultures, possibly withdrawn from the cell cycle due to the earlier arrest with colchicine, and their numbers may have differed between control and mdx cultures.

MyoD is a muscle regulatory factor (MRF) that constitutes a focal point for positive and negative control of myogenesis. MyoD expression initiates myogenic differentiation, and induces

inhibition during the G_1 phase of the cell cycle (Martelli et al., 1994). The control of myogenesis by MyoD is complex. For example, in experiments on MyoD knockout mice (Megeney et al. 1996), muscles *in vivo* showed dramatically less effective regeneration than wildtype mice, and significantly decreased proliferation by myogenic cells labelled by myogenin expression and ³H-thymidine uptake. In the *in vitro* studies, however, myogenic cell numbers were not reduced, but elevated. Those results suggested that self-renewal by early stem cells, rather than myogenic differentiation, occurs in the absence of MyoD. Growth factors may repress MyoD function by stimulating expression of very early response genes which repress MyoD transactivation (Megeney et al., 1996; Li et al., 1992b). Negative regulation of MyoD function by growth signals (such as bFGF) occurs in proliferating myoblasts, while withdrawl of exogenous growth factors triggers MyoD's action to arrest cell cycling and activate the myogenic program (Martelli et al., 1994). It is not known if control and mdx myoblasts express different levels of bFGF, or how myoblasts and fibroblasts might differ in that regard, although a report of greater sensitivity to exogenous bFGF by mdx versus control myoblast cultures (DiMario and Strohman, 1988) might be explained in part, by a differential expression of the mitogen (Garrett and Anderson, 1995). Unpublished observations (Anderson et al., 1997b, submitted), using immunocytochemistry, do show an increased expression of MyoD protein in myotubes in regenerating mdx mice. Interestingly, the same increase was far less dramatic in control regenerating muscle. Those observations would support the idea of differential regulation of MyoD expression in control and mdx muscle regeneration.

The high level of proliferation shown by untreated mdx mixed cells, in comparison to either low or high mdx cells alone, suggests that myoblasts and fibroblasts interact positively to promote mitogenesis, possibly by the addition of bFGF and/or other factors contributed by the fibroblasts or through direct cell-to-cell contact. However, mixing control myoblasts and fibroblasts in the same untreated conditions does not appear to have an additive effect on proliferation. The difference between

the two strains regarding separate versus mixed populations may also relate to differences in mitogen production, receptor expression, or interaction with MyoD and other MRFs.

Other important findings in this study confirm that sorting mixed myoblast and fibroblast cell populations according to 90° light scatter (cytoplasmic granularity) permits the distinction of low (myoblast) and high (fibroblast) light scatter populations in mdx and control cultures as reported (Yablonka-Reuveni, 1988). The sorted cells were further separated from cells with intermediate scatter which remain an uncharacterized mixed population of cells. The expression of skeletal muscle myosin in early differentiated control and mdx low cells further confirms that the low population contains a very large majority of myoblasts that are separated from a mixed population by flow cytometry, and that the population sorted as high contains a large majority of skeletal muscle myosin-negative fibroblasts.

The observed increase in ^{3}H-thymidine uptake per cell in the mdx fibroblast population after T3 treatment is puzzling, particularly since both myoblast and mixed populations of mdx cells in the same experiment showed decreased uptake per cell with T3 treatment. In the same experiment, there were significant effects on cell cycling attributable to a low frequency of mdx T3-treated fibroblasts in G_0/G_1. However, the change was small (only 15% of the total significant Chi-squared value for the differences in G_0/G_1), and the distribution was the lowest in frequency among the other fibroblast cultures. However, S-phase for fibroblasts did not contribute to significant Chi-squared changes with T3 treatment. Thus, there is a difference between S-phase estimation by PI staining and flow cytometry, and estimates of proliferation in a population based on ^{3}H-thymidine uptake per cell, even in a single experiment. The latter method estimates DNA synthesis over a one hour pulsed exposure in a population presumed to be moving through various phases of the cell cycle in a continuous sequence. The cells replicating their DNA are only observed in a very restricted window in S-phase itself. The histograms in Figure 5 show a small proportion of cells in S-phase, and ^{3}H-thymidine uptake analysis will only identify small numbers of cells

that may be either at the begining, the middle or at the end of S-phase and which cannot be distinquished from one another. Thus, in view of the flow cytometry findings, observations of increased ^{3}H-thymidine uptake per cell in mdx T3-treated fibroblasts indicate that additional experiments are needed to follow a particular phase of the cell cycle (S-phase for example) through a cycle by bromodeoxyuridine (BrdU) and PI double labelling. Those experiments would determine three aspects of a differential effect of T3 on cell cycling: a) if the cells in the ^{3}H-thymidine uptake experiments are present as a group just entering S-phase from G_0/G_1 or just about to leave S-phase and enter G_2/M, b) if that cell population is more synchronized in activity in response to T3 treatment than untreated populations and c) if that T3-treated population is synchronized more due to endogenous regulation of proliferation or myogenesis.

The interesting aspect of the uptake by mdx fibroblasts (comparison between untreated and T3-treated cells) is that fibroblasts also appear to show a differential effect of T3 treatment. That observation suggests that fibroblasts deserve renewed study for their role in the possible endocrine mediation of muscle repair processes such as remodelling of the extracellular matrix, and the dynamics of cell recruitment during wound repair. There clearly are strain-specific effects of T3 on cell cycling that differ between myoblasts and fibroblasts, and which appear to be modified by cell-to-cell interactions.

Fig. 4.1. Bivariate contour plots of forward angle scatter (cell size) data versus 90° light scatter (cytoplasmic granularity). Channel numbers are in arbitrary units. Accompanying single parameter histograms are also shown. (A) control (B) mdx. Boxes indicate gates used for sorting. Box #1: mdx high cells, Box #2: mdx low cells, Box #3: control high cells, and Box #4: control low cells.

control   mdx

cell size

cytoplasmic granularity

A   B
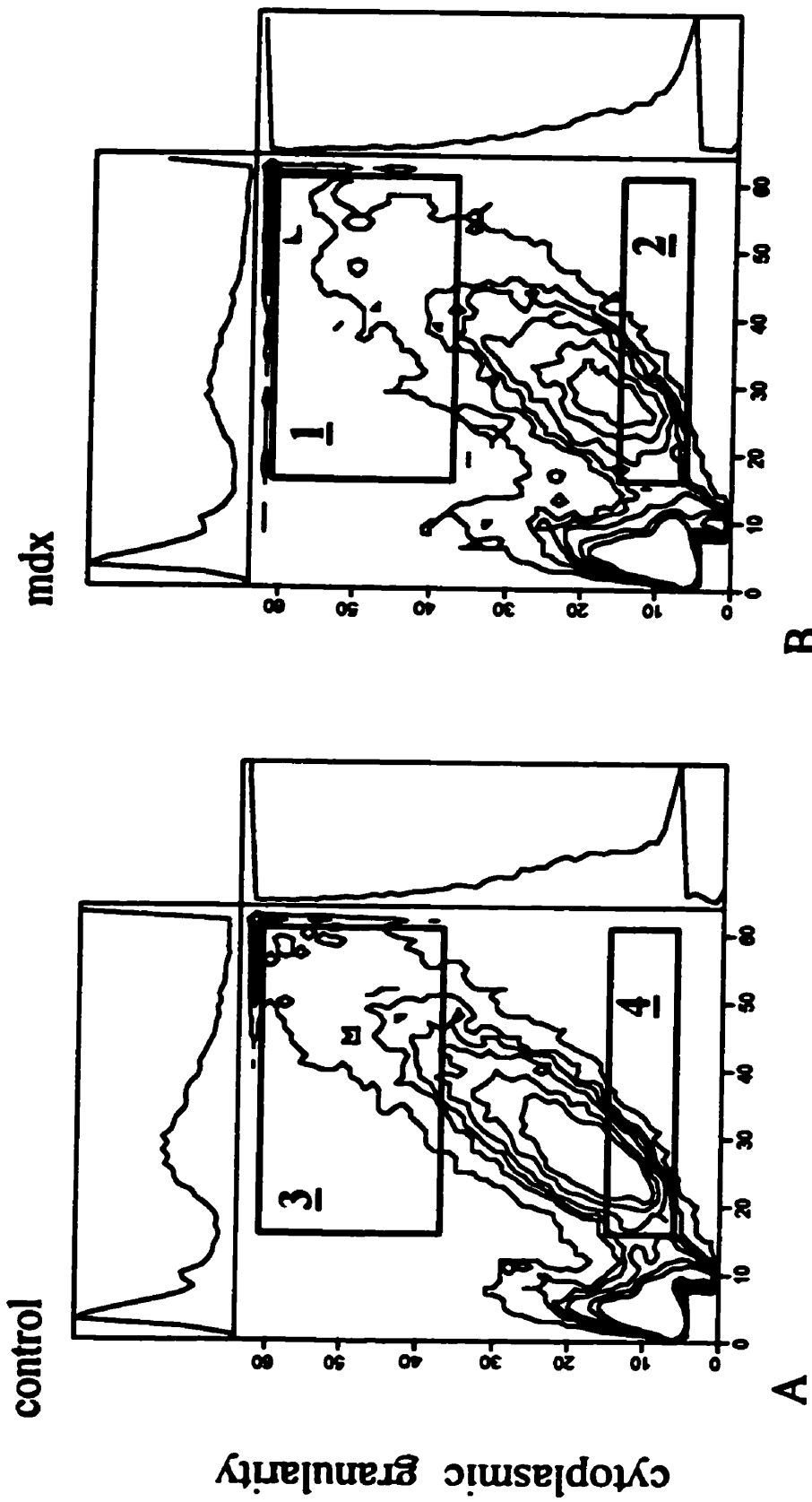
Fig. 4.2. Micrographs of immunocytochemistry for skeletal muscle myosin and bisbenzimide staining for

nuclei in sorted mdx low (A and B) and high cells (C and D). (A) Nuclear staining of a field of mdx low

cells. Note the two nuclei in the small myotube (arrowheads). (B) The same small myotube as in panel

A is positive for anti-skeletal muscle myosin immunostaining (arrow). (C) Nuclear staining of a field of

mdx high cells. (D) In the same field as panel C, the majority of cells do not show anti-skeletal muscle

myosin fluorescence. Bar=55μm, 220X.
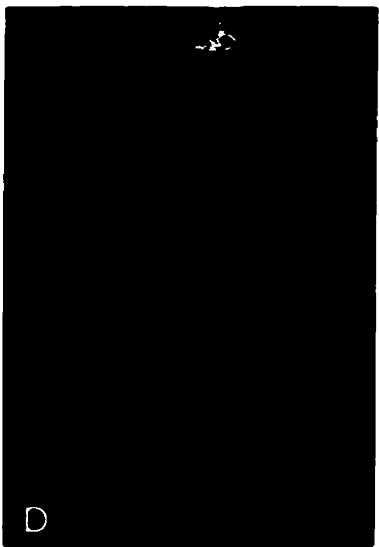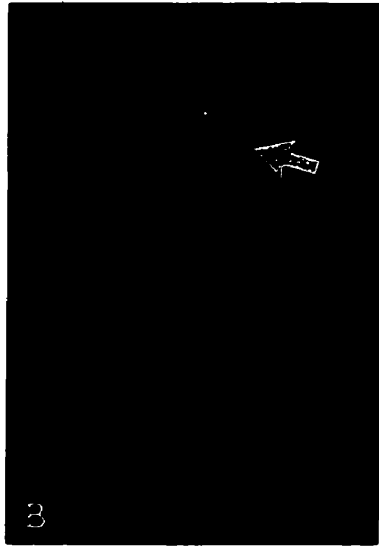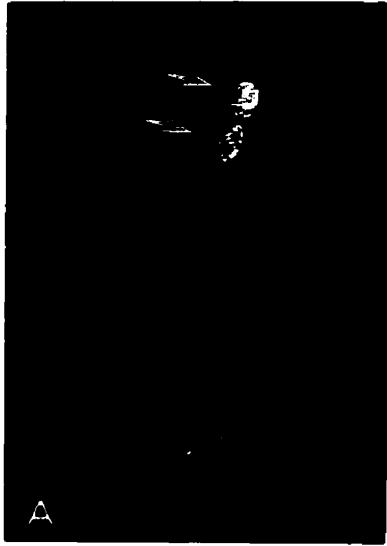
Fig. 4.3. Line graph comparing ^{3}H-thymidine uptake (nmols per cell) in control (C57, open squares) and mdx (solid diamonds) unsorted cells after stimulation out of colchicine arrest in metaphase. Values are expressed as the mean ± SE of duplicate samples. Where standard error bars are not shown they were too small to be resolved on the graph.
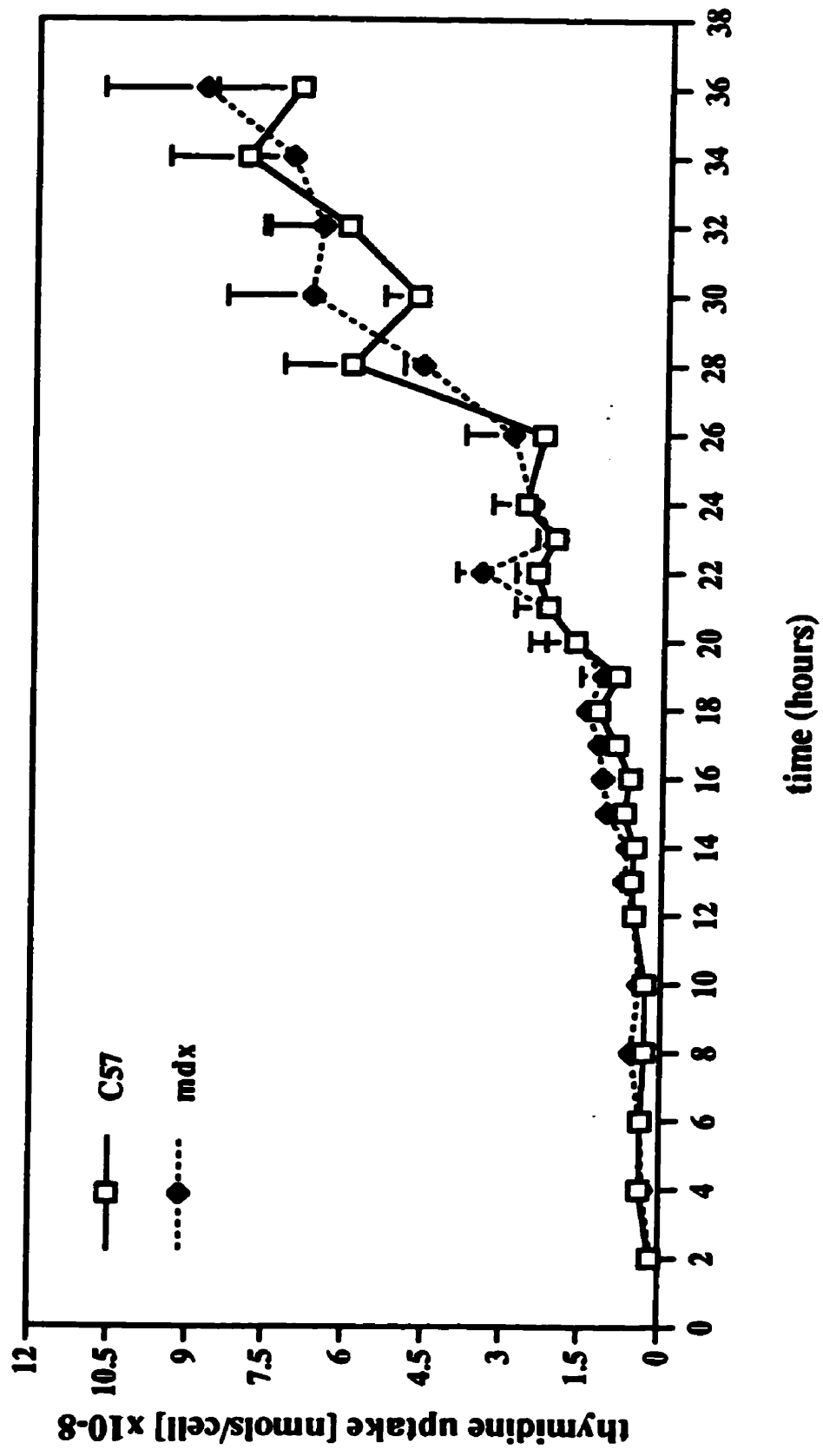
Fig. 4.4. Bar graph comparing ^{3}H-thymidine uptake (nmols per cell) in control (C57) and mdx cells grouped into low, high and remixed populations, and grown in MEM supplemented with 15% carbon-stripped HS and 4% CEE, with T3 and without T3 treatment. Bars represent duplicate DPM readings from a single sample. Values are expressed as a mean ± SE. Missing standard error bars were too small to be resolved on the graph. Comparison of strains and cell populations each showed significant differences, and each interacted with T3.

99

Fig. 4.5. Histograms of flow cytometric analysis of control and mdx low (left column), high (middle column) and mixed cells (right column) and displayed by treatment (with T3 and without T3) by propidium iodide staining of DNA. Data represent the proportion of cells in G_0/G_1 phase (first peak = 2N amount of DNA), S-phase (middle = between 2N and 4N amounts of DNA) and G_2/M phase (second peak = 4N amount of DNA). Five thousand cells were analyzed from each population. Significant differences were determined by Chi-squared. Significant differences were observed between control and mdx low cell types, particularly in G_0/G_1 and S phases affected by T3.
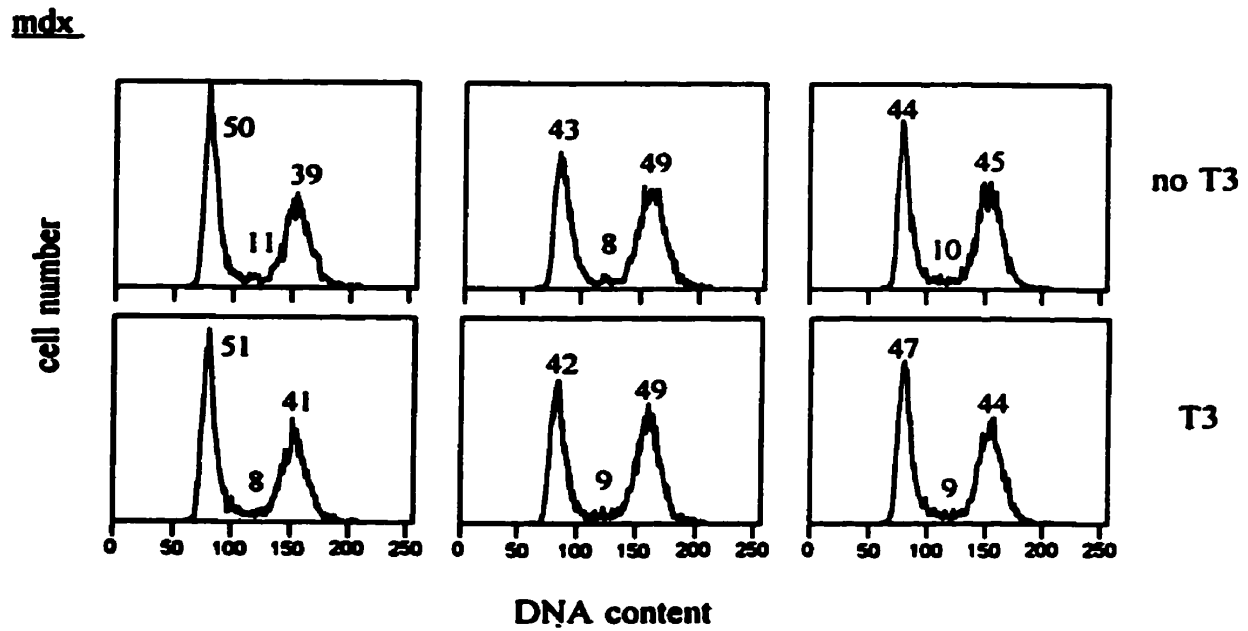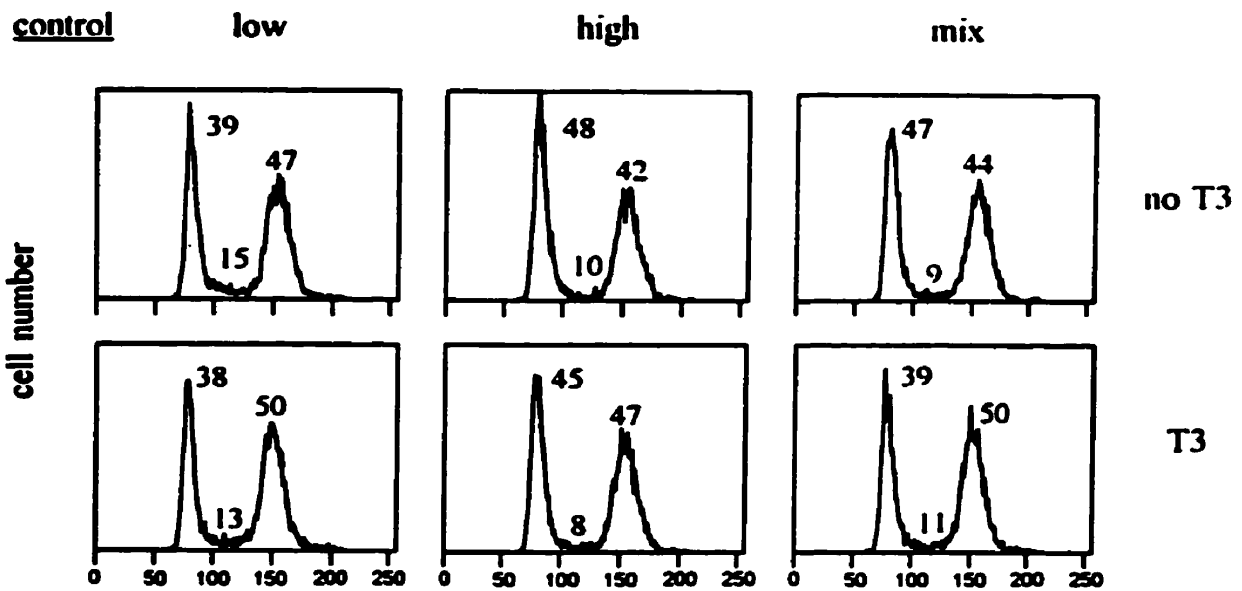
Chapter 5

The Transition into S-Phase is Affected by T3 in Control

But Not in mdx Primary Muscle Cell Cultures

5.0 Introduction

As previously discussed, excess thyroid hormone (T3) alters the proportion of slow and fast fibers in rodent skeletal muscle (Ianuzzo et al., 1977), can change myosin isoform expression (Izumo et al., 1986), and leads to precocious maturation of muscle fibers in humans (Butler-Browne et al., 1990). These and other studies have helped to define thyroid hormone's differentiative role during the development of skeletal muscle fibers. More recently, T3 was shown to interact directly with the muscle-specific regulatory factors (MRFs) MyoD and myogenin to promote terminal muscle differentiation (Carnac et al., 1992; Muscat et al., 1994) in various muscle cell lines.

Based on extracellular conditions, such as the presence of growth factors or hormones, the decision for G_0 cells in most tissues to enter the cycle is made shortly before the commitment to S-phase in the late G_1 period (reviewed in Reddy, 1994). It is the extracellular factor-dependent commitment of late G_1 cells to enter S that is the rate limiting step in determining the ability of cells to complete a cell cycle (reviewed in Reddy, 1994). Therefore, once cells are in S-phase they will proceed through that cycle regardless of their extracellular environment. When the cells reach the next G_0/G_1 phase, and an extracellular factor is presented (e.g., growth factor or hormone), the cells will respond either by continuing to cycle or by arresting in G_0.

Since muscle regeneration involves the formation of new fibers and their differentiation and maturation, it was our initial intent to examine the effects of T3 on muscle regeneration in control and mdx mice (Pernitsky et al., 1996; chapter three). The dystrophic mdx mouse shows X-linked dystrophin-deficient myopathy and fiber necrosis (Bulfield et al., 1984; Koenig et al., 1987). However, unlike human Duchenne muscular dystrophy (DMD), limb muscles in mdx mice can effectively regenerate and maintain function throughout the lifespan (Anderson et al., 1987; Anderson et al., 1988). After a crush injury, muscle regeneration in mdx mice is more effective than in muscle of the normal parent strain (Pernitsky

et al., 1996; McIntosh et al., 1994; McIntosh and Anderson, 1995; chapter three). *In vivo* experiments (Pernitsky et al., 1996; chapter three) showed that control muscle regeneration was altered by T3 treatment while mdx muscle regeneration was not substantially affected by T3. This was observed as fewer nuclei in new myotubes in T3-treated control muscle compared to untreated control muscle. Therefore, by comparing muscle regeneration in both strains under the influence of T3, some of the mechanism(s) underlying the very successful regeneration by mdx muscle might be determined.

Initial *in vivo* studies showed that T3 appeared to speed the transition from proliferation to fusion in control and mdx mouse myoblasts (activated satellite cells) found within muscle regenerating from crush injury. Interestingly, T3 only reduced overall repair in normal control muscle, suggesting that mdx myoblasts may have a large enough proliferative capacity (or level of activation) to prevent a T3-induced shift from proliferation to fusion (Pernitsky et al., 1996; chapter three). In agreement with the *in vivo* data, further *in vitro* studies (Pernitsky and Anderson, 1996; chapter four) demonstrated that the cycling and proliferation of control and mdx sorted myoblasts may also be differentially modulated by T3. Analysis of sorted myoblasts at one time point, revealed that in the absence of T3, fewer mdx myoblasts were in S-phase than control myoblasts. In the presence of T3, the proportion of mdx myoblasts in S-phase was reduced, while control proportions of S-phase myoblasts remained unchanged. Conversely, there were more mdx than control myoblasts in G_0/G_1 without T3. This analysis was performed using only propidium iodide (PI, a marker for DNA content) which limited our ability to follow a specific population over time. It did, however, lead us to question whether T3 affects the transition from one phase of the cell cycle to the next, particularly those involving transitions out of and into S-phase.

Questions regarding cell cycle transitions were raised during the experiments of chapter four which were carried out using myoblasts sorted from fibroblasts and maintained for long periods in

culture (up to one month). The experiments discussed in the following work addressed such questions using mass cultures that consisted of mixed muscle cells (myoblasts and some fibroblasts) which were primary isolates of muscle in order to emulate the *in vivo* condition as closely as possible.

To provide further examination of the differences between control and mdx muscle cell cycle activity, specifically the transitions out of and into S-phase following T3 treatment of cycling cells, we tested the hypothesis, as in 2.0 (C), that T3 would slow down or stop those muscle cells in S-phase from passing through the next late S - G_2/M and G_0/G_1 - early S transitions of the cell cycle. We also tested whether the passage through each transition might be differentially affected by T3 in the control and mdx muscle cell cultures, based on previous observations of differences between the two strains (Pernitsky et al., 1996; Pernitsky and Anderson, 1996; chapters three and four).

5.1 Materials and Methods

5.1.0 Animals, Cell Culture, and BrdU Labelling for Experiment #1

Young (5 to 8-week-old) control (C57BL10/ScSn) and mdx dystrophic mice (C57BL10/ScSn mdx) were used for all the experiments in this chapter. Primary muscle cells were isolated as reported in chapter four. Briefly, on day 0, two control mice were anesthetised (ethyl ether) and sacrificed by cervical dislocation according to the Canadian Council on Animal Care guidelines. Muscles were dissected from the hindlimb, forelimb, and back using aseptic technique. Tissues were further dissected to remove tendons and fat, and chopped into a sludge using a sterile razor blade. The sludge was placed into 25cm^2 (50ml) flasks (Falcon, Lincoln Park, NJ) with warm minimal essential medium (MEM) (Gibco BRL, Grand Island, NY) supplemented with 15% horse serum (HS) (Hyclone Laboratories Inc., Logan, UT) and 2% chick embryo extract (CEE (Gibco), containing < 0.3 nmols/L T3 by commercial assay) and incubated at 37°C in 5% O_2 and 95% CO_2 for 72 hours. This technique increases cell yield by maximal activation of quiescent satellite cells in non-dystrophic (control) muscle, and homogeneously activates

satellite cells in dystrophic (mdx) muscle, probably due to soluble factors released from damaged muscle (Chen and Quinn, 1992; Chen et al., 1994; Allen, personal communication).

On day 3, the flask contents were emptied into 50ml centrifuge tubes (Falcon), vortexed for 1 minute and filtered 1-2X through gauze (Nitex) to remove larger pieces of debris. Filtrates were centrifuged at 1200rpm for 10 minutes at 4°C (Heraeus Sepatech Varifuge RF, Baxter Inc., McGaw Park, IL), resuspended in MEM supplemented with 15% HS and 2% CEE, and plated onto two 100X20mm Primaria (Falcon) culture dishes containing pre-warmed MEM supplemented as above. On day 7, cells were passaged at equal density into 8 dishes and allowed to proliferate for 3 days. Although T3 was not used in this experiment, the basal medium used as a vehicle for T3 treatment in experiment #3 (consisting of MEM supplemented with carbon-stripped HS (15%)(modified after Tanswell et al., 1983) and 4% CEE (see chapter 4), was applied on day 10 for 24 hours in order to adapt the cells. On day 11, cells were fed again and after 2 hours were pulsed (in the dark) for 2, 4, or 6 hours with [1X] BrdU labelling solution (500X stock containing 5-bromo-2'-deoxyuridine and 5-fluoro-2'-deoxyuridine in a 10:1 ratio) (Amersham Life Science Inc., Arlington Heights, IL) to label cells in S-phase. Two plates were not exposed to a BrdU pulse and served as the no-BrdU control.

5.1.1 Preparation of Cells for Anti-BrdU-FITC Antibody and PI Staining

After 2, 4, or 6 hours, cells were trypsinized (0.05% trypsin-EDTA, Gibco, 1-3mins) from culture dishes and enzyme action was quenched with equal volumes of HS. Cells were centrifuged at 1200rpm for 10 minutes at 4°C, resuspended in 3ml 0.05M PBS, counted, centrifuged at 1200rpm for 7 minutes at 4°C and resuspended in 500µL of sterile 0.9% NaCl on ice. Cells from each group were then added to 5mls of ice-cold 70% ethanol while vortexing and incubated on ice for 30 minutes. Cells were centrifuged at 2100rpm for 15 minutes at room temperature on a table-top centrifuge (International Equipment Co., Needham Hts., MA). The supernatant was removed and 500µL of sterile 0.9% NaCl was

added, followed by 500µL of 4M HCL/Triton X-100. The cells were incubated for 30 minutes at room temperature to produce single stranded DNA molecules. After an additional 500µL of 0.9% NaCl was added, the cells were centrifuged at 2100rpm for 7 minutes. Denaturing of the DNA was neutralized by the addition of 1.5ml of 0.1M sodium tetraborate ($Na_2B_4O_7$). Cells were centrifuged as above and rinsed with 1ml of 0.05M PBS/1.0% bovine serum albumin (BSA) (Gibco, Grand Island, NY). After resuspending the cells in 100µL of PBS/BSA, they were transfered to a 500µL microcentrifuge tube and 10µL of FITC-linked anti-BrdU antibody (Becton Dickinson Immunocytochemistry Systems, San Jose, CA) was added. The tubes were covered with foil and mixed on a bio-rotator for 1-2 hours at room temperature. The contents of the tubes were transfered back to 15ml glass tubes, backwashed with an additional 1ml of PBS/BSA and centrifuged at 2100rpm for 7 minutes. Cells were resuspended (in the dark) in 500µL of a solution containing 10µg/ml PI (Molecular Probes Inc., Eugene, OR) and 50µg/ml RNAse (ICN Biochemicals Inc., Cleaveland, OH) solution and stored in the dark at 4°C overnight.

5.1.2 Flow Cytometry Analysis

Flow cytometry analysis was performed on a Coulter Electronics Inc. (Hialeah, FL) EPICS 753 fluorescence-activated cell sorter (FACS) with laser excitation set at 488nm (500mW). Forward versus side light scatter histograms were used to gate on intact cells and eliminate debris, while peak versus integrated PI derived fluorescence signals were used for doublet discrimination gating. FITC and PI fluorescence signals were separated by a 550nm dichroic long pass filter and detected through 525BP and 630LP filters respectively. Two colour fluorescence histograms were based on 5000 (experiments #1 and #2) or 10000 cells (experiment #3) satisfying both the light scatter and doublet discrimination gating criteria. Subsequent analysis was performed using Coulter Elite workstation software, version 4.01 (Burlington, ON). Control (no-BrdU) histograms were derived from cells which had not been exposed to BrdU, but were otherwise treated the same as the test samples.

5.1.3 Animals, Cell Culture, and BrdU Labelling for Experiment #2

Primary muscle cells were isolated exactly as in experiment #1 (see section 5.1.0) and passaged once to amplify numbers. On day 4, cells were trypsinized, pelleted, resuspended in 6ml of MEM supplemented with 15% HS and 2% CEE and counted, before plating at 3 different densities. Twelve dishes were divided into 3 sets of 4 dishes. The first set of 4 dishes was plated directly from the first suspension (1ml per dish) and the remaining volume (2ml) was diluted with 4ml of MEM. The second set of dishes was plated with the diluted suspension (1ml per dish), and the remaining volume (2ml) was diluted with 4ml of MEM. This final dilution was plated (1ml per dish) on the remaining 4 dishes. Again, the basal medium for T3 treatment was used to adapt the cells. On day 10 cells were fed and after 2 hours, 2 of the 4 dishes in each set were pulsed (in the dark) for 4 hours with [1X] BrdU labelling solution. The remaining 2 dishes in each set were used as no-BrdU controls.

After 4 hours, cells were trypsinized from culture dishes, collected, washed, and prepared for BrdU/PI staining and analysis by flow cytometry exactly as in experiment #1 (see section 5.1.1).

5.1.4 Animals and Cell Culture for Experiment #3

Six mice from each of control and mdx dystrophic strains were used in the following experiment. On day 0, muscle cells were isolated as described in experiments #1 (section 5.1.0) and #2 (section 5.1.3) with the exception that 20% HS was used, in order to ensure that cells remained proliferative. As well, the cultures in experiment #3 were not passaged. On day 3, cells were plated directly onto fourteen 100X20mm Primaria dishes (1.1×10^5 cells per dish) to be used for flow cytometry analyses and six 35X10mm culture dishes (1.8×10^4 cells per dish) for analysis with immunocytochemistry (see below). Cell populations were grown for 7 days until semi-confluent in MEM supplemented with 20% HS and 2% CEE.

5.1.5 T3 Treatment and BrdU Labelling

Semi-confluent (70-80% of the surface of the dish was occupied by cells) cells were switched to MEM containing 20% carbon-stripped HS and 4% CEE, and allowed to adapt for 24 hours. Cells were fed once again with the above MEM and supplements. At this time, T3 (Sigma Chemical Co., St. Louis, MO) (10^{-9}M in 0.05M NaOH vehicle) was added to half of the dishes in each group (control and mdx), while the other half of the dishes remained untreated and received only the vehicle. Two hours later, cells were pulsed with [1X] BrdU labelling solution for 4 hours. A set of two untreated dishes from each strain did not receive BrdU and served as no-BrdU controls. After the 4 hour BrdU pulse, one set of cells that included both control and mdx, untreated and T3-treated cells was prepared immediately (4 hour time interval) for BrdU/PI staining and analysis by flow cytometry as above. The remaining cells were refed with MEM supplemented with 20% carbon-stripped HS and 4% CEE but without T3, and sets of dishes were sampled after an additional 6 (10 hour time interval) and 10 additional hours (20 hour time interval), and prepared for BrdU/PI staining and analysis by flow cytometry.

5.1.6 Immunocytochemistry

To characterize the proliferating cell populations in cultures with and without T3 treatment, mdx and control cells grown on 35X10mm culture dishes were prepared for immunocytochemistry at identical time intervals as the above BrdU/PI samples. Cells were fixed in 1ml of 1.0% paraformaldehyde over ice for 15 minutes. After rinsing in 0.01M PBS, 2ml of ice cold PBS/0.1% TritonX-100 was added and the cells were incubated on ice for a further 15 minutes. Cells were rinsed 1X with cold PBS and stored at 4°C in PBS containing 0.05% sodium azide for 7 days. After a PBS wash, cells were blocked on ice for 2 hours with PBS containing 0.5%Tween and 1.0%bovine serum albumin (PBS-BSA). Cells were then incubated in 500µl of primary anti-MyoD rabbit polyclonal IgG (Santa Cruz Biotechnology, Inc., Santa Cruz, CA). Antibody was diluted 1:100 in PBS-BSA and applied overnight to cells in a dark, humidified

chamber at 4°C. Cells were rinsed for 2-3 minutes in PBS-BSA, and incubated in 500μl of secondary

anti-rabbit whole Ig, conjugated to Texas Red (from donkey). The secondary antibody was diluted 1:150

in PBS-BSA (Amersham Life Science Inc., Mississauga, ON.) and applied to cells for 2 hours at 4°C in

a dark, humidified chamber, followed by a 1 hour incubation at room temperature. Cells were rinsed 2X

with PBS-BSA. Glass coverslips were mounted onto the dishes with Immumount (Lipshaw Immunon,

Pittsburgh, PA). Cells were observed and photographed with Kodak Ektachrome Colour film (ASA

1600) on a BHT-2 Olympus photomicroscope equipped with epifluorescence and phase contrast optics,

and copied onto black and white film for photoreproduction.

Counts of MyoD-positive and MyoD-negative cells were made by scanning multiple fields across

coverslips. Phase contrast and then fluorescence optics were used to count total cells and MyoD-positive

cells, respectively while distinguishing between MyoD-positive nuclei that were elongated or round.

5.1.7 Analysis of BrdU-FITC/PI Histograms and Statistics

BrdU/PI histograms were converted to contour plots (Coulter Electronics of Canada, Elite 4.01

Analysis Software, Burlington, ON). Each plot was divided into 4 rectangles to delineate the 4 cell cycle

phases: G_0/G_1, early S, late S, and G_2/M as indicated in Figures 5.1 - 5.3. The same rectangle coordinates

were superimposed on each plot for experiment #3, except for the no-BrdU control. In the no-BrdU

control, overall fluorescence was lower and the rectangle coordinates were adjusted to accomodate the

shift. The proportion of cells plotted in each rectangle was determined by the Elite 4.01 Analysis Software

Program. Chi-squared contingency tests for 2 independent variables were used to analyze the frequency

distributions of cells in different phases of the cell cycle, comparing the two strains, and the effects of T3

treatment over time (Stats Plus, Human Systems Dynamics, Northridge, CA). Histograms of the BrdU/PI

fluorescence in experiments #1 and #2 were converted to contour plots and analyzed for the effects on

cell cycle activity of BrdU pulse time and cell confluence respectively, prior to the start of experiment #3.

A probability of p<0.05 was used to accept a difference as significant.

5.2 Contributions by Others

During the course of these experiments, Dr. E.S. Rector kindly performed the operations required to collect flow cytometric data and transferred the data to disk for further analysis and graphical representation.

5.3 Results

5.3.0 Experiment #1 - Selection of an Appropriate BrdU-Pulse Time

This experiment was designed to determine the length of the BrdU labelling pulse that would maximize S-phase cell labelling. We chose to test 3 different pulse times, 2, 4, and 6 hours and expected increases in the number of labelled S-phase cells with increasing pulse time. However, there was very little S-phase cell labelling and little change with increasing pulse time, possibly due to the inactive state of the cultures which were grown to a relatively high density, comparable to cells in experiment #2 (see below). Figure 5.1 A-D shows contour plots of each sample, including the no-BrdU control. The no-BrdU control allows confirmation of the specificity of labelling cells in S-phase. The S-phase percentages in the presence of BrdU were all very low (early S = 0.7-1.7% and late S = 1.5-1.9%, Fig. 5.1 B-D). However, all labelling was higher than the background delineated by the no-BrdU control (Fig. 5.1A). Approximately 90% of the cells from each sample were in the G_0/G_1 phase and 5-8% were in the G_2/M phase for each pulse time. At the time of sampling, the cultures had similar cell densities as follows: no-BrdU control, 5.4×10^4 cells/cm^2; 2 hour pulse, 5.9×10^4 cells/cm^2; 4 hour pulse, 5.2×10^4 cells/cm^2; and 6 hour pulse, 5.1×10^4 cells/cm^2. Since the use of pulse times from 2-6 hours did not significantly affect S-phase labelling, a mid-range pulse of 4 hours duration was used for the following experiments to ensure sufficient S-phase cell labelling with a relatively short pulse (< 17% of the total cell cycle time).

5.3.1 Experiment #2 - Increased Cell Density Decreases Cell Cycle Activity

To determine an optimal cell density in which treatment-induced changes in activity in all 4 phases of the cell cycle might be observed, cells were cultured and grown to different final densities as follows: confluent cells, 7.2×10^4 cells/cm^2; first dilution, 3.6×10^4 cells/cm^2; and second dilution, 1.1×10^4 cells/cm^2. Figure 5.2 A-F shows contour plots of each sample (including no-BrdU controls), after a 4 hour BrdU pulse. Panels A,C, and E show the no-BrdU controls. The background level of FITC in cells was 0.3-1.7% in early S, and 0.1-2.1% in late S. Panel B shows that at high density (confluent), only 2.2% and 2.2% of cells were in early and late S phase respectively, while 91.5% of the cells were in G_0/G_1 and 4.1% were in G_2/M. At a moderate density (1st dilution, panel D), there was a change in cell cycling activity. Compared to confluent cultures, more cells in the first dilution cultures were in early (4.2%) and late (7.7%) S-phase, and 79.0% and 9.1% of the cells were in G_0/G_1 and G_2/M respectively. Finally, at the lowest density (2nd dilution, panel F), there was a further dramatic change in cell cycling activity, with 7.4% and 13.9% of the cells in early and late S-phase respectively, and 55.8% in G_0/G_1 and 13.9% of the cells in G_2/M. Therefore, at the lowest cell density (2nd dilution), the highest proportions of cells were distibuted into early and late S-phase compared to the confluent and 1st dilution cultures, and lower proportions were found in the G_0/G_1 and G_2/M phases of the cell cycle.

The proportions of cell populations in each phase of the cell cycle (frequency data) were analyzed (Chi-square statistics) to determine differences among populations based on cell density. There were significant differences among distributions found in the cultures of different densities (Chi-square = 176.6, P<0.001, df = 6). The differences originated in the smaller proportion of cells in late S and G_2/M in confluent cultures than in the 2nd dilution cultures (partitioned Chi-square = 41.2 and 74.1 respectively). This was also reflected in the significant decrease in the proportion of cells in G_0/G_1 (partitioned Chi-squared = 25.3) in the shift from confluent cultures to 2nd dilution cultures. Together these changes

contributed to 80% of the total value of Chi-square.

Since changes in late S - G_2/M and G_0/G_1 were resolved in this experiment, and cells were most optimally spread throughout the cell cycle in cultures at the lowest density (2nd dilution), experiment #3 was conducted with cells at a density similar to that reached by 2nd dilution cultures.

5.3.2 Experiment #3 - Cell Cycle Activity in Control and mdx Muscle Cells

Strain Effects

Chi-square values were significantly different (P<0.001) for comparisons among cell cycle phases at all time points examined (4, 10 and 20 hours) (Chi-square = 38.0, 65.0, and 172.2). Only significant changes are reported below. Specifically, untreated control cultures had more cells in G_0/G_1 at 20 hours compared to untreated mdx cells (Fig. 5.3) (partitioned Chi square = 20.2). Chi-square values were also different for the comparisons among cell cycle phases and between strains over time (Chi-square = 131.4 and 388.2 respectively). Over time, the proportion of untreated mdx cells in G_0/G_1 had decreased by 20 hours (partitioned Chi-square = 39.6).

Untreated mdx cultures had more cells in early S-phase compared with untreated control cultures at 4, 10 and 20 hours (partitioned Chi-square = 3.8, 13.8, and 38.0 respectively). Examined over time, untreated cells from both control and mdx strains showed greater proportions in early S-phase at 20 hours than at 4 hours. These results can be observed in Figure 5.3 and the line graph in Figure 5.4A shows early S-phase specific differences clearly.

Untreated mdx cultures also had more cells in late S-phase at 4 hours (partitioned Chi-square = 7.2) and 10 hours (partitioned Chi-square = 10.1) compared to untreated control cells at 4 and 10 hours (Figs. 5.3 and 5.4B).

Untreated mdx cultures had fewer cells in G_2/M at all time points examined (partitioned Chi-square = 6.1, 6.5, and 27.6 respectively) compared to untreated control cells. Over time, the proportion

of untreated control and mdx cells in G_2/M decreased by 20 hours (partitioned Chi-square = 15.3).

In summary, mdx cultures had significantly fewer cells in G_0/G_1 at 20 hours and more cells in early and late S-phase at all time points compared with control cultures. Only mdx cells showed changes in proportions of cells in G_0/G_1 over time, while both control and mdx cells showed changes in proportions of cells in G_2/M over time.

T3 Treatment Effects

In comparisons of T3-treated control and mdx cultures over time, Chi-square values were significant for the comparisons among cell cycle phases and between strains (Chi-square = 265.1 and 242.0 respectively). Again, only significant changes are reported below. The proportion of cells in early S-phase increased between 4 and 20 hours in both T3-treated control and mdx cultures (partitioned Chi-square = 174.0 and 145.3 respectively). At the 20 hour time point, the proportion of control cells in early S-phase increased with T3 treatment compared with untreated control cells (Figs. 5.3 and 5.4A). Finally, T3-treated control cultures showed a decrease in cell proportions in G_2/M between 4 and 20 hours (partitioned Chi-square = 24.5). In summary, only control cells in early S-phase and G_2/M appeared to be affected by T3 treatment.

5.3.3 Immunocytochemistry

Immunostaining for nuclear MyoD protein was applied to determine the myogenic character of the control and mdx cultures in experiment #3. Three main cell types were observed in all cultures. These three types of cells were found in mostly homogeneous colonies and contained small nuclei. A fourth cell type, rarely observed, was large and flat with a large round nucleus, and was characteristic of fibroblast or endothelial-like cells. Only nuclei in smaller cells were stained positive for MyoD protein.

Two types of colonies were observed based on MyoD staining alone: MyoD-positive cells that had either elongated or round nuclei (Fig. 5.5 A-D), and MyoD-negative cells that had only round nuclei

(Fig.5.5 E,F). Cells with elongated nuclei were found in mixed colonies of cells, where cells were present with both round and elongated nuclei that were 90-100% positive for MyoD. Cells with round nuclei that were observed in mixed colonies were also mostly positive (80-100%) for MyoD. For example, in the untreated control culture at 4 hours, there were 47 MyoD-positive cells counted out of 47 cells with elongated nuclei, and 39 MyoD-positive cells out of 40 cells with round nuclei. By contrast, the colonies that contained only cells with round nuclei were virtually unstained for MyoD (0-1% positive, Fig.5.5 E,F).

Therefore, according to distributions of MyoD staining, and nuclear shape, MyoD-positive and negative cells were likely differentiated and uncommitted myoblasts respectively. The differentiated and undifferentiated myoblasts were growing in separate colonies. Alternatively, 2 different types of cells could be present in these primary cultures (e.g. myoblast or fibroblast). However, since MyoD-positive staining was present in cells with elongated or round nuclei in the same colony and MyoD-negative cells with the same morphology were nearly always in homogeneous colonies, the MyoD-positive and negative cells were probably both myogenic cells observed at different stages of differentiation.

These cells were identified to quantify differences between cultures, based on the shape of their nuclei and MyoD staining. Cells with nuclei that were MyoD positive and elongated; MyoD positive and round; and MyoD negative and round were counted and expressed as a proportion of total cells counted. Table 5.1 shows the calculated proportions of those three groups of cells in each culture over time.

In control cultures, the proportions of differentiated myogenic cells, i.e., cells with MyoD-positive/elongated nuclei, decreased during the 20 hours in culture. The decrease in proportions of differentiated myogenic cells (MyoD-positive/elongated) was larger in T3-treated control cultures compared to untreated control cultures, since there was a large proportionate increase in cells with MyoD-negative/round nuclei and no change in proportions of cells with MyoD-positive/round nuclei.

Untreated mdx cultures had similar proportionate decreases in cells with MyoD-positive/elongated nuclei compared to untreated control cultures. In contrast to T3-treated control cultures, mdx cells grown with T3 maintained the same proportions of both differentiated cells with MyoD-positive/elongated nuclei and non-differentiated cells with MyoD-negative/round nuclei.

These tabulations confirm that T3 treatment affects differentiation of control muscle cells, but does not change the differentiation sequence or timing of mdx muscle cells in culture. The data are consistent with flow cytometry analysis of the parallel cultures in which only control cells in early S-phase and G_2/M were affected by T3 treatment.

5.4 Discussion

The present experiments examined cell cycle activity in control and mdx primary muscle cell cultures. The incorporation of BrdU into nuclear DNA of cycling muscle cells and double staining those cells with anti-BrdU FITC and PI permitted the separation and analysis of distinct populations of cells at four phases of the cell cycle (G_0/G_1, early S, late S, and G_2/M). The results indicate that there were significant differences between control and mdx muscle cells in their progression through the cell cycle over a 20 hour time period and in their response to T3. The differences were particularly evident by 20 hours in culture, when there were significantly fewer mdx than control cells in G_0/G_1, and a concommitantly larger proportion of mdx cells in early S and late S phases at that time. Therefore, under the influence of T3, mdx cultures continued to cycle regardless of commitment to MyoD expression, while control cultures showed a larger tendency to partition into either cycling or differentiating MyoD-expressing muscle cells.

At 4 hours, control and mdx cultures had approximately equal proportions of cells in G_0/G_1, while mdx cultures had a somewhat larger proportion of cells in early and late S phases. The data are consistent with the possibility that the cycling rate of mdx muscle cells may be faster than that of control

muscle cells: most of the mdx cells in S-phase at 4 hours had reached the next early and late S phases by 20 hours. By comparison, a large proportion of control muscle cells still resided in G_0/G_1 and G_2/M at 20 hours, although some did progress to S-phase since the total S-phase population had doubled by 20 hours.

These data are in agreement with an earlier *in vivo* study of satellite cell proliferation using autoradiography (Anderson et al., 1987). It is very interesting that the proportions of mdx cells in G_0/G_1 decreased over time, while the proportions of control muscle cells in the same phase remained stable. This suggests that the mdx cell population was quite homogeneous in that cells cycled at approximately the same rate, and remained proliferative over 20 hours in culture regardless of MyoD expression. It is known that very high proportions of proliferating myogenic cells are present *in vivo* in mdx regenerating muscle, where 18% of myf5-positive and 30% of myogenin-positive mononuclear cells are proliferative (McIntosh et al., 1997, submitted). In contrast, the control population of cells may have been more heterogeneous, and may have contained cells which cycled at more variable rates. However, it is more likely, judging by the proportions of MyoD staining and the observation of nuclear and cell shape all the control cells were likely myoblasts. According to that characterization of the cultures, some of the control cells began to differentiate earlier than in mdx cultures and did not pass from G_0/G_1 into early S-phase. By comparison, the other control cells stayed proliferative and cycling. This may explain why the S-phase population doubled in control cultures and at the same time was accompanied by a large proportion of cells in G_0/G_1 at 20 hours. Therefore, the present results suggest that mdx muscle cells may cycle faster than control cells. That difference may be due in large part to a lower trend toward differentiation and arrest in mdx than control myogenic cells under the same conditions.

It is not clear why mdx primary muscle cell cultures would be more homogeneously activated to cycle or to differentiate than control primary muscle cell cultures. The procedure used to isolate the

myoblasts should produce relatively evenly activated cells (Chen and Quinn, 1992; Chen et al., 1994). However, immunocytochemistry results support the above reasoning that there may be two distinct populations based on degree of myogenic differentiation in both control and mdx muscle cell cultures. Anti-MyoD antibodies were used to identify committed myoblasts early in differentiation since MyoD is a muscle regulatory factor and its expression is known to initiate myogenic differentiation (Martelli et al., 1994; Muscat et al., 1994). MyoD is also observed in myoblasts which are proliferative *in vivo* (Garrett and Anderson, 1995; Anderson et al., 1997a, submitted) and in satellite cells on intact fiber preparations (Yablonka-Reuveni and Rivera, 1994). MyoD-positive and negative colonies were typically growing separately from one another in all the culture dishes in the present study. Some of the colonies were myoblasts that were proliferative because they had small cells with round MyoD-positive nuclei. Other colonies contained very similar small cells with rounded nuclei that did not express MyoD. It cannot be determined from these observations and data whether the MyoD-negative cells were "pre-MyoD" myoblasts, defined as myogenic cells before the expression of MyoD (Yablonka-Reuveni and Rivera, 1997 in press), or another type of cell such as fibroblasts. However, since there were colonies of cells that included both elongated (an indication that differentiation was taking place) and round nuclei (a proliferative state) that were both MyoD-positive, it is very likely that the observed cell heterogeneity in cultures of experiment #3 was largely due to variations in the state or degree of commitment and differentiation to muscle, rather than to large numbers of contaminating fibroblasts.

The two types of muscle cells, proliferative and MyoD-positive, and proliferative but MyoD-negative, were observed in both control and in mdx cultures. While, it is not possible to conclude that the MyoD-positive myoblasts and MyoD-negative cells cycled in the same manner in mdx cultures, MyoD-positive myoblasts and MyoD-negative cells were both proliferative. Anderson et al. (1991, 1993, and 1995) and DiMario and Strohman (1988) showed that mdx muscle contains larger amounts of the potent

mitogen basic fibroblast growth factor (bFGF) than control muscle. It is also known that mdx myoblasts express and synthesize bFGF (Garrett and Anderson, 1995). The high levels of mitogenic bFGF may have enabled mdx myoblasts to proliferate long enough to allow the G_0/G_1-early S-phase transition to occur. There is evidence that fibroblasts in a myoblast culture can affect cycling behavior (Pernitsky and Anderson, 1996; chapter four). MyoD-negative cells and fibroblasts might play a role in maintaining myoblast proliferation (Morin et al., 1995). In addition, two studies from our laboratory demonstrate that committed myoblasts expressing any of the four MRF genes are capable of proliferating and that in mdx muscle the proliferative proportion can reach up to 30% *in vivo* (Anderson et al., 1997a, submitted; McIntosh et al., 1997, submitted). Since the cultures were not confluent, contact inhibition of cell division (Ferrari et al., 1988) did not likely prevent a cell transition into or from S-phase. Fusion may have just begun in the larger colonies of MyoD-positive cells, since very occasional myotubes with 3 nuclei were observed.

T3 treatment only affected cycling behavior in control cultures. The effects of T3 were observed at the 20 hour time point as an increase in the proportion of cells in early S-phase with treatment. The proportions of control cells in G_2/M decreased significantly between 4 and 20 hours while the proportions of control cells in G_0/G_1 did not. Therefore, T3 treatment in control cells invoked changes across most phases of the cell cycle over time. It appears that all of the cells in the control T3-treated cultures cycled continuously, with few myoblasts entering G_0. It is well-known that T3 can initiate the myogenic program (Muscat et al., 1994) by inducing the expression of the MyoD gene and subsequently leading cells into the G_0 state (Martelli et al., 1994). Indeed, the increase in cell cycle activity with T3 treatment is difficult to explain, since the expectation was a decrease in cycling activity. As stated earlier, fibroblast cell cycling changes with T3 and can affect cycling behavior in mixed cultures (Pernitsky and Anderson, 1996; chapter four), but the proportion of fibroblasts in the primary cultures was low. It is not known if

fibroblasts could have altered or contributed to the cycling behavior of the control primary myoblasts under the T3 treatment conditions used in this study. However, while a subset of control myoblasts, just prior to or beginning to express MyoD, were sensitive to T3, it is clear that T3 had no direct effect on the cycling behavior of mdx muscle cells.

In summary, cycling control untreated primary muscle cell cultures behaved less uniformly or synchronously than mdx untreated primary muscle cell cultures as suggested earlier (Pernitsky and Anderson, 1996; chapter four). T3 treatment altered the cycling of control cells, and resulted in changes in the proportions of cells in all 4 phases of the cell cycle over time. Ultimately that produced an increased distribution of cells in S-phase and decreased the distribution in G_2/M. In our earlier *in vivo* studies of muscle regeneration 4 days after a crush injury, T3 treatment reduced the proliferation of myoblasts in control muscle. That shift resulted in precocious myoblast differentiation and decreased muscle regeneration (smaller myotubes with few nuclei). The present *in vitro* results suggest an additional short term effect of T3 to increase proliferation in undifferentiated pre-MyoD cells, at least for 1 further cycle over the 20 hours after T3 treatment. That additional effect may only occur *in vitro* or may only be observable with detailed flow cytometric analysis. The high proportions of untreated mdx cells in early and late S phases support the idea that mdx muscle has a large number of activated and/or proliferating myoblasts when challenged to regenerate after an imposed injury *in vivo*. Clearly, there were strain-specific effects of T3 on cell cycling, but T3 did not slow down or stop control or mdx muscle cells from passing through the late $S-G_2/M$ or G_0/G_1-early S transitions of the cell cycle.

Table 5.1: Proportions of cells positive and negative for MyoD in control and mdx cultures with and without T3 treatment.

strain and treatment	time(hrs)	MyoD+ and elongated	MyoD+ and round	MyoD- and round	total cells
control noT3	4hr	0.32	0.26	0.42	149
	10hr	0.2	0.14	0.65	96
	20hr	0.17	0.04	0.76	262
control T3	4hr	0.61	0.11	0.28	215
	10hr	0.16	0.13	0.67	290
	20hr	0.12	0.13	0.75	271
mdx noT3	4hr	0.56	0.18	0.21	206
	10hr	0.54	0.18	0.29	330
	20hr	0.21	0.08	0.72	274
mdx T3	4hr	0.42	0.08	0.51	229
	10hr	0.42	0.07	0.5	177
	20hr	0.36	0.11	0.53	412

Note: Where the total of 3 proportions does not total 1.0 (across the columns), there were a small number of cells with elongate or round nuclei that were not MyoD positive (first 2 columns) or a small number of round cells that were MyoD positive (third column).

Fig.5.1. Contour plots of flow cytometric analysis of primary control muscle cells pulsed with BrdU labelling solution for 2, 4, and 6 hours (panels B, C, and D respectively). Panel A shows the no-BrdU control. Data represent the proportions of cells in the 4 phases of the cell cycle as labelled in Panel A (G_0/G_1, early S, late S, and G_2/M). Five thousand cells were analyzed from each population.

control cells

FITC fluorescence (S-phase)

PI fluorescence (DNA content)
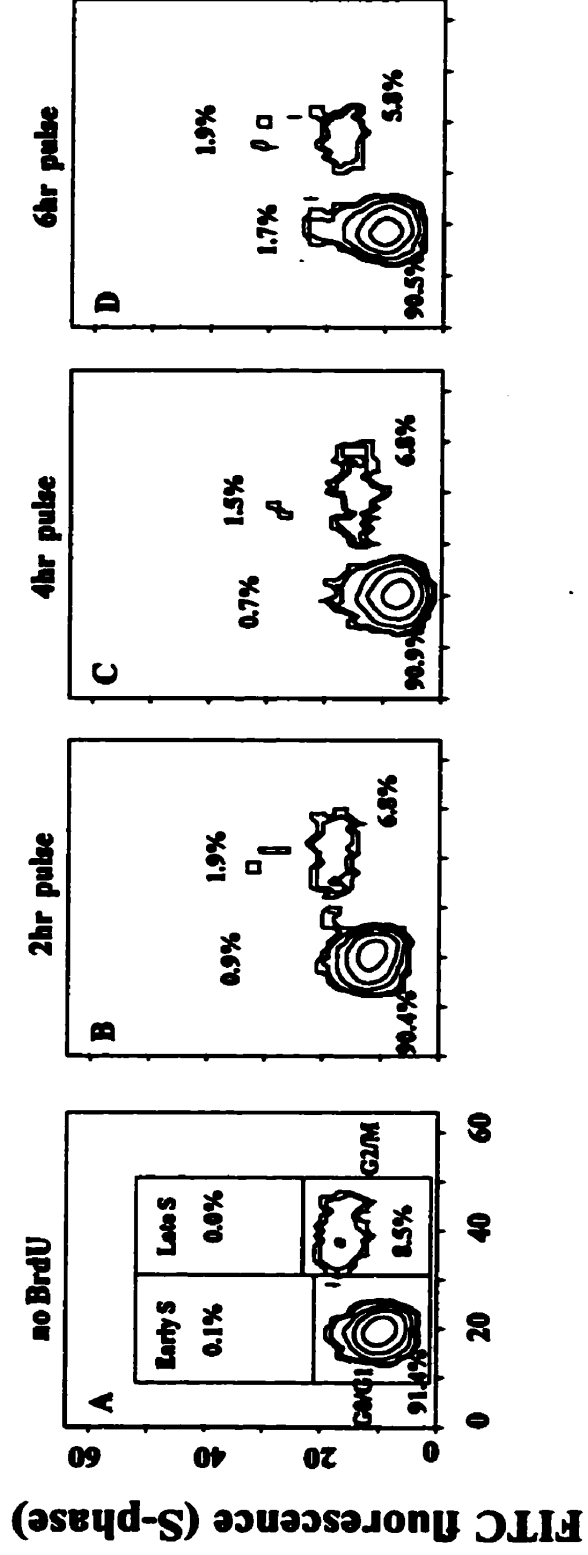
Fig. 5.2. Contour plots of flow cytometric analysis of primary mdx muscle cells pulsed with BrdU labelling

solution for 4 hours. Panels B, D, and F show cell cycle dynamics in a confluent culture, a moderate

density culture, and a low density culture respectively. Panels A, C, and E show the no-BrdU controls.

Data represent the proportions of cells in the four phases of the cell cycle as labelled in Panel A (G_0/G_1,

early S, late S, and G_2/M). Five thousand cells were analyzed from each population. Significant

differences were determined by Chi-square. Significant differences were observed in the low density

cultures, showing an increase in the proportions of cells in the early and late S phases.

mdx cells

FITC fluorescence (S-phase)

PI fluorescence (DNA content)

125
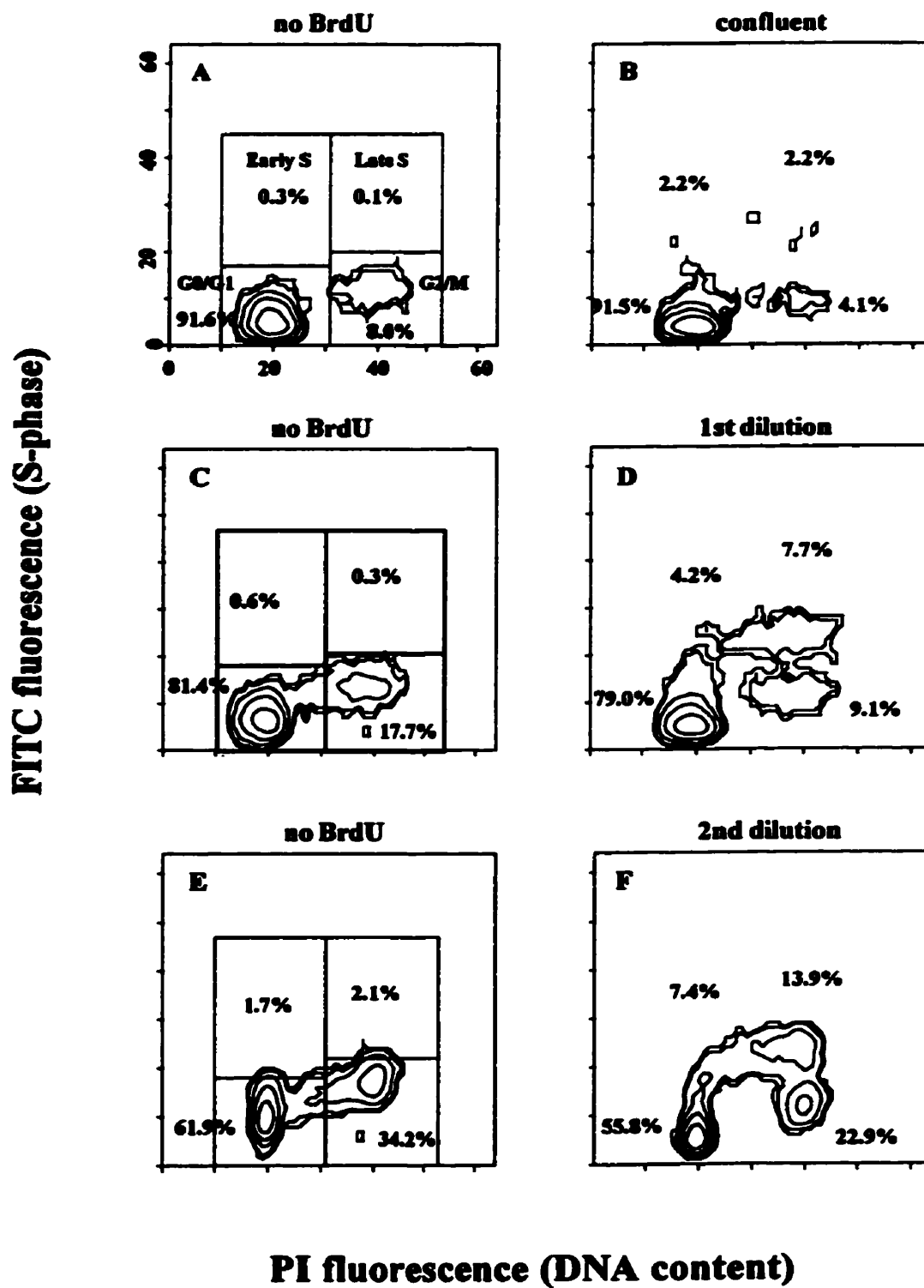
Fig.5.3. Contour plots of flow cytometric analysis of primary control and mdx muscle cells with and without T3 (for 6 hours), sampled after a 4 hour pulse with BrdU labelling solution (4 hour column). After the BrdU labelling solution and T3 were removed, additional samples were taken after 6 and 10 hours had passed (10 and 20 hour columns respectively). Data represent the proportions of cells in the 4 phases of the cell cycle as labelled in the first panel (G_0/G_1, early S, late S, and G_2/M). Ten thousand cells were analyzed from each population. Significant differences (Chi-square statistics) were observed between untreated control and untreated mdx cultures in early S-phase over all time points and in G_0/G_1 at 20 hours. T3 treatment increased cell cycling, but only in control cultures.

FITC fluorescence (S-phase)

FITC fluorescence (S-phase)

no BrdU

Early S 0.1%	Late S 0.1%
53.0%	46.7%
G0/G1	G2/M

no T3/4hr

3.7% 9.2%

51.1% 35.9%

no T3/10hr

12.1% 9.9%

30.6% 27.4%

no T3/20hr

17.7% 14.0%

43.0% 24.4%

T3/4hr

4.3% 11.5%

50.2% 33.9%

T3/10hr

16.0% 15.4%

43.5% 25.0%

T3/20hr

25.5% 20.7%

35.1% 18.7%

mdx

noT3/4hr

6.0% 14.2%

50.4% 29.3%

noT3/10hr

18.7% 13.0%

47.1% 21.2%

noT3/20hr

36.4% 22.3%

29.3% 12.0%

T3/4hr

6.3% 14.0%

52.6% 27.1%

T3/10hr

20.9% 16.1%

42.9% 20.1%

T3/20hr

32.7% 19.6%

33.1% 14.6%

PI fluorescence (DNA content)

Fig.5.4 Line graphs representing the changes in proportions of control and mdx early (A) and late (B)

S-phase cells (untreated and T3-treated) over time. Time 0 represents the time when the cells were pulsed

with BrdU. At time 4 the BrdU was removed and cells were sampled. Additional samples were taken at

10 and 20 hours after the initiation of the BrdU pulse.
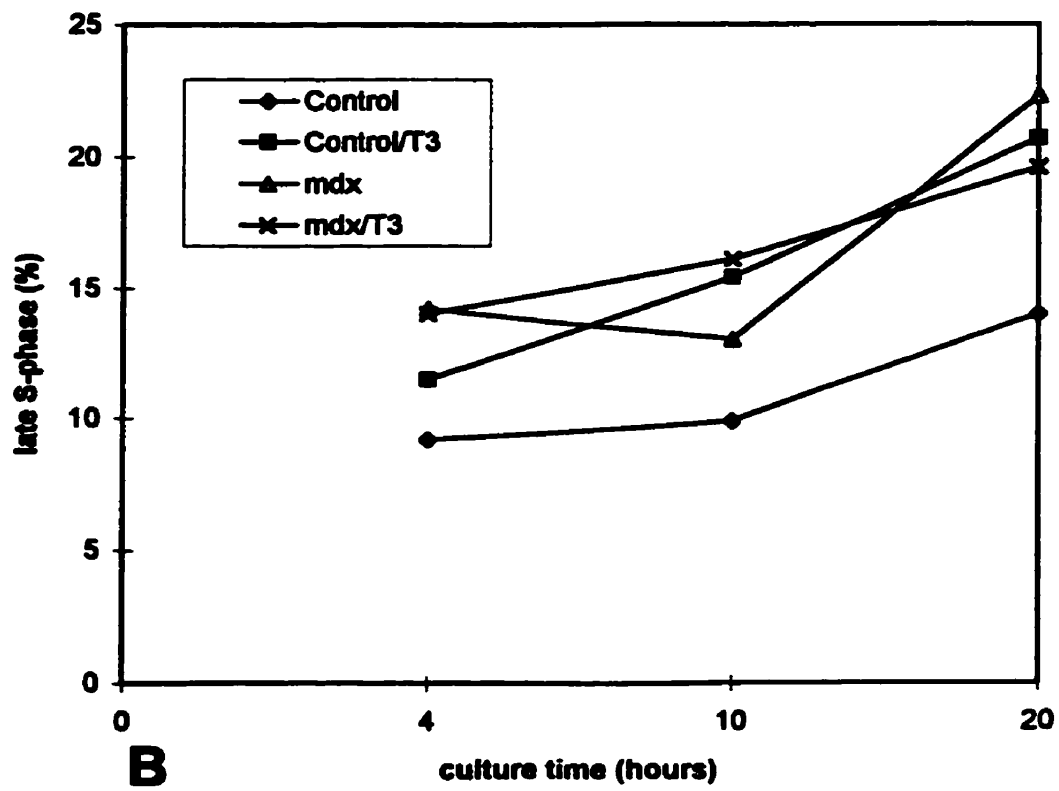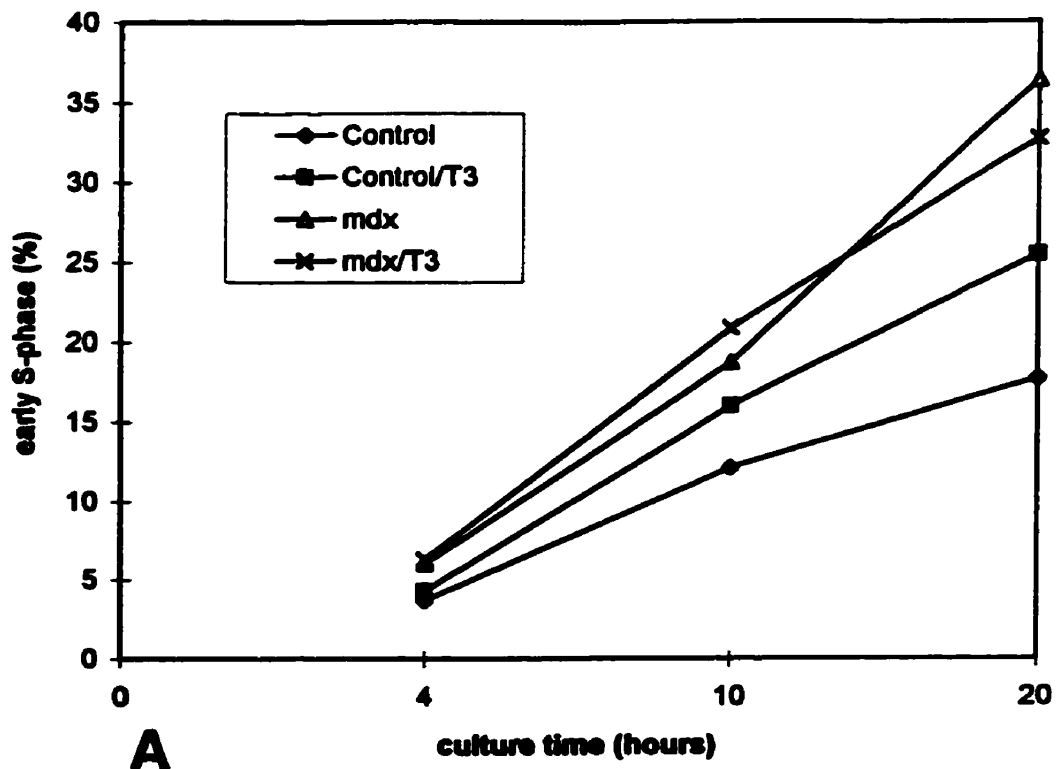
Fig.5.5 Micrographs of immunocytochemistry for the muscle regulatory factor MyoD. Panels A, C, and E are phase contrast pictures of the fluorescent and non-fluorescent cells in Panels B, D, and F respectively. (A and B) show cells with nuclei that were MyoD-positive and elongated. (C and D) show cells with MyoD-positive nuclei that were both elongated and round. (E and F) show cells with nuclei that were all round but MyoD-negative. These colonies were observed in both control and mdx muscle cell cultures. Bar=30μm, 342X.
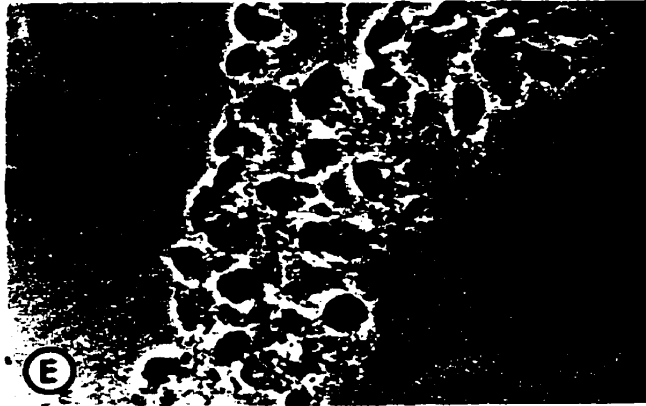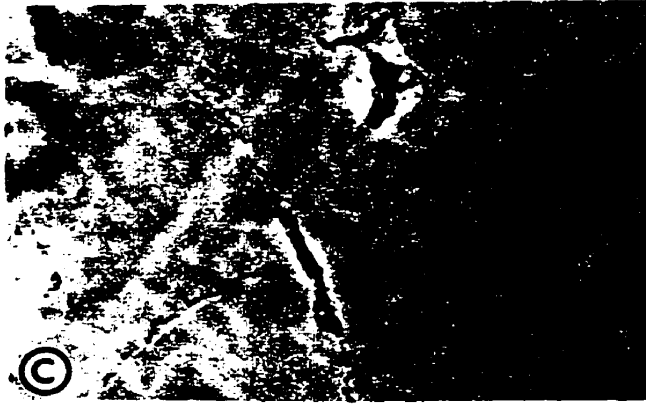
Chapter 6 - General Discussion

The experiments compiled in this thesis were undertaken to gain a better understanding of proliferation and differentiation during muscle regeneration in control and mdx mice. Previous studies in our laboratory (Anderson et al., 1994a; McIntosh et al., 1994; McIntosh and Anderson, 1995) revealed that normal TH levels played an important role during muscle regeneration. We have also demonstrated that alteration of TH levels (hyperthyroidism or hypothyroidism) can affect the regenerative process. Therefore, T3 was used to alter the muscle regeneration process during the course of the current studies, and that treatment became a valuable tool for helping us to uncover differences between control and mdx muscle regeneration both *in vivo* and *in vitro*.

Chapter three describes *in vivo* experiments and data demonstrating, for the first time, that mdx muscle maintains a larger regenerative capacity than control muscle under hyperthyroid conditions. It was shown that, not only was regeneration different in control and mdx muscle, but that T3 differentially affected control and mdx muscle repair. These important findings lead us to ascertain what might be different between control and mdx myoblasts, i.e. at the mononuclear cell level, that might be observed as their differential response to T3.

It was postulated at the end of chapter three, that differences may originate early in muscle regulatory gene expression (e.g., MyoD and Myf-5) in control and mdx myoblasts. Further work on the same *in vivo* muscles used in chapter three, showed the anticipated findings that MyoD immunostaining of mononuclear cell nuclei (myoblasts) was observed in regenerating control muscles under hyperthyroid conditions and in myoblasts aligned prior to fusion into myotubes (Anderson et al., 1997b, submitted). However, in regenerating muscles of hyperthyroid mdx mice, both myoblast nuclei and new myotube nuclei were positive for MyoD protein (Anderson et al., 1997b, submitted). This counterpart immunocytochemistry study verified the idea that the regulation of MyoD expression can be altered by

T3, as found in other reports (Muscat et al., 1994; Carnac et al., 1992). The work also showed that MyoD expression is controlled differently in control and mdx muscle treated with T3. Bhagwati et al. (1996) addressed the importance of MyoD during muscle regeneration in the mdx mouse, and showed that MyoD was expressed in satellite cells and in small regenerating muscle fibers (myotubes) surrounding necrotic fibers. These authors hypothesized that MyoD plays a critical role in the initiation and progression of events which lead to regeneration in mature skeletal muscle (Bhagwati et al., 1996). Collaborative work with our laboratory further substantiates this hypothesis (Megeney et al., 1996; McIntosh et al., 1997, submitted). Therefore, the idea that differences between control and mdx muscle regeneration might originate in the control of MRF gene expression should be an important consideration in the design of future experiments.

To further examine myoblasts at the mononuclear cell level, the technical focus of the work turned to exploring myoblast cell cycle dynamics and proliferation in control and mdx muscle (chapter four). In order to study the dynamics of the cell cycle with and without T3, it was decided that we would use a tissue culture or *in vitro* environment. Myoblasts and fibroblasts were sorted in the chapter four experiments to determine how the two cell types might behave, if they were affected differently by T3 and if there might be strain differences in fibroblast behavior, as suspected for myoblasts. By no means did this study try to mimic the *in vivo* environment. Myoblasts in a regenerating muscle do not exist by themselves. They are surrounded by many types of mononuclear cells in addition to fibroblasts. These experiments were performed to determine if there were direct effects of T3 treatment on cell cycling of myoblasts, fibroblasts and remixed myoblasts and fibroblasts.

The ^{3}H-thymidine incorporation and propidium iodide studies (chapter four) revealed that control and mdx muscle cells did indeed demonstrate different changes in proliferation and cell cycling when treated with T3. Those differences were also cell-type specific. The results further supported the

hypothesis that the regenerative capability of mdx myoblasts may be as a result of differential regulation of cell cycling. The results obtained in chapter four clearly expanded earlier work (chapter three) on the effects of T3 on muscle regeneration in both strains. However, an important question still remained unanswered. Did mdx myoblasts cycle faster than control myoblasts?

It was exciting to observe distinct responses in control and mdx fibroblasts with T3 treatment, and to discover that myoblast and fibroblast interactions did occur *in vitro*. Studies are still needed to determine the exact nature of T3 effects on fibroblasts. These studies might include resolving how T3 actually interacts with fibroblasts on T3 receptors, and what genes, if any, might be regulated by T3 in fibroblasts. Perhaps the influence of growth factors like bFGF is also regulated by T3 in fibroblasts. Morin et al. (1995) have shown that mdx fibroblasts do contain a growth factor activity that appears to stimulate the proliferation of mdx myoblasts *in vitro*. Therefore, regulation of bFGF expression by T3 in fibroblasts could result in a change in cycling behavior that may have negative or positive effects on myoblasts both *in vivo* and *in vitro*. The negative result would be that this growth factor activity would not be produced in fibroblasts, and myoblasts would not be stimulated by this source. On the other hand, perhaps less fibroblast activity means that less fibrosis would occur during muscle regeneration, giving the advantage to myoblast proliferation and new myotube formation, which ultimately leads to effective muscle regeneration.

During the course of the experiments in chapter four, it was decided that the potential differences in cycling between mdx diaphragm and limb muscle myoblasts and fibroblasts should be examined. Since the diaphragm in the mdx mouse appears to be affected by dystrophy much more than limb muscle, but retains function, it was thought that cell cycle dynamics might play a role in determining the two very different phenotypes of muscular dystrophy in the same mouse. The diaphragms were collected at the same time and in the same way as the limb muscles and prepared for culture and cell cycle analysis with

or without T3 treatment exactly as reported in chapter four. The cell cycle distributions of myoblasts (low) and fibroblasts (high) in the diaphragm are shown in Figure 6.1. The following results are described in Anderson et al. (1997a, submitted). The proportion of mixed cells (myoblasts recombined with fibroblasts) in S-phase was lower in diaphragm cultures than limb cultures. T3-treatment resulted in a decreased proportion of diaphragm myoblasts in S-phase compared to T3-treated limb myoblasts. Smaller proportions of diaphragm fibroblasts were also observed in S-phase with T3 compared to limb fibroblasts with T3. In contrast, T3 treatment resulted in a larger proportion of limb fibroblasts in S-phase compared to untreated limb fibroblasts. These results agree with decreases in new repair in diaphragm tissue from hyperthyroid mdx mice (Anderson et al., 1997a, submitted) and with data described in chapter four for limb muscle cell cycling. It is apparent from these results that diaphragm myoblasts may be more sensitive to T3 than limb myoblasts. Further studies are required to reveal potential differences in cell cycle rates between mdx diaphragm myoblasts and limb myoblasts (and even purified fibroblasts). Those studies could be done easily by pulsing primary diaphragm and limb myoblasts with BrdU for a period of time and subsequently following that labelled S-phase population (as in chapter five) over 1 cell cycle.

The next logical step to our work was to follow control and mdx myoblast movement through the cell cycle. If differences between control and mdx myoblast cell cycling could be observed at one point in time (as in chapter four), we should also be able to observe differences over time. As well, the effects of T3 might also be more readily observed. With the use of BrdU, an S-phase cell labelling agent, a particular population of myoblasts was marked and followed over time. PI was used for the determination of proportions of cells in the remaining phases of the cell cycle (G_0/G_1 and G_2/M).

In an attempt to minimize the manipulation of myoblasts in culture, the purification and subculturing steps were not used for the studies in chapter five. The continued subculturing of cells (after

cell sorting) to obtain optimal numbers for cell cycle analysis using PI (as in chapter four) would likely change cell cycle behavior over time. By comparison, myoblasts in primary cultures (over a short period of time) emulate more closely the *in vivo* muscle regenerating environment. To reiterate, while the *in vitro* setting was not meant to mimic *in vivo* muscle regeneration in these studies, the differences between different model systems were taken into account. The main goal was to further examine cell cycle activity in control and mdx primary muscle cell cultures, and to observe the effects of T3 on these muscle cells.

The results from the chapter five studies were consistent with previous work (chapter three and four). Differences in cycling activity were observed between control and mdx muscle cell (myoblast) cultures. Additionally, the differences in cycling behavior were observed as they developed over time. Control muscle cells appeared to cycle less uniformly than mdx muscle cells. Even more exciting was the observation that the proportions of muscle cells in early and late S-phases were higher in mdx cultures compared to control cultures at all time points. This result leads us closer to the possibility that there are differences in cycling rate between control and mdx myoblasts. A simple visual experiment could be performed to examine this likely possibility. Using clonal myoblasts from both strains, control and mdx myoblasts could be cultured on a dish that was partitioned into two halves, with control cells on one side and mdx cells on the other side. Using a sterile video camera apparatus set up in the incubator, it would be possible to capture on video, the cell cycle activity of the two different cell types over the period of one or even two cell cycles to see if there are any differences in cell cycle rate (by observing the events of mitosis). Cell counts could track the rate of doubling in the population and by single cells over time.

T3 treatment only altered the cycling of control muscle cells, suggesting that they may be more sensitive to the effects of T3 than mdx muscle cells. This is an important finding. Throughout all of the studies in this thesis, the control mouse strain was more susceptible to the effects of T3. Perhaps mdx muscles *in vivo* metabolize the excess T3 differently than control muscles due to the ongoing muscle

regeneration occurring in mdx muscle. That regeneration requires that sufficient quantities of thyroid hormones are present. Conceivably the number of thyroid hormone receptors present in mdx muscle may not change or could be saturated and more quickly down-regulated by excess T3 than in control muscle. That could leave the excess T3 relatively ineffective in altering myoblast cell cycle activity in mdx muscle. To address such a possibility, thyroid hormone receptor binding and density studies are necessary. These techniques could provide us with information about T3 binding affinity with its receptor, and whether there are differences in T3 binding, T3 receptor density, or receptor turnover between control and mdx myoblasts during muscle regeneration.

In the chapter five experiments, T3 did not slow down or stop control or mdx muscle cells from passing through the late $S-G_2/M$ or G_0/G_1-early S-phase transitions of the cell cycle, as was originally hypothesized. Perhaps the muscle cells needed to be exposed to T3 for a longer period of time to actually see muscle cells totally arrested in G_0. The experiments in chapter five only used a short exposure time (6 hours) as we were interested in examining immediate effects of T3 on a single or the next cell cycle. Results of T3 exposure indicated that there was a short-term effect of T3 on control pre-MyoD muscle cells or fibroblasts in addition to the longer term effects on regeneration (chapter three) and cell cycle distribution (chapter four). A longer T3 exposure might have altered more committed myogenic cells expressing MyoD and/or other MRFs, and produced the anticipated result that was in the initial hypothesis.

Observed changes in the proportions of cells in particular phases of the cell cycle with various hormone or drug treatments can provide information about changes in cell cycle time and rate. These observations are made relatively easily with the use of fluorescent-tagged antibodies to BrdU and PI, given a well-controlled experiment and access to a flow cytometer. However, other questions may be addressed regarding what genes, specifically cyclins, might control a muscle cell's ability to cycle in the

presence of excess thyroid hormone. The production of the different cyclin proteins over the period of one cell cycle could be followed using specific anti-cyclin antibodies tagged with fluorescent markers and analyzed by flow cytometry. For example, the G_1 cyclin proteins can be observed in the G_1-S-phase transition, since those specific cyclins are not produced and are lost as cells progress through S-phase. However, they will reappear as the cells re-enter G_1. Thus, T3 treatment might alter the expression of those specific cyclin genes and this may present as a change in cyclin protein translation. It is unknown if thyroid hormones interact with the cell cycle machinery at this level, but that information certainly will be important to determine by future experiments.

Muscle regeneration in mdx muscle is special indeed! The results from the studies in this thesis can now be added to the many studies on the mdx mouse that have shown its enhanced capability to successfully regenerate muscle tissue compared to controls and patients with DMD. Future studies of cell cycle regulation by cyclin genes and their Cdk partners in myogenic cells that are committed and proliferative, and experiments that explore the nature of myoblast and fibroblast interactions will, without a doubt, contribute further to our understanding of muscle regeneration. It is the hope that this knowledge will point to new treatments that might benefit muscle regeneration processes in individuals with neuromuscular diseases and other muscle-related disorders.

138

Fig.6.1. Histograms of flow cytometric analysis of cycling cells from mdx diaphragm (top) and mdx limb

muscles that were separated by light scatter into myoblast (low) and fibroblast (high) populations or

remixed 1:1 (mix). T3-treated cultures are labelled as "T3" and untreated cultures are indicated as "no

T3". Data represent the proportions of cells in G_0/G_1 (first peak = 2N amount of DNA), S-phase

(between 2N and 4N amounts of DNA), and G_2/M (second peak = 4N amount of DNA). Five thousand

cells were analyzed from each population and significant differences were analyzed by Chi-squared

statistics. The proportion of mixed cells (myoblasts recombined with fibroblasts) in S-phase was lower

in diaphragm cultures than limb cultures (p = 0.002, Chi-squared = 20.7, df = 6). T3-treatment resulted

in a decreased proportion of diaphragm myoblasts in S-phase compared to T3-treated limb myoblasts.

Smaller proportions of diaphragm fibroblasts were observed in S-phase with T3 compared to limb

fibroblasts with T3. In contrast, T3 treatment resulted in a larger proportion of limb fibroblasts in S-

phase compared to untreated limb fibroblasts (p<0.001, Chi-squared = 33.5, df = 6) (after Anderson et

al., 1997a, submitted).

mdx diaphragm muscle

DNA content
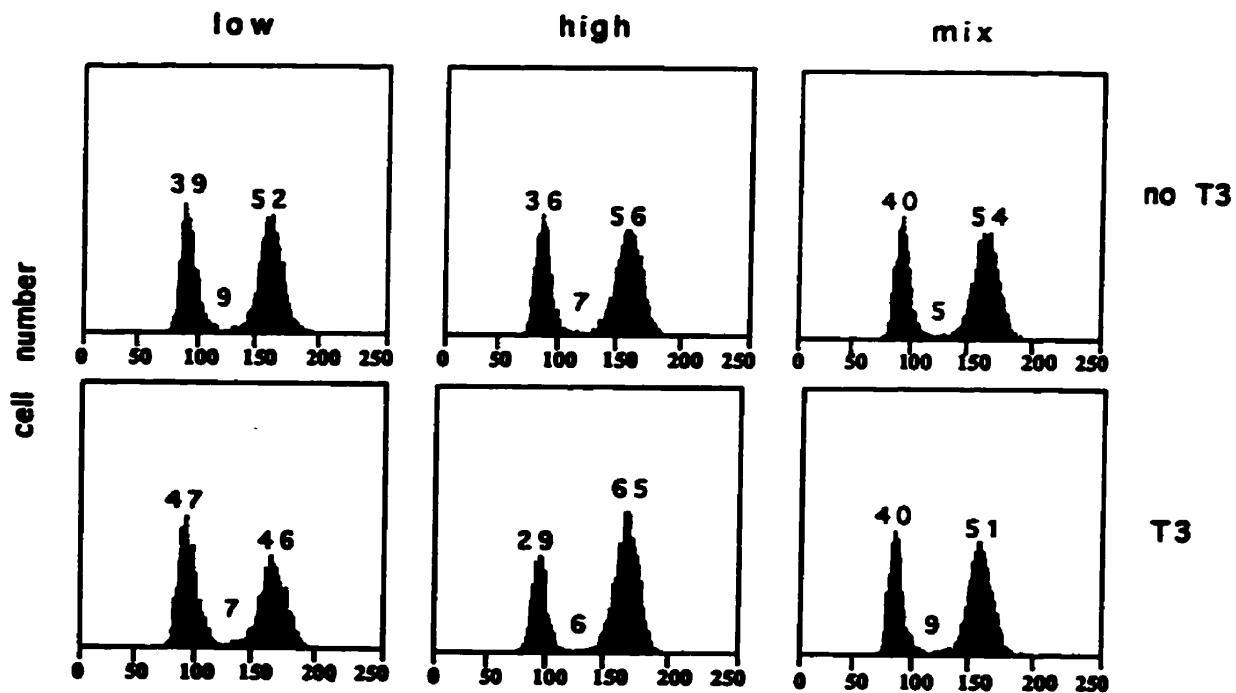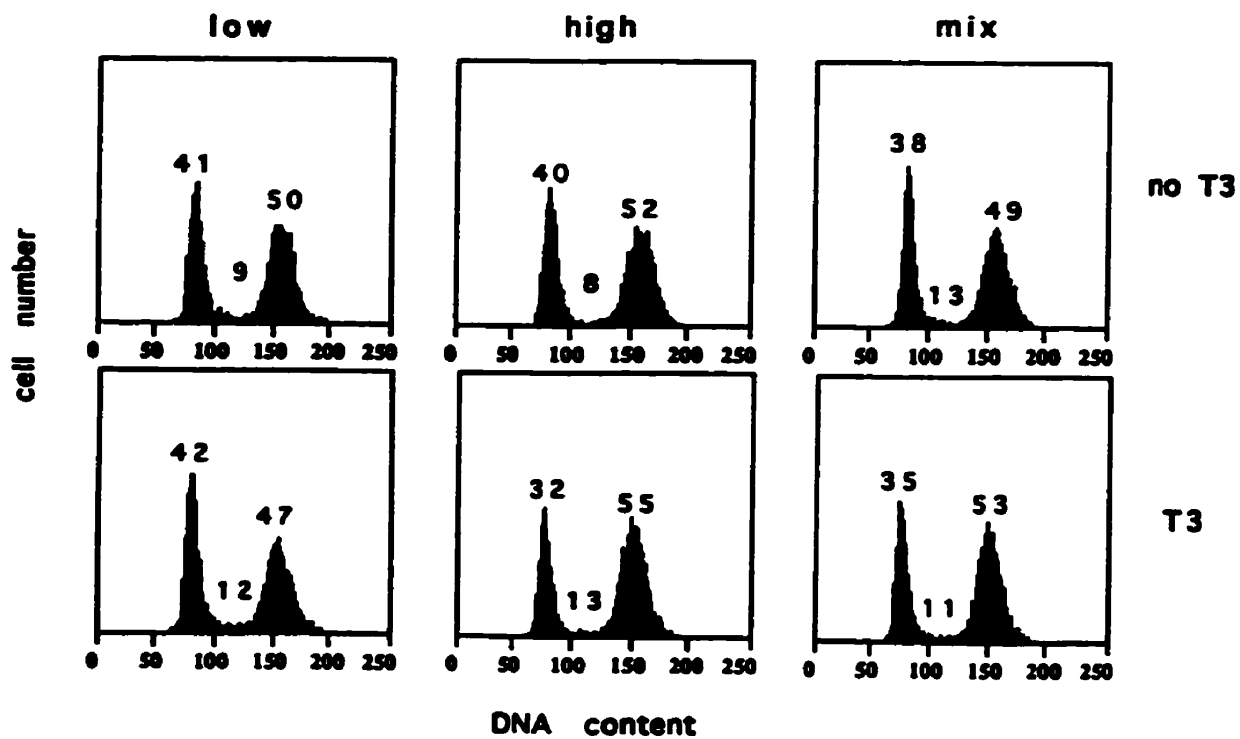
References

Allen RE, MV Dodson, and LS Luiten (1984) Regulation of skeletal muscle satellite cell proliferation by bovine pituitary fibroblast growth factor. Exp. Cell Res., 152: 154-160.

Allen RE, MV Dodson, LK Boxhorn, SL Davies, and KL Hossner (1986) Satellite cell proliferation in response to pituitary hormones. J. Anim. Sci., 62: 1596-1601.

Anderson JE, WK Ovalle, and BH Bressler (1987) Electron microscopic and autoradiographic characterization of hindlimb muscle regeneration on the mdx mouse. Anat. Rec., 219: 243-257.

Anderson JE, BH Bressler, and WK Ovalle (1988) Functional muscle regeneration in the hindlimb skeletal muscle of the mdx mouse. J. Muscle Res. Cell Motil., 9: 499-516.

Anderson JE, L Liu, and E Kardami (1991) Distinctive patterns of basic fibroblast growth factor (bFGF) distribution in degenerating and regenerating areas of dystrophic mdx striated muscles. Dev. Biol., 147: 96-109.

Anderson JE, BA Kakulas, PF Jacobsen, RD Kornegay, and MD Grounds (1993) Comparison of basic fibroblast growth factor in X-linked dystrophin-deficient myopathies of human, dog, and mouse. Growth Factors, 9: 107-121.

Anderson JE, L Liu, and E Kardami (1994a) The effects of hyperthyroidism on muscular dystrophy in the mdx mouse: greater dystrophy in cardiac and soleus muscle. Muscle Nerve, 17: 64-73.

Anderson JE, L Liu, E Kardami, and LJ Murphy (1994b). The pituitary-muscle axis in mdx dystrophic mice. J. Neurol. Sci., 123: 80-87.

Anderson JE, CM Mitchell, JK McGeachie, and MD Grounds (1995) The time course of basic fibroblast growth factor expression in crush-injured skeletal muscles of SJL/J and BALB/c mice. Exp. Cell Res., 216: 325-334.

Anderson JE, KL Garrett, MJ Krahn, AN Moor (neé Pernitsky), LM McIntosh, and KAH Penner (1997a) Dytrophy and myogenesis in mdx diaphragm muscle. (submitted to Dev. Biol. April, 1997).

Anderson JE, LM McIntosh, AN Moor (neé Pernitsky), and Z Yablonka-Reuveni (1997b) Levels of MyoD protein expression following injury of mdx and normal limb muscle are modified by thyroid hormone. (submitted to J. Histoch. Cytoch. March, 1997).

Bagust J, DM Lewis, and RA Westerman (1981) Motor units in cross-reinnervated fast and slow-twitch muscle of the cat. J. Physiol., 313: 223-235.

Baldwin KM, AM Hooker, PJ Campbell, and RE Lewis (1978) Enzyme changes in neonatal skeletal muscle: effect of thyroid deficiency. Am. J. Physiol., 235: C97-C102.

Balogh S, CCG Naus, and PA Merrifield (1993) Expression of gap junctions in cultured rat L6 cells during myogenesis. Dev. Biol., 155: 351-360.

Bandman E, R Matsuda, and RC Strohman (1982) Developmental appearance of myosin heavy and light chain isoforms *in vivo* and *in vitro* in chicken skeletal muscle. Dev. Biol., 93: 508-518.

Bandman E (1985) Myosin isozyme transitions in muscle development, maturation, and disease. Int. Rev. Cytol., 97: 97-131.

Bárány M and RI Close (1971) The transformation of myosin in cross-innervated rat muscles. J. Physiol., 213: 455-474.

Benbrook D and M Pfahl (1987) A novel thyroid hormone receptor encoded by a cDNA clone from a human testis library. Science, 238: 788-791.

Bengal E, L Ransone, R Scharfmann, VJ Dwarki, SJ Tapscott, H Weintraub, and IM Verma (1992) Functional antagonism between c-jun and MyoD proteins: a direct physical association. Cell, 68: 507-519.

Bischoff R (1975) Regeneration of single skeletal muscle fibers *in vitro*. Anat. Rec., 182: 215-236.

Bischoff R (1994) The satellite cell and muscle regeneration. *In: Myology-basic and clinical*, Engel AG, and C Franzini-Armstrong (Eds.) New York: McGraw-Hill, 97-118.

Bhagwati S, A Ghatpande, SA Shafiq, and B Leung (1996) In situ hybridization analysis for expression of myogenic regulatory factors in regenerating muscle of mdx mouse. J. Neuropathol. Exp. Neurol., 55: 509-514.

Blau HM and D Baltimore (1991) Differentiation requires continuous regulation. J. Cell Biol., 112: 781-783.

Bober E, G Lyons, T Braun, G Cossu, M Buckingham, and HH Arnold (1991) The muscle regulatory gene myf-6 has a biphasic pattern of expression during early mouse development. J. Cell Biol., 113: 1255-1265.

Braun T, E Bober, B Winter, N Rosenthal, and HH Arnold (1990) Myf-6, a new member of the human gene family of myogenic determination factors: Evidence for a gene cluster on chromosome 12. EMBO. J., 9: 821-831.

Braun T, MA Rudnicki, HH Arnold, and R Jaenisch (1992) Targeted inactivation of the muscle regulatory gene Myf5 results in abnormal rib development and perinatal death. Cell, 71: 369-382.

Brooke MH and KK Kaiser (1970) Muscle fiber types: how many and what kind? Arch. Neurol. (Chicago) 23: 369-379.

Buckingham M (1992) Making muscle in mammals. Trends Genet., 8: 144-148.

Bulfield G, WGF Siller, PAL Wight, and KJ Moore (1984) X-chromosome-linked muscular dystrophy mdx in the mouse. Proc. Natl. Acad. Sci. USA, 81: 1189-1192.

Buller AJ, JC Eccles, and RM Eccles (1960) Differentiation of fast and slow muscles in the cat hindlimb. J. Physiol., 150: 399-416.

Buskin JN and SD Hauschka (1989) Identification of a myocyte nuclear factor that binds to the muscle-specific enhancer of the mouse creatine kinase gene. Mol. Cell Biol., 9: 2627-2640.

Butler-Browne GS, LB Bugaisky, S Cuenod, K Schwartz, and RG Whalen (1982) Denervation of newborn rat muscle does not block the appearance of adult fast myosin heavy chain. Nature, 299: 830-833.

Butler-Browne GS, JP Barbet, and LE Thornell (1990) Myosin heavy and light chain expression during human skeletal muscle development and precocious muscle maturation induced by thyroid hormone. Anat. Embryol., 181: 513-522.

Carlson BM, FM Hansen-Smith, and DK Magon (1979) The life history of a free muscle graft. In: Muscle Regeneration, A Mauro et al. (Eds.) New York: Raven Press, 493-507.

Carlson BM and JA Faulkner (1983) The regeneration of skeletal muscle fibers following injury: A review. Med. Sci. Sport. Exerc., 15: 187-198.

Carnac G, O Albagli-Curiel, M Vandromme, C Pinset, D Montarras, V Laudet, and A Bonnieu (1992) 3,5,3'-Triiodothyronine positively regulates both MyoD1 gene transcription and terminal differentiation in C2 myoblasts. Mol. Endocrinol., 6: 1185-1194.

Caruso M, F Martelli, A Giordano, and A Felsani (1993) Regulation of MyoD gene transcription and protein function by the transforming domains of the adenovirus E1A oncoprotein. Oncogene, 8: 267-278.

Cattini PA, TR Anderson, JD Baxter, P Mellon, and NL Eberhardt (1986). The human growth hormone gene is negatively regulated by triiodothyronine when transfected into rat pituitary tumor cells. J. Biol. Chem., 261: 13367-13372.

Chen G and LS Quinn (1992) Partial characterization of skeletal myoblast mitogens in mouse crushed muscle extract. J. Cell. Physiol., 153: 563-574.

Chen G, BH Bressler, and LS Quinn (1994) Extracts from mdx and normal mouse skeletal muscle contain similar levels of mitogenic activity for myoblasts. Cell Biol. Int., 18: 229-235.

Cobrinik D (1996) Regulatory interactions among E2Fs and cell cycle control proteins. In: Transcriptional Control of Cell Growth: The E2F Gene Family. Ch. 2, PJ Farnham (Ed.), Springer-Verlag, Berlin, Heidelberg, 31-61.

D'Albis A, C Pantaloni, and JJ Bechet (1979) An electrophoretic study of native myosin isozymes and of their subunit content. Eur. J. Biochem., 99: 261-272.

D'Albis A, C Janmot, and JJ Bechet (1985) Myosin switches in skeletal muscle development of an urodelan amphibian, *Pleurodeles waltlii*. Comparison with a mammalian, *Mus musculus*. Biochem. Biophys. Res. Commun., 128: 94-100.

D'Albis A, M Lenfant-Guyot, C Janmot, C Chanoine, J Weinman, and CL Gallien (1987) Regulation by thyroid hormones of terminal differentiation in the skeletal dorsal muscle: 1. neonate mouse. Dev. Biol., 123: 25-32.

Darling DS, JS Beebe, J Burnside, ER Winslow, and WW Chin (1991) 3,5,3'-triiodothyronine (T3) receptor-auxiliary protein (TRAP) binds DNA and forms heterodimers with the T3 receptor. Mol. Endocrinol., 5: 73-84.

Daughaday WH and P Rotwein (1989). Insulin-like growth factors I and II: peptide messenger ribonucleic acid and gene structures, serum, and tissue concentrations. Endocr. Rev., 10: 68-91.

Davis CE, JB Harris, and LVB Nicholson (1991) Myosin isoform transitions and physiological properties of regenerated and re-innervated soleus muscles of the rat. Neuromuscular Disord., 1: 411-421.

Davis FB, JH Kite Jr., PJ Davis, and SD Blas (1982) Thyroid hormone stimulation *in vitro* of red blood cell Ca^{+2}-ATPase activity: Interspecies variation. Endocrinol., 110: 297-298.

Davis RL, H Weintraub, and AB Lassar (1987) Expression of a single transfected cDNA converts fibroblasts to myoblasts. Cell, 51: 987-1000.

DeCaprio JA, JW Ludlow, J Figge, JY Shew, CM Huang, WH Lee, E Marsilio, E Paucha, and DM Livingston (1988) SV40 large tumor antigen forms a specific complex with the product of the retinoblastoma suseptibility gene. Cell, 54: 275-283.

DiMario J and RC Strohman (1988) Satellite cells from dystrophic mdx mouse muscle are stimulated by fibroblast growth factor *in vitro*. Differentiation, 39: 42-49.

DiMario J, N Buffinger, S Yamada, and RC Strohman (1989) Fibroblast growth factor in the extracellular matrix of dystrophic mdx mouse muscle. Science, 244: 688-690.

Downes M, R Griggs, A Atkins, EN Olson, and GEO Muscat (1993) Identification of a thyroid hormone response element in the mouse myogenin gene: characterization of the thyroid hormone and retinoic-X-receptor heterodimeric binding site. Cell Growth Differ., 4: 901-909.

Draeger A, AG Weeds, and RB Fitzsimmons (1987) Primary, secondary and tertiary myotubes in developing skeletal muscles: a new approach to the analysis of human myogenesis. J. Neurol. Sci., 81: 19-43.

Dupont-Versteegdon EE and RJ McCarter (1992) Differential expression of muscular dystrophy in diaphragm versus hindlimb muscles of mdx mice. Muscle Nerve, 15: 1105-1110.

Edgar BA and CF Lehner (1996) Developmental controls of cell cycle regulators: a fly's perspective. Science, 274: 1646-1652.

Edmondson DG and EN Olson (1989) A gene with homology to the myc similarity region of MyoD1 is expressed during myogenesis and is sufficient to activate the muscle differentiation program. Genes Dev., 3: 628-640.

El-Deiry WS, T Tokino, VE Velculescu, DB Levy, R Parsons, JM Trent, D Lin, WE Mercer, KW Kinzler, and B Vogelstein (1993) WAF1, a potential mediator of p53 tumor suppression. Cell, 75: 817-825.

Elledge SJ (1996) Cell cycle checkpoints: preventing an identity crisis. Science, 274: 1664-1672.

Emerson CP (1990) Myogenesis and developmental control genes. Curr. Opin. Cell Biol., 2: 1065-1075.

Evans RM (1988) The steroid and thyroid hormone receptor superfamily. Science, 240: 889-895.

Ferrari S, B Calabretta, R Battini, SC Cosenza, TA Owen, KJ Soprano, and R Baserga (1988) Expression of c-myc and induction of DNA synthesis by platelet-poor plasma in human diploid fibroblasts. Exp. Cell Res., 174: 25-33.

Fischman D (1970) The synthesis and assembly of myofibrils in embryonic muscle. Curr. Top. Dev. Biol., 5: 235-280.

Florini JR, DZ Ewton, SL Falen, and JJ Van Wyk (1986). Biphasic concentration dependency of stimulation of myoblast differentiation by somatomedins. Am. J. Physiol., 250: C771-C778.

Forman BM, J Casanova, BM Raaka, J Ghysdael, and H Samuels (1992) Half-site spacing and orientation determines whether thyroid hormone and retinoic acid receptor and related factors bind to DNA response elements as monomers, homodimers, or heterodimers. Mol. Endocrinol., 6: 429-442.

Füchtbauer EM and H Westphal (1992) MyoD and myogenin are coexpressed in regenerating skeletal muscle of the mouse. Dev. Dyn., 193: 34-39.

Gambke B, GE Lyons, J Haselgrove, AM Kelly, and NA Rubinstein (1983) Thyroidal and neural control of myosin transitions during development of rat fast and slow muscles. FEBS Lett., 156: 335-339.

Garrett KL and JE Anderson (1995) Colocalization of bFGF and the myogenic regulatory gene myogenin in dystrophic mdx muscle precursors and young myotubes in vivo. Dev. Biol., 169: 596-608.

Glass CK, OV Devary, and MG Rosenfeld (1990) Multiple cell type-specific proteins differentially regulate sequence recognition by the alpha retinoic acid receptor. Cell, 63: 729-738.

Goodrich DW and WH Lee (1993) Molecular characterization of the retinoblastoma suseptability gene. Biochim. Biophys. Acta., 1155: 43-61.

Gospodarowicz D (1975) Purification of a fibroblasts growth factor from bovine pituitary. J. Biol. Chem., 250: 2515-2520.

Gospodarowicz D, J Weseman, and J Moran (1975) Presence in brain of a mitogenic agent promoting proliferation of myoblasts in low density culture. Nature, 256: 216-219.

Gospodarowicz D J Weseman, JS Moran, and J Lindstrom (1976) Effect of fibroblast growth factor on the division and fusion of bovine myoblasts. J. Cell. Biol., 70: 395-405.

Gospodarowicz D, N Ferrara, L Schweigerer, and G Neufeld (1987) Structural characterization and biological functions of basic fibroblast growth factor. Endocr. Rev., 8: 95-114.

Greif RL and D Sloane (1978) Mitochondrial binding sites for triiodothyronine. Endocrinology, 103: 1899-1902.

Grounds MD and JK McGeachie (1989) A model of myogenesis in vivo derived from detailed autoradiographic studies of regenerating skeletal muscle challenges the concept of quantal mitosis. Cell Tissue Res., 250: 563-569.

Grounds MD (1991) Towards understanding skeletal muscle regeneration. Path. Res. Pract., 187: 1-22.

Grounds MD, KL Garrett, MC Lai, WE Wright, and MW Beilharz (1992) Identification of skeletal muscle precursor cells *in vivo* by use of MyoD1 and myogenin probes. Cell Tissue Res., 267: 99-104.

Grounds MD and Z Yablonka-Reuveni (1993) Molecular and cell biology of skeletal muscle regeneration. *In: Molecular and Cell Biology of Muscular Dystrophy*, T Partridge (Ed.) London: Chapman & Hall, 210-256.

Gu W, JW Schneider, G Condorelli, S Kaushal, S Mahdavi, and B Nadal Ginard (1993) Interaction of myogenic factors and the retinoblastoma protein mediates muscle cell commitment and differentiation. Cell, 72: 309-324.

Gunning P and E Hardeman (1991) Multiple mechanisms regulate muscle fiber diversity. FASEB J., 5: 3064-3070.

Halevy O, BG Novitch, DB Spicer, SX Skapek, J Rhee, GJ Hannon, D Beach, and AB Lassar (1995) Correlation of terminal cell cycle arrest of skeletal muscle with induction of p21 by MyoD. Science, 267: 1018-1021.

Hannon K, CK Smith II, KR Bales, and RF Santerre (1992) Temporal and quantitative analysis of myogenic regulatory and growth factor gene expression in the developing mouse embryo. Dev. Biol., 151: 137-144.

Hartwell LH and TA Weinert (1989) Checkpoints: controls that ensure the order of cell cycle events. Science, 246: 629-634.

Hashizume K, K Ichikawa, and M Kobayashi (1984) Effect of calcium ion on triiodothyronine binding to kidney outer mitochondrial membrane *in vitro*. Endocrinol. Jpn., 31: 311-320.

Hastings KEM and CP Emerson (1982) Gene sets in muscle development. *In: Muscle Development: Molecular and Cellular Control,* ML Pearson and HF Epstein (Eds.) New york: Cold Springs Harbor Laboratory, 215-236.

Hasty P, A Bradley, JH Morris, DG Edmondson, JM Venuti, EN Olson, and WH Klein (1993) Muscle deficiency and neonatal death in mice with a targeted mutation in the myogenin gene. Nature, 364: 501-506.

Hinterberger T, D Sassoon, S Rhodes, and S Koneiczny (1991) Expression of the muscle regulatory factor MRF4 during somite and skeletal myofiber development. Dev. Biol., 147: 144-156.

Hoffman EP, RH Brown, Jr, and LM Kunkel (1987) Dystrophin: The protein product of the Duchenne muscular dystrophy locus. Cell, 51: 919-928.

Holloway JM, CK Glass, S Adler, CA Nelson, and M Rosenfeld (1990) The C'-terminal interaction domain of the thyroid hormone receptor confers the ability of the DNA site to dictate positive or negative transcriptional activity. Proc. Natl. Acad. Sci. USA, 87: 8160-8164.

Hughes SM, JM Taylor, SJ Tapscott, CM Gurley, WJ Carter, and CA Peterson (1993) Selective accumulation of MyoD and myogenin in fast and slow adult skeletal muscle is controlled by innervation and hormones. Development, 118: 1137-1147.

Ianuzzo D, P Patel, V Chen, and C Williams (1977) Thyroidal tropic influence on skeletal muscle myosin. Nature, 270: 74-76.

Ichikawa K and K Hashizume (1991) Cellular binding proteins of thyroid hormones. Life Sci., 49: 1513-1522.

Izumo S, B Nadal-Ginard, and V Mahdavi (1986) All members of the MHC multigene family respond to thyroid hormone in a highly tissue-specific manner. Science, 231: 597-600.

Karin M (1990) The AP-1 complex and its role in transcriptional control by protein kinase C *In: Molecular Aspects of Cellular Recognition,* vol. 6, P Cohen and G Foulkes (eds.), Elsevier, Amsterdam, 143-161.

Karpati G, S Carpenter, and S Prescott (1988) Small caliber skeletal muscle fibers do not suffer necrosis in mdx mouse dystrophy. Muscle Nerve, 11: 795-803.

Kelly AM (1983) Emergence of specialization in skeletal muscle. *In: Handbook of Physiology,* LD

Peachy (Ed.) Baltimore: Williams and Wilkins, 507.

King RW, RJ Deshaies, JM Peters, and MW Kirschner (1996) How proteolysis drives the cell cycle. Science, 274: 1652-1659.

Kimura I, Y Gotoh, and E Ozawa (1989) Further purification of a fibroblast growth factor-like factor from chick-embryo extract by heparin-affinity chromatography. In Vitro Cell Dev. Biol., 25: 236-242.

Kliewer SA, K Umesono, DJ Mangelsdorf, and R Evans (1992) Retinoid-X-receptor interacts with nuclear receptors in retinoic acid, thyroid hormone, and vitamin D3 signalling. Nature, 355: 446-449.

Koenig M, EP Hoffman, CJ Bertelson, AP Monaco, C Feener, and LM Kunkel (1987) Complete cloning of the Duchenne muscular dystrophy (DMD) cDNA and preliminary genomic organization of the DMD gene in normal and affected individuals. Cell, 50: 509-517.

Koenig RJ, RL Warne, GA Brent, JW Harvey, PR Larsen, and DD Moore (1988) Isolation of a cDNA clone encoding a biological active thyroid hormone receptor. Proc. Natl. Acad. Sci. USA, 85: 5031-5035.

Lazar MA and WW Chin (1990) Nuclear thyroid hormone receptors. Clin. Invest., 86: 1777-1782.

Lazar MA, TJ Berrodin, and HH Harding (1991) Differential DNA binding by monomeric, homodimeric, and potentially heteromeric forms of the thyroid hormone receptor. Mol. Cell Biol., 11: 5005-5015.

Leid M, P Kastner, R Lyons, H Nakshartri, M Saunders, T Zachareweski, J Chen, A Staub, J-M Garnier, S Mader, and P Chambon (1992) Purification, cloning, and RXR identity of the HeLa cell factor with which RAR or TR heterodimerizes to bind target sequences efficiently. Cell, 68: 377-395.

Li L, J Zhou, G James, R Heller Harrison, MP Czech, and EN Olson (1992a) FGF inactivates myogenic helix-loop-helix proteins through phosphorylation of a conserved protein kinase C site in their DNA-binding domains. Cell, 71: 1181-1194.

Li L, JC Chambard, M Karin, and EN Olson (1992b) Fos and jun repress transcriptional activation by myogenin and MyoD: the amino terminus of jun can mediate repression. Genes Dev., 6: 676- 689.

Liu L, BW Doble, and E Kardami (1993) Perinatal phenotype and hypothyroidism are associated with elevated levels of 21.5- to 22-kDa basic fibroblast growth factor in cardiac ventricles. Dev. Biol., 157: 507-516.

Longobardi-Given A (1992) Cells from within: DNA and molecular biology. In: Flow Cytometry, New York: John Wiley and Sons, Inc., 103-133.

Mai B and M Lipp (1993) Identification of a protein from Saccharomyces cerevisiae with E2F-like DNA-binding and transactivating properties. FEBS Lett., 321: 153-158.

Malhotra P, CF Manohar, S Swaminathan, R Toyama, R Dhar, R Reichel, and B Thimmapaya (1993) E2F site activates transcription in fission yeast *Schizosaccharomyces pombe* and binds to a 30-KDa transcription factor. J. Biol. Chem., 268: 20392-20401.

Mangelsdorf DJ, K Umesono, S Kliewer, U Borgmeyer, E Ong, and R Evans (1991) A direct repeat in the cellular retinol-binding protein type II gene confers differential regulation by RXR and RAR. Cell, 66: 555-561.

Marini JF, F Pons, J Leger, N Loffreda, M Anoal, M Chevallay, M Fardeau, and JJ Leger (1991) Expression of myosin heavy chain isoforms in Duchenne muscular dystrophy patients and carriers. Neuromuscular Disord., 1: 397-409.

Martelli F, C Cenciarelli, G Santarelli, B Polikar, A. Felsani, and M Caruso (1994) MyoD induces retinoblastoma gene expression during myogenic differentiation. Oncogene, 9: 3579-3590.

Martin CR (1985) Thyroid hormones, thyrotropin, and thyrotropin-releasing hormone. *In: Endocrine Physiology*, New York: Oxford University Press, 745-784.

Marx J (1995) Cell cycle inhibitors may help brake growth as cells develop. Science, 267: 963-964.

Matsuda R, DH Spector, and RC Strohman (1983) Regenerating adult chicken skeletal muscle and satellite cell cultures express embryonic patterns of myosin and tropomyosin isoforms. Dev. Biol., 100: 478-488.

Mauro A (1961) Satellite cell of skeletal muscle fibers. J. Biophys. Biochem. Cytol., 9: 493-495.

McIntosh LM, AN Pernitsky, and JE Anderson (1994) The effects of altered metabolism (hypothyroidism) on muscle repair in the mdx dystrophic mouse. Muscle Nerve, 17: 444-453.

McIntosh LM and JE Anderson (1995). Hypothyroidism increases muscle precursor proliferation and reduces myotube fusion in mdx limb muscle. Biochem. Cell. Biol., 73: 181-190.

McIntosh LM (1997) Tandem changes in myogenic cell proliferation, muscle regeneration and muscle taurine levels in MyoD(-/-), mdx dystrophic and double mutant mice. (submitted).

McLennan IS (1994) Neurogenic and myogenic regulation of skeletal muscle formation: a critical evaluation. Prog. Neurobiol., 44: 119-140.

Megeney LA, B Kablar, K Garrett, JE Anderson, and MA Rudnicki (1996) MyoD is required for myogenic stem cell function in adult skeletal muscle. Genes Dev., 10: 1173-1183.

Minor JH and BJ Wold (1990) Herculin, a fourth member of the MyoD family of myogenic regulatory genes. Proc. Natl. Acad. Sci. USA., 87: 1089-1093.

Mitchell CA, JK McGeachie, and MD Grounds (1992) Cellular differences in the regeneration of murine

skeletal muscle: a quantitative histological study in SJL/JeBALB/C mice. Cell Tissue Res., 269: 159-166.

Morin A, J Louette, MLJ Vos, A Tixier-Vidal, A Belayew, and JA Martial (1990). Triiodothyronine inhibits transcription from the human growth hormone promoter. Mol. Cell Endocrinol., 71: 261-267.

Morin S, S de-la-Porte, M Fiszman, and J Koenig (1995) Inhibition of proliferation in 8-week-old mdx mouse muscle fibroblasts *in vitro*. Differentiation, 59: 145-154.

Moss FP and CP LeBlond (1971) Satellite cells as the source of nuclei in muscles of growing rats. Anat. Rec., 170: 421-436.

Murray A, G Evan, T Hunt, and P Nurse (1994) The cell division cycle. *In: Molecular Biology of the Cell*, 3rd Ed., B Alberts, D Bray, J Lewis, M Raff, K Roberts, and JD Watson (Eds.), Garland Publishing, Inc., New York and London, 864-906.

Murray MB and HC Towle (1989) Identification of nuclear factors that enhance binding of the thyroid hormone receptor to a thyroid hormone response element. Mol. Endocrinol., 3: 1434-1442.

Muscat GEO, R Griggs, M Downes, and J Emery (1993) Characterization of the thyroid hormone response element in the skeletal α-actin gene: negative regulation of T3 receptor binding by the retinoid X receptor. Cell Growth Differ., 4: 269-279.

Muscat GEO, L Mynett-Johnson, D Dowhan, M Downes, and R Griggs (1994) Activation of MyoD gene transcription by 3,5,3'-triiodo-L-thyronine: a direct role for the thyroid hormone and retinoid X receptors. Nucleic Acids Res., 22: 583-591.

Muscat GEO, M Downes, and DH Dowhan (1995) Regulation of vertebrate muscle differentiation by thyroid hormone: the role of the MyoD gene family. BioEssays, 17: 211-218.

Nabeshima Y, K Hanaoka, M Hayasaka, E Esumi, S Li, I Nonaka, and Y Nabeshima (1993) Myogenin disruption results in perinatal lethality because of severe muscle defects. Nature, 364: 532-535.

Naar AM, J-M Boutin, S Lipkin, V Yu, J Holloway, C Glass, and MG Rosenfeld (1991) The orientation and spacing of core DNA-binding motifs dictate selective transcriptional responses to three nuclear receptors. Cell, 65: 1267-1279.

Nevins JR (1992) E2F: a link between the Rb tumor suppressor protein and viral oncoproteins. Science, 258: 424-429.

Nixon BT and H Green (1984) Growth hormone promotes the differentiation of myoblasts and preadipocytes generated by azacytidine treatment of 10T1/2 cells. Proc. Natl. Acad. Sci. USA., 81: 3429-3432.

Ohtani K and JR Nevins (1994) Functional properties of a Drosophila homolog of the E2F1 gene. Mol. Cell. Biol., 14: 1603-1612.

Olwin BB and SD Hauschka (1988) Cell-surface fibroblast growth factor and epidermal growth factor receptors are permanently lost during skeletal muscle terminal differentiation in culture. J. Cell Biol., 107: 761-769.

Olson E (1990) MyoD family: a paradigm for development. Genes Dev., 4: 1454-1461.

Olson E (1992) Interplay between proliferation and differentiation within the myogenic lineage. Dev. Biol., 154: 261-272.

Olson E (1993) Signal transduction pathways that regulate skeletal muscle gene expression. Mol. Endocrinol., 7: 1369-1378.

Ontell M (1978) Neonatal muscle: an electron microscopic study. Anat. Rec., 189: 669-690.

Ontell M and K Kozeka (1984a) The organogenesis of murine striated muscle: a cytoarchitectural study. Am. J. Anat., 171: 133-148.

Ontell M and K Kozeka (1984b) Organogenesis of the mouse extensor digitorum longus muscle: a quantitative study. Am. J. Anat., 171: 149-161.

Ontell M, D Hughes, and D Bourke (1988a) Morphometric analysis of the developing mouse soleus muscle. Am. J. Anat., 181: 279-288.

Ontell M, D Bourke, and D Hughes (1988b) Cytoarchitecture of fetal murine soleus muscle. Am. J. Anat., 181: 267-278.

Oppenheimer JH, D Körner, HL Shwartz, and MI Surks (1972) Specific nuclear triiodothyronine binding sites in rat liver and kidney. J. Clin. Endocrinol. Metab., 35: 330-333.

Oppenheimer JH (1979) Thyroid hormone action at the cellular level. Science, 203: 971-979.

Ott M, E Bober, G Lyons, HH Arnold, and M Buckingham (1991) Early expression of the myogenic regulatory gene Myf-5, in precursor cells of skeletal muscle in the mouse embryo. Development, 111: 1097-1107.

Parker SB, G Eichele, P Zhang, A Rawls, AT Sands, A Bradley, EN Olson, JW Harper, and SJ Elledge (1995) p53-independent expression of p21^{Cip1} in muscle and other terminally differentiating cells. Science, 267: 1024-1027.

Partridge TA (1982) Cellular interactions in the development and maintenance of skeletal muscle. In: Cell Behavior, Bellairs et al.(Eds.) Cambridge University Press, 555-580.

Pernitsky AN, LM McIntosh, and JE Anderson (1996) Hyperthyroidism impairs early repair in normal but not dystrophic mdx mouse tibialis anterior muscle. An in vivo study. Biochem. Cell Biol., 74: 315-324.

Pernitsky AN and JE Anderson (1996) Differential effects of 3,5,3'-triiodothyronine on control and mdx myoblasts and fibroblasts: analysis by flow cytometry. Exp. Cell Res., 227: 214-222.

Philpott A and SH Friend (1994) E2F and its developmental regulation in Xenopus laevis. Mol. Cell. Biol., 14: 5000-5009.

Polyak K, JY Kato, MJ Soloman, CJ Sherr, J Massague, JM Roberts, and A Koff (1994) p27Kip1, a cyclin-Cdk inhibitor, links transforming growth factor-beta and contact inhibition to cell cycle arrest. Genes Dev., 8: 9-22.

Proulx A, PA Merrifield, and CCG Naus (1997) Blocking gap junctional intercellular communications in myoblasts inhibits myogenin and mrf4 expression. Dev. Genetics, in press.

Ransone AJ and IM Verma (1990) Nuclear proto-oncogenes fos and jun. Annu. Rev. Cell Biol., 6: 539-557.

Rapraeger AC, A Krufka, and BB Olwin (1991) Requirement of heparan sulfate for bFGF-mediated fibroblast growth and myoblast differentiation. Science, 252: 1705-1708.

Reddy GPV (1994) Cell Cycle: regulatory events in G_1-S transition of mammalian cells. J. Cell. Biochem., 54: 379-386.

Rhodes SJ and SF Konieczny (1989) Identification of MRF4: a new member of the muscle regulatory gene family. Genes Dev., 3: 2050-2061.

Robertson TA, MD Grounds, CA Mitchell, and JM Papadimitriou (1990). Fusion between myogenic cells in vivo: an ultrastructural study in regenerating murine skeletal muscle. J. Struct. Biol, 105: 170-182.

Rodriques-Arnao J, JP Miell, and RJM Ross (1993) Influence of thyroid hormones on the GH-IGF-I axis. TEM, 4: 169-173.

Ross JJ, MJ Duxson, and AJ Harris (1987) Formation of primary and secondary myotubes in rat lumbrical muscles. Development, 100: 383-394.

Rudnicki MA, T Braun, S Hinuma, and R Jaenisch (1992) Inactivation of MyoD in mice leads to up-regulation of the myogenic HLH gene Myf-5 and results in apparently normal muscle development. Cell, 71: 383-390.

Rudnicki MA, PNJ Schneglesberg, RH Stead, T Braun, HH Arnold, and R Jaenisch (1993) MyoD or Myf-5 is required for the formation of skeletal muscle. Cell, 75: 1351-1359.

Rudnicki MA and R Jaenisch (1995) The MyoD family of transcription factors and skeletal myogenesis. BioEssays, 17: 203-209.

Samuels HH and JS Tsai (1973) Thyroid hormone action in cell culture: demonstration of nuclear

receptors in intact cells and isolated nuclei. Proc. Natl. Acad. Sci. USA., 70: 3488-3492.

Sartore S, L Gorza, and S Schiaffino (1982) Fetal myosin heavy chains in regenerating muscle. Nature, 298: 294-296.

Sassoon D, G Lyons, WE Write, V Lin, A Lassar, H Weintraub, and M Buckingham (1989) Expression of two myogenic regulatory factors myogenin and MyoD1 during mouse embryogenesis. Nature, 344: 303-307.

Sassoon D (1992) Myogenic regulatory factors: Dissectng their role and regulation during vertebrate embryogenesis. Dev. Biol., 156: 11-23.

Schiaffino S, L Gorza, G Pitton, L Saggin, S Ausoni, S Sartore, and T Lomo (1988) Embryonic and neonatal myosin heavy chain in denervated and paralyzed rat skeletal muscle. Dev. Biol., 127: 1-11.

Schiaffino S, L Gorza, S Ausoni, R bottinelli, C Reggiani, L Larsson, L Edstrom, K Gundersen, and T Lomo (1990) Muscle fiber types expressing different myosin heavy chain isoforms. Their functional properties and adaptive capacity. In: The Dynamic State of Muscle Fibers, D Pette (Ed.) Berlin: de Gruyter, 329-341.

Schiaffino S, and C Reggiani (1994) Myosin isoforms in mamalian skeletal muscle. J. Appl. Phisiol., 77(2): 493-501.

Schmalbruch H (1986) Muscle regeneration: Fetal myogenesis in a new setting. Biblithca. Anat., 29: 126-153.

Schultz E (1976) Fine structure of satellite cells in growing skeletal muscle. Am. J. Anat., 147: 49-70.

Schultz E (1989) Satellite cell behavior during skeletal muscle growth and regeneration. Med. Sci. Sport. Exerc., 21: 181-186.

Sherr CJ (1993) Mammalian G_1 cyclins. Cell, 73: 1059-1069.

Sherr CJ (1994) G1 phase progression: cycling on cue. Cell, 79: 551-555.

Sherr CJ (1996) Cancer cell cycles. Science, 274: 1672-1677.

Simonides WS and C van Hardeveld (1989) The postnatal development of sarcoplasmic reticulum Ca^{2+} transport activity in skeletal muscle of the rat is critically dependent on thyroid hormone. Endocrinol., 124: 1145-1152.

Slansky JE and PJ Farnham (1996) Introduction to the E2F family: protein structure and gene regulation. In: Transcriptional Control of Cell Growth: The E2F Gene Family. Ch. 1, PJ Farnham (Ed.), Springer-Verlag, Berlin, Heidelberg, 1-30.

Smith BT, W Galaugher, and WM Thurlbeck (1980) Serum from pneumonectomized rabbits stimulates alveolar type II cell proliferation *in vitro*. Am. Rev. Respir. Dis., 121: 701-707.

Smith CK, MJ Janney, and RE Allen (1994) Temporal expression of myogenic regulatory genes during activation, proliferation, and differentiation of rat skeletal muscle satelite cells. J. Cell. Physiol., 159: 379-385.

Smith TH, NE Block, SJ Rhodes, SF Konieczny, and JB Miller (1993) A unique pattern of expression of the four muscle regulatory factor proteins distinguishes somitic from embryonic, fetal, and newborn mouse myogenic cells. Development, 117: 1125-1133.

Soboll S (1993) Thyroid hormone action on mitochondrial energy transfer. Biochim. et Biophys. Acta, 1144: 1-16.

Sréter FA, J Gergely, S Salmons, and F Romanul (1973) Synthesis by fast muscle of myosin light chains characteristic of slow muscle in response to long-term stimulation. Nature London New Biol. 241: 17-19.

Stedman HH, HL Sweeney, JB Shrager, HC Maquire, RA Panettieri, B Petrof, M Narusawa, JM Leferovich, JT Sladky, and AM Kelly (1991) The mdx mouse diaphragm reproduces the degenerative changes of Duchenne muscular dystrophy. Nature, 352: 536-538.

Sterling K and PO Milch (1975) Thyroid hormone binding by a component of mitochondrial membrane. Proc. Natl. Acad. Sci. USA, 72: 3225-3229.

Sterling K, GA Campbell, GS Taliadouros, and EA Nunez (1984a) Mitochondrial binding of triiodothyronine (T3). Demonstration by electron-microscopic radioautography of dispersed liver cells. Cell Tissue Res., 236: 321-325.

Sterling K, GA Campbell, and MA Brenner (1984b) Purification of the mitochondrial triiodothyronine (T3) receptor from rat liver. Acta Endocrinol., 105: 391-397.

Stockdale FE (1992) Myogenic cell lineages. Dev. Biol., 154: 284-298.

Tanswell AK, MG Joneja, J Lindsay, and E Vreeken (1983) Differentiation-arrested rat fetal lung in primary monolayer cell culture. I. Development of a differentiation-arrested and growth-supporting culture system using carbon-stripped bovine fetal calf serum. Exp. Lung Res., 5: 37-48.

Tapscott SJ, RL Davis, MJ Thayer, PF Cheng, H Weintraub, and AB Lassar (1988) MyoD1: A nuclear phosphoprotein requiring a myc region to convert fibroblasts to myoblasts. Science, 242: 405-411.

Thomas MR, JP Miell, AM Taylor, RJM Ross, JR Arnao, DE Jewitt, and AM McGregor (1993) Endocrine and cardiac paracrine actions of insulin-like growth factor-I (IGF-I) during thyroid dysfunction in the rat: is IGF-I implicated in the mechanism of heart weight/body weight change during abnormal thyroid function? J. Mol. Endocrinol., 10: 313-323.

Ullman M and A Oldfers (1991) Skeletal muscle regeneration in young rats is dependent on growth hormone. J. Neurol. Sci., 106: 67-74.

Voytik SL, M Przyborski, SF Badylak, and S Konieczny (1993) Differential expression of muscle regulatory factor genes in normal and denervated adult rat hindlimb muscles. Dev. Dynamics, 98: 214-224.

Wakayama Y (1976) Electron microscopic study on the satellite cell in the muscle of Duchenne muscular dystrophy. J. Neuropath. Exp. Neurol., 35: 532-540.

Webster C and HM Blau (1990) Accelerated age-related decline in replicative life-span of Duchenne muscular dystrophy myoblasts: implications for cell and gene therapy. Somatic Cell Molec., 16: 557-565.

Weintraub H, R Davis, S Tapscott, M Thayer, M Krause, R Benezra, TK Blackwell, D Turner, R Rupp, and S Hollenberg (1991) The MyoD gene family: nodal point during specification of the muscle cell lineage. Science, 251: 761-766.

Weintraub H (1993) The MyoD family and myogenesis: redundancy, networks, and thresholds. Cell, 75: 1241-1244.

Wentworth B, MJ Donoghue, J Engert, E Berglund, and N Rosenthal (1991) Paired MyoD binding sites regulate myosin light chain gene expression. Proc. Natl. Acad. Sci. USA., 88: 1242-1246.

Whalen RG, K Schwartz, P Bouveret, SM Sell, and F Gros (1979) Contractile protein izozymes in muscle development: identification of an embryonic form of myosin heavy chain. Proc. Natl. Acad. Sci. USA, 76: 5197-5201.

White TP and KA Esser (1989) Satellite cell and growth factor involvment in skeletal muscle growth. Med. Sci. Sport. Exerc., 21: S158-S163.

Williams BO, EM Schmitt, L Remington, RT Bronson, DM Albert, RA Weinberg, and T Jacks (1994) Extensive contribution of Rb-deficient cells to adult chimeric mice with limited histopathological consequences. EMBO J., 13: 4251-4259.

Wong A, KL Garrett, and JE Anderson (1997) Myoid cell density in the thymus is lower during mdx dystrophy and is reduced after muscle crush-injury. (in prep).

Write WE, DA Sassoon, and VK Lin (1989) Myogenin, a factor regulating myogenesis, has a domain homologous to MyoD. Cell, 56: 607-617.

Yablonka-Reuveni Z and M Nameroff (1987) Skeletal muscle cell populations. Separation and partial characterization of fibroblast-like cells from embryonic tissue using density centrifugation. Histochemistry, 87: 27-38.

Yablonka-Reuveni Z (1988) Discrimination of myogenic and nonmyogenic cells from embryonic skeletal

muscle by 90 degrees light scattering. Cytometry, 9: 121-125.

Yablonka-Reuveni Z and AJ Rivera (1994) Temporal expression of regulatory and structural muscle proteins during myogenesis of satellite cells on isolated adult rat fibers. Dev. Biol., 164: 588-603.

Yablonka-Reuveni Z and AJ Rivera (1997) Influence of PDGF-BB on proliferation and transition through the MyoD-myogenin-MEF2A expression program during myogenesis in mouse C2 myoblasts: An analysis of cell phenotypes. Growth Factors, in press.

Yamada S, N Buffinger, J DiMario, and RC Strohman (1989) Fibroblast growth factor is stored in fiber extracellular matrix and plays a role in regulating muscle hypertrophy. Med. Sci. Sports Exerc., 21: S173-S180.

Yen PM, DS Darling, RL Carter, M Forgione, PK Umeda, and WW Chin (1992) T3 decreases binding to DNA by T3-receptor homodimers but not receptor-auxiliary protein heterodimers. J. Biol. Chem., 267: 3565-3568.

Yu VC, C Delsert, B Anderson, JM Holloway, O Devary, A Naar, S Kim, J-M Boutin, C Glass, and MG Rosenfeld (1991) RXRß: a coregulator that enhances binding of retinioc acid, thyroid hormone, and vitamin D receptors to their cognate response elements. Cell, 67: 1251-1266.

Zacharias JM and JE Anderson (1991) Muscle regeneration after imposed injury is better in younger than older dystrophic mice. J. Neurol. Sci., 104: 190-196.

Zhang M and IS McLennan (1994) Use of antibodies to identify satellite cells with a light microscope. Muscle Nerve, 17: 987-994.

Zhang XK, KN Wills, M Husmann, T Hermann, and M Pfahl (1991) Novel pathway for thyroid hormone receptor action through interaction with jun and fos oncogene activities. Mol. Cell. Biol., 11: 6016-6025.

Zhang XK, B Hoffman, PBV Tran, G Graupner, and M Pfahl (1992) Retinoid X receptor is an auxillary protein for thyroid hormone and retinoic acid receptors. Nature, 355: 441-449.

Appendix #1

Hyperthyroidism impairs early repair in normal but not dystrophic *mdx* mouse tibialis anterior muscle. An in vivo study

A.N. Pernitsky, L.M. McIntosh, and J.E. Anderson

Abstract: The effect of hyperthyroidism on muscle repair was examined in *mdx* and control mice injected with triiodothyronine (T3) for 4 weeks. On day 24 of treatment, the right tibialis anterior (TA) muscle was crush-injured; 3 days later, mice received intraperitoneal [^{3}H]thymidine to label newly synthesized DNA. One day later, muscles from both limbs were removed to study the severity of dystrophy (uncrushed muscle) and the regeneration response (crushed muscle). In uncrushed TA muscle, the area of active dystrophy (fiber damage and infiltration as a proportion of muscle cross-sectional area) was reduced by half after T3 treatment. Uncrushed muscle fiber diameter was lower in T3-treated control muscles. In crushed muscles, the diameter of new myotubes was larger in *mdx* mice than in controls and was reduced after T3 treatment in control regenerating muscle. In the same muscles, developmental myosin heavy chain was present in new myotubes and in small numbers of mononuclear cells (possibly differentiating myoblasts) near new myotubes and surviving fibers. Myotube density in the regenerating muscles was not changed by T3 treatment, although the number of myotube nuclei per field was decreased in control and increased in *mdx* T3-treated mice. Results extend previous reports of T3 effects on dystrophy and the strain difference in muscle precursor cell (mpc) proliferation. The results also suggest the hypothesis that excess T3 affects muscle regeneration either by reducing mpc proliferation or by increasing mpc fusion early in regeneration in control and *mdx* muscle.

Key words: hyperthyroid, muscle regeneration, crush injury, proliferation, *mdx* mouse.

Résumé : L'effet d'une hyperthyroïdie sur la régénération musculaire a été étudié chez des souris *mdx* et des souris témoins ayant reçu des injections de triiodothyronine (T3) pendant 4 semaines. Au 24e jour du traitement, le muscle jambier antérieur droit a été écrasé; 3 jours après cette blesssure, les souris ont reçu une injection intrapéritonéale de [^{3}H]thymidine afin de marquer l'ADN nouvellement synthétisé. Le jour suivant, les muscles des deux pattes ont été prélevés afin de déterminer l'intensité de la dystrophie (muscle non écrasé) et le degré de régénération (muscle écrasé). La surface de dystrophie active dans le muscle jambier antérieur non écrasé (proportion de fibres endommagées et infiltrées dans une coupe transversale du muscle) est réduite de moitié à la suite des injections de T3. Le diamètre des fibres des muscles non écrasés est plus petit dans les muscles des souris témoins traitées avec la T3. Le diamètre des nouveaux myotubes est plus gros dans les muscles écrasés des souris *mdx* que dans ceux des souris témoins et il est réduit dans les muscles en régénération des sosuris témoins traitées avec la T3. La chaîne lourde de la myosine de type foetal est présente dans les nouveaux myotubes des muscles en régénération et dans un petit nombre de cellules mononuclées (probablement des myoblastes en cours de différenciation) près des nouveaux myotubes et des fibres survivantes. La densité des myotubes dans les muscles en régénération n'est pas modifiée par les injections de T3, même si le nombre de noyaux de myotubes par champ diminue dans les muscles des souris témoins et augmente dans ceux des souris *mdx* traitées avec la T3. Ces résultats s'ajoutent à ceux déjà publiés au sujet des effets de la T3 sur la dystrophie et de la prolifération des cellules souches musculaires de différentes souches de souris. Ils suggèrent également qu'un excès de T3 affecterait la régénération musculaire soit en réduisant la proliférationon des cellules souches musculaires, soit en augmentant leur fusion précoce au cours de la régénération des muscules des sosuris *mdx* et des souris témoins.

Mots clés : hyperthyroïde, régénération musculaire, blessure par écrasement, prolifération, souris *mdx*.

[Traduit par la rédaction]

A.N. Pernitsky, L.M. McIntosh, and J.E. Anderson.[1] Department of Anatomy, University of Manitoba, 730 William Avenue, Winnipeg, MB R3E 0W3, Canada.

[1] Author to whom all correspondence should be addressed.

Introduction

The *mdx* mouse model for X-linked Duchenne muscular dystrophy (DMD) (Bulfield et al. 1984) is invaluable for the study of regeneration in dystrophin-deficient (Hoffman et al. 1987) muscle. It has been suggested that *mdx* muscle responds to segmental fiber damage by a larger than normal proliferative response (Anderson et al. 1987), which compensates for ongoing dystrophy. This proliferation may be due in part to an altered control of myogenesis in view of the large amount of a key mitogen, basic fibroblast growth factor (bFGF) (Gospodarowicz et al. 1976), observed in *mdx* muscles (Anderson et al. 1991). bFGF is much lower in DMD or other human muscle neuromuscular disease biopsy samples (Anderson et al. 1993) while it is co-expressed with muscle regulatory genes like myogenin in regenerating *mdx* muscles (Garrett and Anderson 1995).

It is known that DMD muscle precursor cells (mpc) do not proliferate as well in vitro as normal human mpc (Webster and Blau 1990). However, *mdx* mpc proliferation in vivo (Anderson et al. 1987; Zacharias and Anderson 1991; McIntosh and Anderson 1995) and in vitro (Anderson 1991) can compensate for substantial fiber damage resulting from dystrophy and (or) crush injury. If the difference in regenerative capacity between DMD and *mdx* muscle involves mpc cycling, then alteration of proliferation may help to elucidate that distinction. Hyperthyroidism has been shown to increase regions of fiber damage in the soleus and cardiac (but not fast-twitch) muscles of *mdx* mice, possibly in relation to a slow-to-fast transition in myosin heavy chains (MHC), expressed by the soleus (Izumo et al. 1986), increased cardiac work and cardiomyocyte hypertrophy (Anderson et al. 1994a). As well, the relative tissue bFGF content is lower in hyperthyroid muscle. However, it has not been determined if hyperthyroidism had a specific effect on muscle regeneration. Since bFGF expression is down-regulated by excess thyroid hormone (TH) (Liu et al. 1993) and the expression of two muscle regulatory genes, MyoD and myogenin (Muscat et al. 1994; Downes et al. 1993), are stimulated by TH, this hormone has been used to alter proliferation and differentiation in regenerating *mdx* and control muscle.

We hypothesized that hyperthyroidism would impair the growth of new myotubes in regenerating control and *mdx* muscle, either by reducing mpc proliferation and (or) affecting mpc differentiation. To test the hypothesis, the incorporation of mpc nuclei into myotubes and parameters of myotube growth were examined in muscle during the synchronous regeneration resulting from a crush injury (Grounds and McGeachie 1989). The presence of developmental myosin heavy chain (devMHC), transiently and specifically expressed by new myotubes in regenerating muscle in vitro (Sartore et al. 1982) and in vivo (Marini et al. 1991; Davis et al. 1991), was used as a marker for new myotube formation. Autoradiography was used to localize myotube nuclei produced by mpc division in the 24-h period before sacrifice.

Materials and methods

Animals and treatment

Mdx dystrophic (C57BL10/ScSn *mdx*) and control (C57BL10/ScSn) mice were made hyperthyroid by triiodothyronine (T3)

injections (subcutaneous) at a dose of 2 μg/g body weight/day (Anderson et al. 1994a) for 4 weeks beginning at 5.5 weeks of age, after the maximum period of *mdx* fiber damage and repair (Anderson et al. 1987, 1988). Non-dystrophic control and *mdx* littermate mice were untreated for the same period; mice were housed according to the Canadian Council on Animal Care. Multiple experiments were performed to examine histology, myotube density, myotube and myofiber diameter, and devMHC localization and to quantify myoblast proliferation and fusion into myotubes. Sections were omitted if they were not in the required orientation (see below) for assessing different parameters, which accounts for the reported variation in group size (control, untreated, $n = 2$–5; control, T3 treated, $n = 2$–7; *mdx*, untreated, $n = 3$–8; *mdx*, T3 treated, $n = 4$–8).

After 3.5 weeks of treatment, mice were anesthetized (ketamine:xylazine, 1:1, 0.01 cc/10 g body weight) and subjected to a crush injury (Grounds and McGeachie 1989) of the right or both tibialis anterior (TA) muscles. Three days later, mice received [^{3}H]thymidine (Amersham Inc., Oakville, Ont.) (2 μCi/g (1 Ci = 37 GBq) intraperitoneal injection) to label DNA synthesis. One day later (4 days after the crush injury) and under ether anesthesia, the TA muscles were removed rapidly from mice, oriented in Tissue Tek O.C.T. compound (uncrushed TA in cross section and crushed TA longitudinally), and frozen for cryosectioning (8 μm). Soleus and gastrocnemius muscles were dissected from both limbs and weighed to document T3 effects on muscle mass. Alternate serial sections were coded and stained with hematoxylin and eosin (H&E) for morphometric studies, immunostained to localize devMHC (Davis et al. 1991), or prepared for autoradiography.

Uncrushed muscles

Morphometry

In the uncrushed TA muscles, one set of H&E-stained cross sections was used to determine myofiber diameter using a calibrated computerized graphics tablet and the SigmaScan program (Jandel Scientific, Corte Madera, Calif.), as previously reported (Anderson et al. 1994a). *Mdx* uncrushed TA muscles were also examined for the proportionate area of active dystrophy (area of fiber disruption and inflammation as a proportion of muscle cross-sectional area) and the number of foci of active dystrophy per cross section (normalized to area). The proportion of fibers with central nuclei (centronucleation), an index of previous fiber regeneration from dystrophy (Karpati et al. 1988), was also determined. The mean and standard error (SEM) were determined for each parameter, and the frequency distribution of fiber diameter in each group was plotted. Sections were viewed and photographed using an Olympus photomicroscope and TMAX400 B&W film (Kodak).

Crushed muscles

Morphometry

H&E-stained sections were used to examine the extent of regeneration in predefined zones of injured muscle. Data for each zone were averaged from all myotubes observed in microscope fields in the necrotic crushed muscle (crush zone, 2 fields), the adjacent area of mononuclear cells and new myotube formation (adjacent zone, 4 fields), and the surviving

muscle furthest from the crush site (surviving zone, 3 fields) exactly as reported (McIntosh et al. 1994, after Mitchell et al. 1992). The crush, adjacent, and surviving zones of injured TA were examined in 200× fields, corresponding to $4.4 \times 10^5 \ \mu m^2$ of tissue area. Selected fields were strictly examined at preset distances from the geometric centre of the necrotic crush zone follows. The crush zone was sampled in 2 fields in a horizontal row across the muscle. Fields in the adjacent zone were sampled at a width of 1 field diameter either proximal (toward the knee, 3 fields) or distal (toward the ankle, 1 field) from the crush zone. Fields in the surviving zone were sampled either 1 field diameter proximal (2 fields) or 1.5 field diameters distal (1 field) to the adjacent zone. Sampling was carried out systematically to standardize analysis, taking into account the architecture of the TA muscle.

The area of the central necrotic portion of the crushed muscle, surrounded by many mononuclear cells, was measured using SigmaScan. In addition, the mean ($\pm$ SEM) density of small myotubes in each zone (the number of myotubes per field averaged over the fields in that zone) and myotube diameter (and frequency distribution) in the adjacent zone were determined.

Immunostaining
A separate set of sections was blocked with a solution of 10% horse serum and 1% bovine serum albumin in phosphate-buffered saline (0.01 M) for 1h and incubated overnight with a monoclonal antibody against devMHC (diluted 1:5), a gift from Dr. L.V.B. Anderson, or 1:250 dilution of the same antibody (Novocastra Inc., Newcastle, UK). According to standard methods (Anderson et al. 1991), antibody binding was detected using biotinylated goat anti-mouse antibody (1:100) and Texas Red – streptavidin (Amersham Inc., Oakville, Ont.). Negative controls for immunostaining included the omission of primary or secondary antibodies in each staining experiment. Fluorescence for devMHC was viewed along with phase contrast to examine myotube structure.

Autoradiography
One set of crushed *mdx* and control TA muscle sections (from untreated and T3-treated mice) were prepared for autoradiography as previously reported (McIntosh and Anderson 1995). The incorporated [^{3}H]thymidine was allowed to expose the emulsion in darkness for 6 weeks at 4°C. Autoradiograms were developed, fixed, and stained with modified Gomori's trichrome. In coded sections, counts were made of the number of nuclei in new myotubes within the adjacent zone as follows. The above sampling method of fields and zones (McIntosh et al. 1994) was modified to examine 400× fields using an ocular grid ($3.53 \times 10^4 \ \mu m^2$ in area at 400×). Two rows of 3 fields each were sampled in the adjacent zone proximal from the crush, and two rows of 3 fields each were sampled distal to the crush. The proportion of labelled (more than five grains per nucleus) myotube nuclei and the mean ($\pm$ SEM) number of nuclei per field were counted as an indicator of myoblast fusion that had occurred over 4 days of muscle regeneration.

Statistics
Differences in data (mean $\pm$ SEM) from each group or time point were tested using two-way analysis of variance (ANOVA) to study the effects of strain (*mdx* versus control), T3 treatment, and the interaction between strain and T3. Duncan's test was used post hoc where appropriate to compare individual group means. A Student's *t*-test (unpaired) was used to compare *mdx*-treated and untreated groups where appropriate. Chi-square statistics were used to assess differences in the frequency distribution of the diameter of myofibers or myotubes between groups. In all cases, a probability of $p < 0.05$ was used to accept a difference as significant.

Results

Uncrushed muscles
Gastrocnemius mass was greater in *mdx* mice than in treatment-matched control mice (Table 1) and was reduced after T3 treatment in both strains ($p < 0.01$). Soleus mass was also lower ($p < 0.01$) after T3 treatment in *mdx* mice but not in control mice. TA muscle weight was previously reported to decrease in hyperthyroid control and *mdx* mice (Anderson et al. 1994a).

Fiber diameter did not differ between control and *mdx* TA muscle. However, fiber diameter was lower in control TA muscle after T3 treatment, according to changes in the mean ($p < 0.01$, Table 1) and frequency distribution ($p < 0.05$, df = 118, Chi-squared, Fig. 1A). In comparison, the mean and distribution of fiber diameter in *mdx* TA muscles were not changed by T3 treatment (Fig. 1B, Table 1).

In *mdx* mice, the area of active dystrophy (as a proportion of muscle area) was significantly decreased (by half) after T3 ($p < 0.05$, Table 1), although the number of foci of damage per section was not changed. As expected, T3 treatment did not change fiber centronucleation, an index of previous fiber repair (Table 1), likely resulting from the use of older mice (5.5 weeks old) with relatively advanced dystrophy and regeneration at the start of treatment.

Crushed muscles
In regenerating TA muscle, the area of the crush zone did not differ between control and *mdx* muscles and was not affected significantly by T3 treatment (Table 2). Myotubes in the adjacent zone had greater diameter ($p < 0.01$) in *mdx* muscle than in control TA muscle, regardless of treatment (Figs. 1, 2). Myotube density in the proximal surviving zone of control TA muscle was lower after T3 treatment ($p < 0.05$) (Table 2), although it was not changed in adjacent zone fields (Table 2). However, myotube diameter in control TA muscle was significantly reduced by T3 treatment (mean, Table 2; distribution, $p < 0.001$, Chi-square, Figs. 1C, 1D). *mdx* myotube diameter was not affected by T3.

Immunofluorescence for devMHC was absent from sections where either a primary or secondary antibody was omitted (not shown). In stained sections, small myotubes were seen as elongated cells with brightly fluorescent sarcoplasm containing multiple non-fluorescent central nuclei. Surviving fibers in muscle of control and *mdx* mice did not fluoresce (Figs. 3A–3D). In the larger (typically *mdx* not control) devMHC-positive myotubes, fluorescence was oriented in narrow longitudinal bands that often had sarcomeric periodicity (Fig. 3D) around many closely packed nuclei. The identification of multinucleated myotubes with early sarcomere formation was confirmed in phase-contrast observations of the

Fig. 1. The frequency distributions of myofiber diameters from control and *mdx* uncrushed TA muscle (top row) and of myotube diameters from control and *mdx* crushed TA muscle (bottom row). Untreated (solid bars) and T3-treated (cross-hatched bars) groups are indicated. There was a significant shift toward smaller fibers in control myofiber (A) and myotube (C) diameters with T3 treatment in controls, whereas T3 had no effect on the diameter of *mdx* unoperated myofibers (B) or myotubes (D). The numbers of myofibers and myotubes measured in each group are given in Tables 1 and 2, respectively.
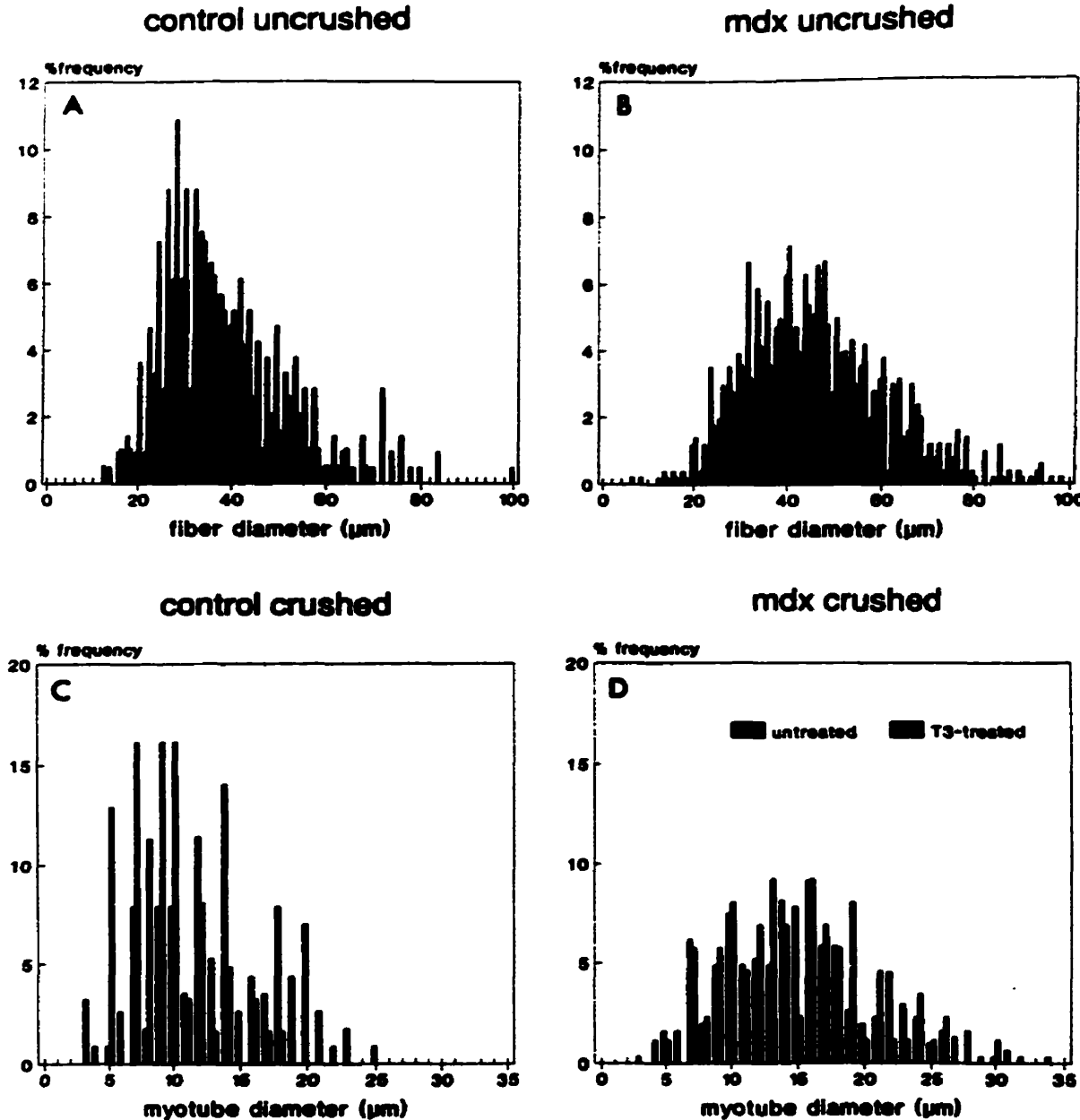
same sections and in H&E-stained serial sections of the same region.

In addition, both control and *mdx* crushed TA demonstrated a small number of ovoid or fusiform mononuclear cells, ranging from 10 to 25 μm in diameter, that also contained devMHC-positive cytoplasm (Figs. 3A, 3D). The devMHC-positive mononuclear cells had a nucleus-to-cytoplasm ratio of about 1:1. The cells were distinguished from endothelial cells around small capillaries and fibroblasts by their shape and

location between or near devMHC-positive myotubes. Fewer of the devMHC-positive mononuclear cells were present in the surviving zone than in the adjacent zone, and there they were closely juxtaposed with devMHC-negative surviving fibers (Figs. 3B, 3D). Where direct close contact was apparent, the sarcoplasm of a devMHC-positive mononuclear cell and a surviving fiber were clearly delineated by the distinct absence of devMHC fluorescence from the sarcoplasm of the older fiber (Fig. 3B). Often the fluorescent mononuclear cells

Table 1. Morphometry data for uncrushed TA, soleus, and gastrocnemius muscles in control and *mdx* groups with and without 4 weeks treatment with T3.

	Control, untreated	Control, T3 treated	*Mdx*, untreated	*Mdx*, T3 treated
Muscle mass (mg)[b]				
Soleus	8.0 ± 0.6 (10)[a]	10.5 ± 1.0 (13)	8.1 ± 0.5 (16)	4.6 ± 0.6 (24)[*†]
Gastrocnemius	126.5 ± 3.8 (10)	114.2 ± 3.3 (13)[*]	152.0 ± 5.5 (16)[†]	127.7 ± 4.5 (24)[*†]
Fiber diameter (μm)[c]	42.1 ± 2.2 (3)	31.5 ± 3.5 (3)[*]	43.1 ± 1.8 (4)	45.5 ± 2.6 (7)[†]
[no. measured]	[213]	[193]	[256]	[509]
Dystrophy (% area),[c]	—	—	2.17 ± 0.6 (6)	1.00 ± 0.3 (6)[*]
no. of foci (no./section)[c]	—	—	6.14 ± 1.11 (7)	5.67 ± 1.72 (6)
Centronucleation (CN)				
(% CN/total)[c]	0.6 ± 0.2 (5)	0.7 ± 0.3 (3)	75.8 ± 3.2 (7)[†]	73.2 ± 2.2 (9)[†]

Note: [*], significant difference from untreated group of same strain ($p < 0.05$); [†], significant difference from control group with same treatment ($p < 0.05$).
[a]Data are mean ± SEM.
[b]Number in parentheses represents number of muscles.
[c]Number in parentheses represents number of animals.

Table 2. Morphometry and autoradiography data for crushed TA muscles in control and *mdx* groups with and without 4 weeks treatment with T3.

	Control, untreated	Control, T3 treated	*Mdx*, untreated	*Mdx*, T3 treated
Area of crush (× 10³ μm²)[a]	67.6 ± 22.4 (6)[a]	38.9 ± 12.9 (6)	51.5 ± 13.1 (10)	27.2 ± 10.0 (8)
Myotube density (no./field)[b]				
Crush zone	5.0 ± 1.0 (3)	7.0 ± 3.0 (2)	7.8 ± 3.1 (6)	5.0 ± 1.5 (3)
Adjacent zone				
Proximal	12.0 ± 2.1 (3)	18.0 ± 5.0 (2)	17.0 ± 3.6 (6)	13.0 ± 7.2 (3)
Distal	17.7 ± 7.6 (3)	12.5 ± 3.5 (2)	21.3 ± 6.9 (6)	11.7 ± 8.0 (3)
Surviving zone				
Proximal	5.0 ± 2.6 (3)	0 (2)[*]	3.5 ± 1.2 (6)	2.0 ± 0.6 (3)[†]
Distal	14.0 ± 3.0 (2)	9.0 ± 5.0 (2)	12.5 ± 2.9 (6)	11.7 ± 9.7 (3)
Myotube diameter (μm)[b]	12.8 ± 1.0 (4)	8.5 ± 0.7 (4)[*]	14.8 ± 0.8 (8)[†]	13.9 ± 0.4 (6)[†]
Labelled myotube nuclei total (%/field)[c]	44.0 ± 3.6 (27)	40.8 ± 3.4 (22)	32.5 ± 2.5 (71)[†]	34.9 ± 3.9 (21)
Proximal	40.3 ± 4.5 (16)	35.5 ± 4.8 (9)	33.5 ± 3.7 (37)	33.9 ± 5.0 (10)
Distal	48.9 ± 6.6 (9)	44.4 ± 4.8 (12)	31.9 ± 3.7 (34)[†]	35.8 ± 6.3 (11)
Number of myotube nuclei (no./field)[c]	15.7 ± 1.2 (26)	12.1 ± 1.7 (22)[*]	14.3 ± 0.9 (69)	18.3 ± 2.2 (21)[†]

Note: [*], significant difference from untreated group of same strain ($p < 0.05$); [†], significant difference from control group with same treatment ($p < 0.05$).
[a]Data are mean ± SEM.
[b]Number in parentheses represents number of animals.
[c]Number in parentheses represents number of fields.

were elongated, apparently extending toward a new myotube (Figs. 3B, 3D). Muscle spindle fibers also contained devMHC fluorescence (not shown).

In the adjacent zone of crushed muscles (Table 2, Fig. 4), the proportion of labelled myotube nuclei was lower ($p < 0.01$, two-way ANOVA, df = 1136) in *mdx* muscle than in control crushed TA muscle and was unaffected by T3 in either strain. Comparison of fields proximal or distal to the crush suggested that the

difference in the proportion of labelled myotube nuclei between control and *mdx* TA was likely due to differences in the distal fields, as in a previous report (McIntosh and Anderson 1995). The number of myotube nuclei per adjacent zone field did not differ between control and *mdx* regenerating muscle. However, there were fewer nuclei in control myotubes after T3 treatment ($p = 0.02$ interaction, df = 1137) but increased numbers of nuclei in *mdx* myotubes in hyperthyroidism.

Fig. 3. Micrographs of developmental MHC immunostaining in crushed TA showing representative stages of myotube development. (A) Mononuclear cells (similar to the mononuclear cell in Fig. 2B), which are presumed to be myoblasts (pmb), and small myotubes (mt) in an untreated control TA are brightly stained with anti-devMHC, while a surviving fiber (S) does not fluoresce. (B) In a control T3-treated crushed TA, a very small devMHC-positive myotube (mt) is well delineated from the directly juxtaposed, unstained surviving myofiber (S). Other small myotubes in the same field are not attached to surviving fibers. (C) A differentiating myotube from an untreated *mdx* TA demonstrates early myofibril formation (arrow) around multiple internal nuclei (short arrows) that do not contain devMHC. (D) Sarcomeric striations (arrows) are present in a more differentiated myotube between two surviving fibers (S) in a T3-treated *mdx* TA. Two devMHC-positive mononuclear cells (pmb) are indicated: one appears to be extending towards a small diameter myotube. Bar, 20 μm; magnification, × 460.

Fig. 2. Myotubes in adjacent zones of crushed TA, 4 days post-injury. (A) Myotubes (large arrow) are present in the adjacent zone of an untreated control TA. Myotubes regenerating in an untreated *mdx* crushed TA (B) are larger in diameter and have more sarcoplasm than control myotubes (A). The *mdx* myotubes also contain many more nuclei than control myotubes after the same recovery period. A mononuclear cell with a round nucleus (small arrow) is seen close to the border of one myotube (B). H&E stain; bar, 20 μm; magnification, × 475.
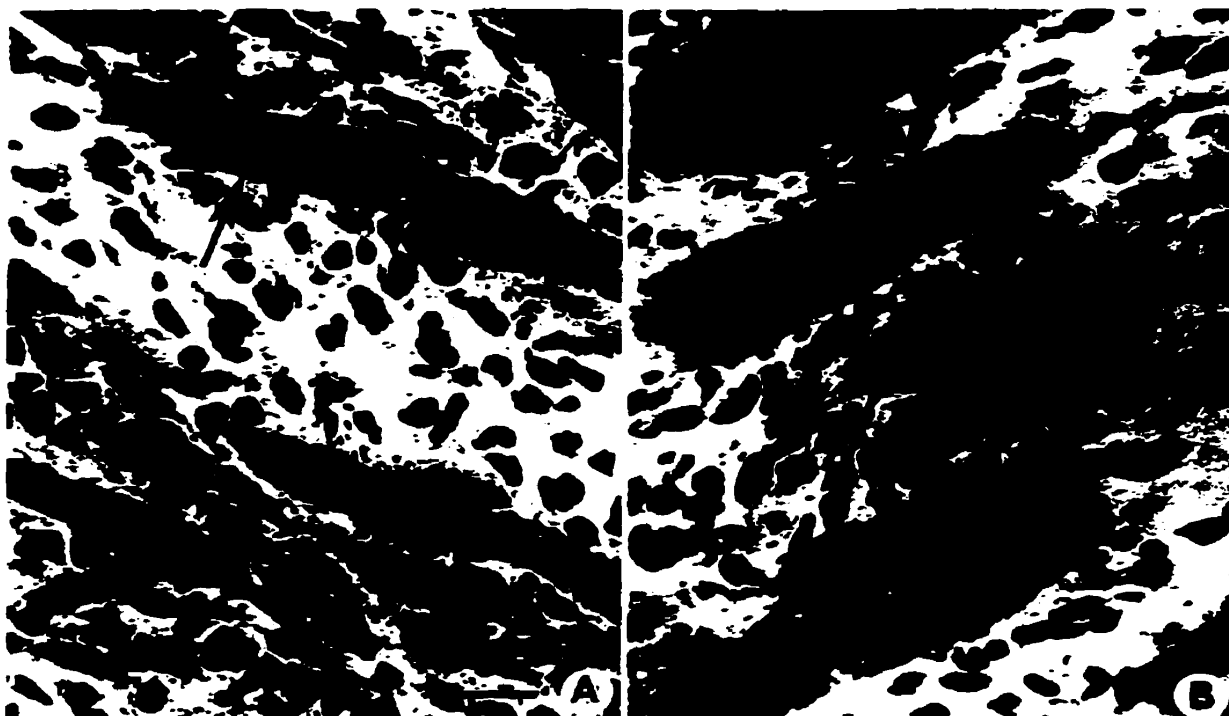
Discussion

The present results show that regeneration was more advanced in crushed *mdx* muscle than in control crushed muscle: specifically, regenerating *mdx* myotubes had a larger diameter with similar numbers of myotube nuclei compared with control myotubes in untreated mice after the same interval of recovery. Hyperthyroidism interfered with muscle repair by different means in control and *mdx* mice. In control regenerating TA muscle, myotube density was decreased in the surviving zone, where repair is stimulated at a distance from the primary site of injury (McIntosh and Anderson 1995). As well, myotube growth (diameter) and the number of nuclei in those myotubes were significantly lower in hyperthyroid than in untreated control muscles. Those changes were not observed in *mdx* regenerating muscle after T3 treatment. Recent mpc proliferation and fusion in control muscle were not significantly affected by T3 treatment. In *mdx* TA muscle by contrast, T3 treatment

actually increased the number of nuclei in myotubes, without effects on myotube diameter, myotube density, or mpc proliferation and fusion in the final day of regeneration. The results suggest that *mdx* mpc have a greater resistance to a treatment that is deleterious to control muscle repair. T3 treatment may reduce control mpc proliferation but does not impair fusion per se and has the general consequence of reducing myotube growth. Thus, although lower mpc proliferation in a regenerative response may be expected to result in the formation of fewer myotubes, the effect of T3 in this study decreased myotube diameter in the area of most intense repair in control muscle and only reduced myotube density in a zone distant from the original injury.

Hyperthyroid-induced fiber atrophy may play a role in decreasing myotube growth since muscle mass and fiber diameter in uncrushed muscles were reduced with T3 treatment (Anderson et al. 1994a; this study). In hyperthyroid control TA, there was a decreased density of new myotubes in the
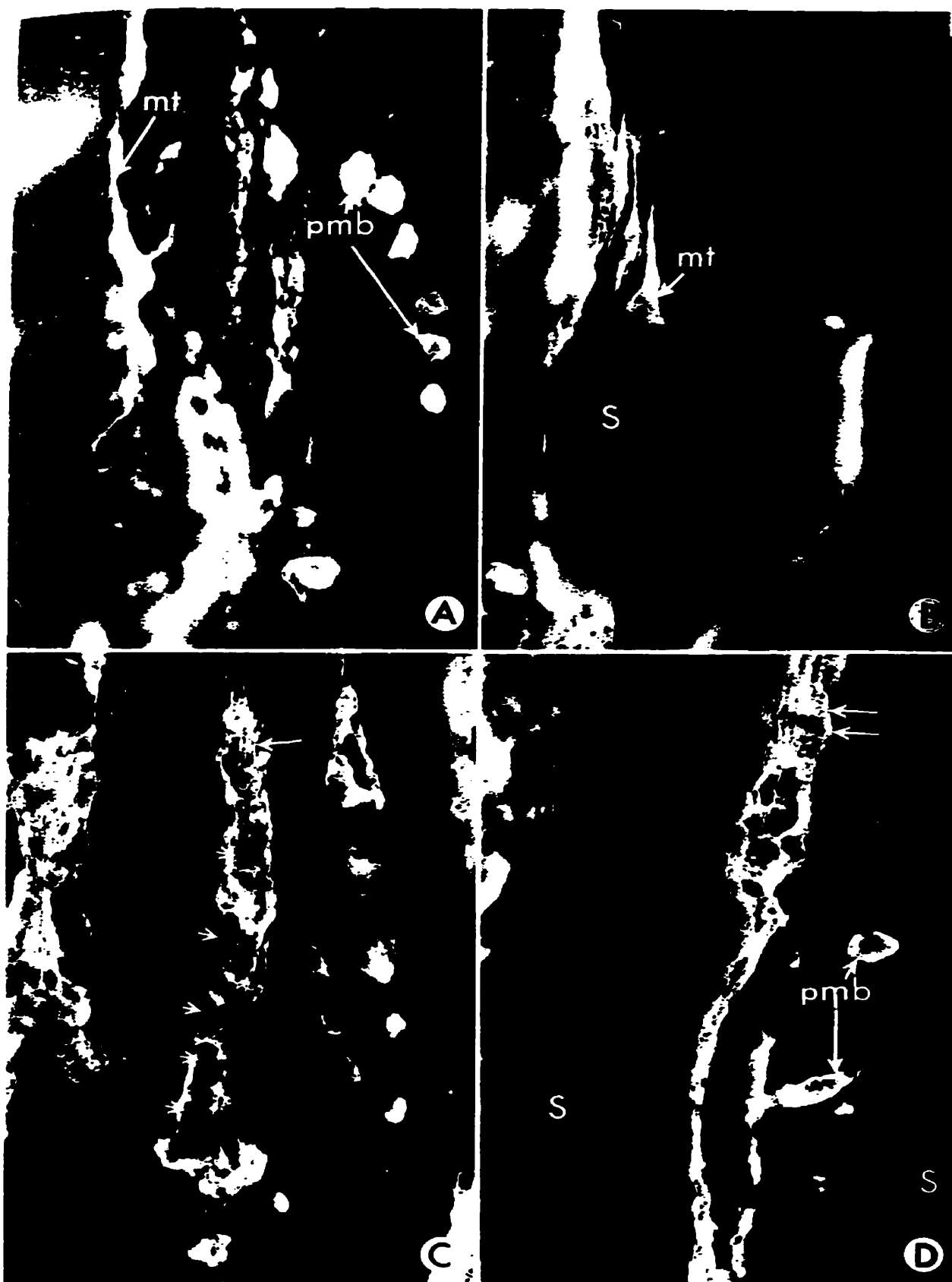
Fig. 4. Autoradiographs of the adjacent zone of TA 4 days after crush injury. (A) In the untreated control TA, most myotube nuclei (large arrows) are labelled by silver grains, as are some large, round (small arrow) mononuclear cells and other smaller ones. (B) Mdx untreated crushed muscle contains large myotubes with many unlabelled (arrowheads) nuclei and some labelled (large arrow) nuclei. Again, some large, round (small arrows) mononuclear cell nuclei are labelled. Note that the grains are in focus and lie above the tissue. Gomori trichrome stain; bar, 20 μm; magnification, × 500.
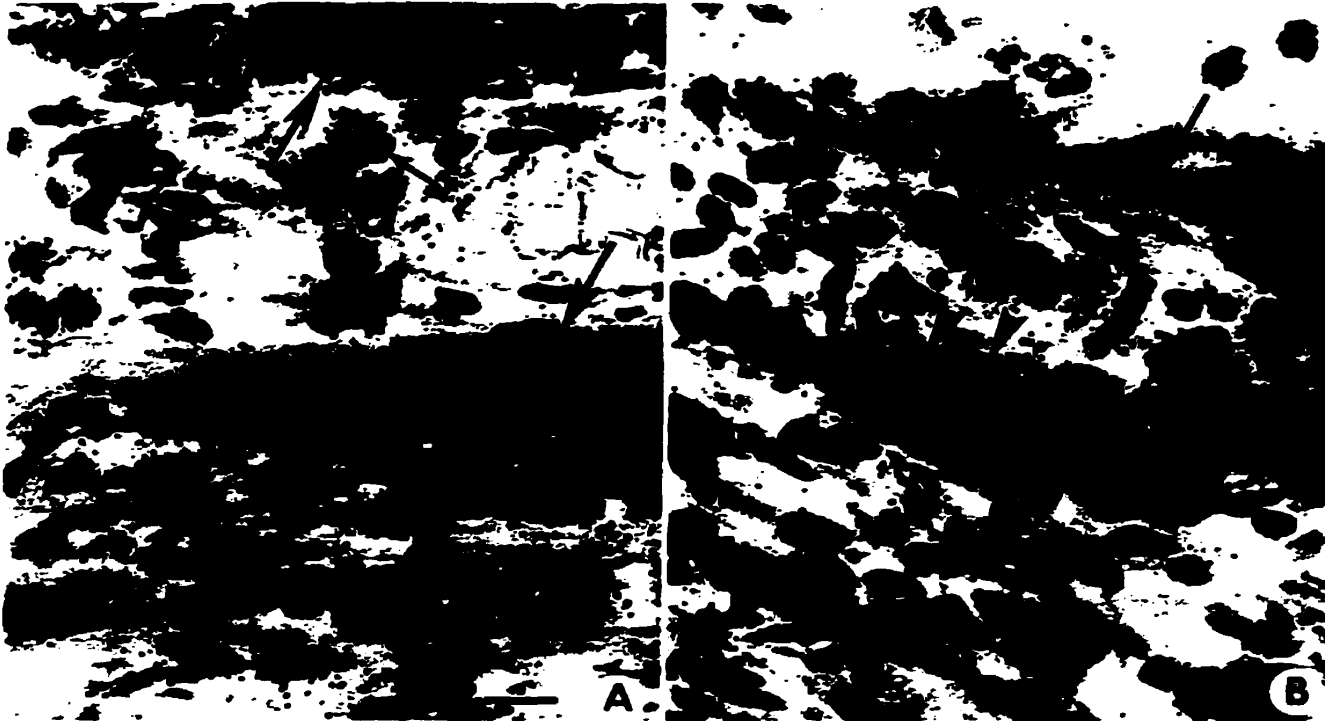
surviving zone. However in *mdx* muscle, myotube growth was not decreased by hyperthyroidism. These results differ from the changes noted in muscle repair under hypothyroid conditions, where myotube density was lower in the distal adjacent zone particularly in *mdx* TA muscle (McIntosh et al. 1994). Hypothyroidism resulted in prolonged and increased *mdx* mpc proliferation and delayed myotube formation in both normal and dystrophic TA muscle (McIntosh and Anderson 1995). Indeed, the presence of new (devMHC-positive) myotubes per se in surviving control fields is interesting, since new myotubes would not typically be expected in surviving non-dystrophic muscle. Again, the observation (McIntosh and Anderson 1995) suggests that the effect of an injury to stimulate mpc proliferation and fusion can be quite far removed from the primary insult to muscle fibers. The distant impact was the only obvious (i.e., myotubes versus none) effect of excess T3 on control muscles, despite the net reduction in mpc proliferation and fusion in the adjacent zone (fewer myotube nuclei per field). In control regenerating TA muscles, it is clear that the reduction in new myotube diameter and lower accumulated incorporation of nuclei within myotubes support the idea that myoblast proliferation and fusion during the early phase of repair (prior to 3 days when [³H]thymidine was injected) may be impaired in hyperthyroidism.

Significant differences in the histology of tissue repair were found between *mdx* and control strains in this study. Myotube diameter in the adjacent zone of crushed muscles (easily distinguished from larger myofibers and previously regenerated

myotubes in the surviving zone using anti-devMHC immunostaining) was always greater in regenerating *mdx* than control TA, regardless of treatment. There may be more favourable growth conditions or faster mitotic cycling and fusion of muscle precursors in *mdx* than control muscles (Anderson et al. 1988). The apparently superior *mdx* response to injury is consistent with previous reports of repair under a variety of conditions (DiMario et al. 1989; Anderson et al. 1991; Zacharias and Anderson 1991; McIntosh et al. 1994) and may derive in part from the action of mitogens including bFGF (DiMario et al. 1989; Anderson et al. 1991, 1993, 1995). The limited effects of T3 on cellular parameters of *mdx* muscle repair after injury are also consistent with the strain differences in bFGF content (DiMario et al. 1989; Anderson et al. 1991) particularly in new myotubes (Anderson et al. 1991). The down-regulation of bFGF by excess T3 (Gospodarowicz et al. 1987; Liu et al. 1993) might have a smaller or more transient effect on mpc proliferation and differentiation in *mdx* than in control regenerating muscle, consistent with the positive relationship between relative bFGF content and muscle repair capacity in two other mouse strains (Anderson et al. 1995).

Thyroid and growth hormone (GH) are both required for normal muscle development and growth, and thyroid hormone also influences the GH-insulin-like growth factor I (IGF-I) axis (Rodriques-Arnao et al. 1993; Thomas et al. 1993). Ullman and Oldfers (1991) demonstrated that GH is required for muscle repair in young rats and for normal skeletal muscle growth in vivo. GH also promotes differentiation of mpcs

transfected from 10T1/2 cells in vitro (Nixon and Green 1984). T3 negatively influences GH gene expression in rats (Cattini et al. 1986) and humans (Morin et al. 1990), so excess T3 could impact on muscle repair via GH. GH-mediated effects, which may contribute to fiber hypertrophy and repair in *mdx* mice ⋯ ⋯ ⋯ n et al. 1994*b*), are compounded by influences on ⋯ ⋯ Daughaday and Rotwein 1989), a mitogen that pro-⋯ ⋯ differentiation (Florini et al. 1986; Rodriques-Arnao et al. 1993). Indeed, since the area of active dystrophy was reduced by half in hyperthyroid *mdx* TA, as opposed to an increase in hyperthyroid *mdx* soleus and cardiac muscle (Anderson et al. 1994a), there may be a fiber-type specific influence of metabolism on mpc responses to fiber injury.

New myotube formation by mpc fusion is clearly critical in determining the effectiveness of muscle repair, and the magni-
⋯e of the response was easily observed by immunostaining ⋯r developmental MHC. Although the identity of the mononuclear cells that also contained devMHC is not certain, the cells are very likely myogenic since they contain a muscle-specific sarcomeric protein as reported for "differentiating myoblasts" (Robertson et al. 1990). The close juxtaposition with new myotubes, morphological features, and the observation that some devMHC-positive mononuclear cells are elongated and appear about to fuse with new myotubes or surviving fibers further suggest that devMHC-positive mononuclear cells may be presumed to be differentiated mpcs or myoblasts. Recent evidence showed that small numbers of mononuclear cells in *mdx* muscle in vivo, which are positive for myogenin mRNA by in situ hybridization, also contain the same devMHC (Garrett and Anderson 1995). That evidence supports the idea that mpcs may be devMHC-positive just before fusion into myotubes or myofibers. It is not known whether such differentiated muscle precursors can still proliferate before contributing to myotube formation and segmental fiber repair.

The present results demonstrate that *mdx* TA muscle maintains a larger regenerative capacity than control muscle under hyperthyroid conditions. The effects of T3 treatment on repair may be related partly to a larger than normal number of mpcs in non-injured *mdx* muscle as a consequence of dystrophy and repair (Zacharias and Anderson 1991), similar to previous comparisons between Duchenne and normal human muscle (Wakayama 1976). We made *mdx* muscle more similar to DMD by T3 treatment (Anderson et al. 1994a) and expected that a change in mpc numbers would be exhibited as reduced myotube number and growth in *mdx* muscle regenerating from a crush injury. However, those effects were only observed in control regenerating muscles. Therefore, if differences in myogenesis do account for the differences between DMD and *mdx* dystrophy, it is early during the mpc proliferation or cell cycling phase, not at the later phase of mpc and myotube differentiation where the differences will be apparent. The differences may originate early in muscle regulatory gene expression (e.g., MyoD and myf-5) or possibly in the proportion of mpcs that co-express those muscle regulatory genes and bFGF (Garret and Anderson 1995) or other mitogens.

Acknowledgements

The authors are grateful for the gift of anti-developmental myosin heavy chain, provided by Dr. Louise V.B. Anderson (née Nicholson), Neurochemistry Department, Newcastle

References

Anderson, J.E. 1991. Myotube phospholipid synthesis and sarcolemmal ATPase activity in dystrophic (*mdx*) mouse muscle. Biochem. Cell Biol. 69: 835–841.

Anderson, J.E., Ovalle, W.K., and Bressler, B.H. 1987. Electron microscopic and autoradiographic characterization of hindlimb muscle regeneration in the *mdx* mouse. Anat. Rec. 219: 243–257.

Anderson, J.E., Bressler, B.H., and Ovalle, W.K. 1988. Functional muscle regeneration in the hindlimb skeletal muscle of the *mdx* mouse. J. Muscle Res. Cell Motility, 9: 499–515.

Anderson, J.E., Liu, L., and Kardami, E. 1991. Distinctive patterns of basic fibroblast growth factor (bFGF) distribution in degenerating and regenerating areas of dystrophic (mdx) striated muscles. Dev. Biol. 147: 96–109.

Anderson, J.E., Kakulas, B.A., Jacobsen, P.F., Kornegay, R.D., and Grounds, M.D. 1993. Comparison of basic fibroblast growth factor in X-linked dystrophin-deficient myopathies of human, dog and mouse. Growth Factors, 9: 107–121.

Anderson, J.E., Liu, L., and Kardami, E. 1994a. The effects of hyperthyroidism on muscular dystrophy in the *mdx* mouse: greater dystrophy in cardiac and soleus muscle. Muscle & Nerve, 17: 64–73.

Anderson, J.E., Liu, L., Kardami, E., and Murphy L.J. 1994b. The pituitary-muscle axis in *mdx* dystrophic mice. J. Neurol. Sci. 123: 80–87.

Anderson, J.E., Mitchell, C.M., McGeachie, J.K., and Grounds, M.D. 1995. The time course of basic fibroblast growth factor expression in crush-injured skeletal muscles of SJL/J and BALB/c mice. Exp. Cell Res. 216: 325–334.

Bulfield, G., Siller, W.G.F., Wight, P.A.L., and Moore, K.J. 1984. X-chromosome-linked muscular dystrophy (*mdx*) in the mouse. Proc. Natl. Acad. Sci. U.S.A. 81: 1189–1192.

Cattini, P.A., Anderson, T.R., Baxter, J.D., Mellon, P., and Eberhardt, N.L. 1986. The human growth hormone gene is negatively regulated by triiodothyronine when transfected into rat pituitary tumor cells. J. Biol. Chem. 261: 13 367 – 13 372.

Daughaday, W.H., and Rotwein, P. 1989. Insulin-like growth factors I and II: peptide messenger ribonucleic acid and gene structures, serum, and tissue concentrations. Endocr. Rev. 10: 68–91.

Davis, C.E., Harris, J.B., and Nicholson, L.V.B. 1991. Myosin isoform transitions and physiological properties of regenerated and re-innervated soleus muscles of the rat. Neuromuscular Disord. 1: 411–421.

DiMario, J., Buffinger, N., Yamada, S., and Strohman, R.C. 1989. Fibroblast growth factor in the extracellular matrix of dystrophic (*mdx*) mouse muscle. Science (Washington, D.C.), 244: 688–690.

Downes, M., Griggs, R., Atkins, A., Olson, E.N., and Muscat, G.E. 1994. Identification of a thyroid hormone response element in the mouse myogenin gene: characterization of the thyroid hormone and retinoid X receptor heterodimeric binding site. Cell Growth & Differen. 4: 901–909.

Florini, J.R., Ewton, D.Z., Falen, S.L., and Van Wyk, J.J. 1986. Biphasic concentration dependency of stimulation of myoblast differentiation by somatomedins. Am. J. Physiol. 250: C771–C778.

Garrett, K.L., and Anderson, J.E. 1995. Co-localisation of bFGF and the myogenic regulatory gene myogenin in dystrophic mdx muscle precursors and young myotubes in vivo. Dev. Biol. 169: 596–608.

Gospodarowicz, D., Weseman, J., Moran, J.S., and Lindstrom, J. 1976. Effect of fibroblast growth factor on the division and fusion of bovine myoblasts. J. Cell Biol. 70: 395–405.

Gospodarowicz, D., Ferrara, N., Schweigerer, L., and Neufeld, G. 1987. Structural characterization and biological functions of fibroblast growth factor. Endocr. Rev. 8: 95–114.

Grounds, M.D., and McGeachie, J.K. 1989. A model of myogenesis in vivo derived from detailed autoradiographic studies of regenerating skeletal muscle challenges the concept of quantal mitosis. Cell Tissue Res. 250: 563–569.

Hoffman, E.P., Brown, Jr., R.J., and Kunkel, L.M. 1987. Dystrophin: the protein product of the Duchenne muscular dystrophy locus. Cell, 53: 219–228.

Izumo, S., Nadal-Ginard, B., and Mahdavi, V. 1986. All members of the MHC multigene family respond to thyroid hormone in a highly tissue-specific manner. Science (Washington, D.C.), 231: 597–600.

Karpati, G., Carpenter, S., and Prescott, S. 1988. Small caliber skeletal muscle fibers do not suffer necrosis in *mdx* mouse dystrophy. Muscle & Nerve, 11: 795–803.

Liu, L., Doble, B.W., and Kardami, E. 1993. Perinatal phenitype and hypothyroidism are associated with elevated levels of 21.5 to 22-kDa basic fibroblast growth factor in cardiac ventricles. Dev. Biol. 157: 507–516.

Marini, J.F., Pons, F., Leger, J., Loffreda, N., Anoal, M., Chevallay, M., Fardeau, M., and Leger, J.J. 1991. Expression of myosin heavy chain isoforms in Duchenne muscular dystrophy patients and carriers. Neuromuscular Disord. 1: 397–409.

McIntosh, L.M., and Anderson, J.E. 1995. Hypothyroidism prolongs and increases *mdx* muscle precursor proliferation and delays myotube formation in normal and dystrophic limb muscle. Biochem. Cell Biol. 73: 181–190.

McIntosh, L.M., Pernitsky, A.N., and Anderson J.E. 1994. The effects of altered metabolism (hypothyroidism) on muscle repair in the *mdx* dystrophic mouse. Muscle & Nerve, 17: 444–453.

Mitchell, C.A., McGeachie, J.K., and Grounds, M.D. 1992. Cellular differences in the regeneration of murine skeletal muscle: a quantitative histological study in SJL/JeBALB/C mice. Cell Tissue Res. 269: 159–166.

Morin, A., Louette, J., Vos, M.L.J., Tixier-Vidal, A., Belayew, A., and Martial, J.A. 1990. Triiodothyronine inhibits transcription from the human growth hormone promoter. Mol. Cell. Endocrinol. 71: 261–267.

Muscat, G.E.O., Mynett-Johnson, L., Dowhan, D., Downes, M., and Griggs, R. 1994. Activation of myoD gene transcription by 3,5,3'-triiodo-L-thyronine: a direct role for the thyroid hormone and retinoid X receptors. Nucleic Acids Res. 22: 583–591.

Nixon, B.T., and Green, H. 1984. Growth hormone promotes the differentiation of myoblasts and preadipocytes generated by azacytidine treatment of 10T1/2 cells. Proc. Natl. Acad. Sci. U.S.A. 81: 3429–3432.

Robertson, T.A., Grounds, M.D., Mitchell, C.A., and Papadimitriou, J.M. 1990. Fusion between myogenic cells in vivo: an ultrastructural study in regenerating murine skeletal muscle. J. Struct. Biol. 105: 170–182.

Rodriques-Arnao, J., Miell, J.P., and Ross, R.J.M. 1993. Influence of thyroid hormones on the GH–IGF-I axis. TEM (Trends Endocrinol. Metab.), 4: 169–173.

Sartore, S., Gorza, L., and Schiaffino, S. 1982. Fetal myosin heavy chains in regenerating muscle. Nature (London), 298: 294–296.

Thomas, M.R., Miell, J.P., Taylor, A.M., Ross, R.J.M., Arnao, J.R., Jewitt, D.E., and McGregor, A.M. 1993. Endocrine and cardiac paracrine actions of insulin-like growth factor-I (IGF-I) during thyroid dysfunction in the rat: is IGF-I implicated in the mechanism of heart weight/body weight change during abnormal thyroid function? J. Mol. Endocrinol. 10: 313–323.

Ullman, M., and Oldfers, A. 1991. Skeletal muscle regeneration in young rats is dependent on growth hormone. J. Neurol. Sci. 106: 67–74.

Wakayama, Y. 1976. Electron microscopic study on the satellite cell in the muscle of Duchenne muscular dystrophy. J. Neuropath. Exp. Neurol. 35: 532–540.

Webster, C., and Blau, H.M. 1990. Accelerated age-related decline in replicative life-span of Duchenne muscular dystrophy myoblasts: implications for cell and gene therapy. Somatic Cell Mol. Genet. 16: 557–565.

Zacharias, J.M., and Anderson J.E. 1991. Muscle regeneration after imposed injury is better in younger than older dystrophic mice. J. Neurol. Sci. 104: 190–196.

Appendix #2

.

Differential Effects of 3,5,3'-Triiodothyronine on Control and *mdx* Myoblasts and Fibroblasts: Analysis by Flow Cytometry

A. N. PERNITSKY AND J. E. ANDERSON[1]

Department of Anatomy, University of Manitoba, Winnipeg, Manitoba R3E 0W3 Canada

The possibility of differential effects of triiodothyronine (T3) treatment *in vivo* on myoblast and fibroblast cell proliferation was examined in control and *mdx* muscle cultures. Cell isolates were purified in a Percoll gradient, sorted by flow cytometry (light scatter), and characterized as myoblasts and fibroblasts using anti-skeletal muscle myosin fluorescence. The two cell types were grown separately or remixed (1:1). Cultures were incubated with or without T3 (10^{-9} M) for 19 h. Cells were either exposed to [^{3}H]thymidine for 1 h and DNA prepared for scintillation counts or stained with propidium iodide for cell cycle analysis by flow cytometry. Overall [^{3}H]thymidine uptake per cell was greater in *mdx* than control cells (mainly fibroblasts and mixed cells) and was decreased by T3 only in myoblast and mixed cultures. Cell cycle data showed that the effects of T3 originated primarily at the G_0/G_1 phase. There were more *mdx* than control myoblasts at G_0/G_1 without T3. After T3 treatment, more control fibroblasts than myoblasts were at G_0/G_1, but more *mdx* myoblasts than fibroblasts were at G_0/G_1. In the absence of T3, there were also fewer *mdx* than control myoblasts in S. After T3, only the proportion of *mdx* myoblasts in S phase was reduced. Results are consistent with distinct T3 effects on muscle regeneration *in vivo* and support the hypothesis that cycling and proliferation of *mdx* and control myoblasts are differentially modulated by T3. As control and *mdx* fibroblasts also showed distinct responses to T3, muscle regeneration likely occurs by a complex regulation of gene expression endogenous to specific cell types as well as interactions between cells of different lineage.
© 1996 Academic Press, Inc.

INTRODUCTION

Thyroid hormone (TH) is known to be critical for the normal growth and metabolism of skeletal muscle [1,

[1] To whom correspondence and reprint requests should be addressed at Department of Anatomy, University of Manitoba, 730 William Avenue, Winnipeg, MB, Canada, R3E 0W3. Fax: 204-772-0622. E-mail: anderson@bldghsc.lan1.umanitoba.ca.

2]. THs, mainly 3,5,3'-triiodothyronine (T3), exert their effects via intranuclear receptors [3]. T3 treatment promotes terminal muscle differentiation and results in increased MyoD (a muscle-specific regulatory factor or MRF) gene transcription in myogenic cell lines [4]. Furthermore, MyoD and fast myosin heavy chain gene expression are both activated in rodent slow-twitch muscle fibers after T3 treatment [4, 5]. Recent studies indicate that T3 directly controls the expression of MRFs [6] and suggest that thyroid response elements on muscle genes are the mechanism underlying changes in the contractile protein isoform profile observed in adult rodents exposed to T3 [7]. Thus, the expression of MRF genes is likely necessary to maintain adult muscle characteristics (and adaptability) in addition to its role in inducing differentiation in developing or regenerating muscle [5].

The dystrophic *mdx* mouse demonstrates X-linked dystrophin myopathy and fiber necrosis [8, 9], but shows effective ongoing limb muscle repair [10, 11]. Recent *in vivo* studies (Pernitsky *et al.*, 1996, in press) indicated that T3 treatment appears to speed the transition from proliferation to fusion in regenerating *mdx* and control mouse myoblasts (activated satellite cells) in muscle regenerating from crush injury. However, T3 treatment reduced overall repair only in control muscle, suggesting that in comparison to control myoblasts, *mdx* myoblasts have a large enough proliferative capacity to accomodate a T3-induced shift from proliferation toward fusion. That capacity may permit the very effective recovery of *mdx* muscle from an imposed injury compared to control muscle [12]. Other reports from this laboratory [12, 13] show that the opposite trend occurs under hypothyroid conditions, that of slowed myoblast proliferation and fusion, which delays repair in regenerating *mdx* muscle. Since we know that *mdx* mice are euthyroid [14], the alteration of various features of muscle repair in *mdx* mice under both hypothyroid and hyperthyroid conditions suggests that there may be a differential response to T3 by regenerating control and *mdx* muscle tissue and possibly in myoblasts isolated from those two strains.

To date there are few studies which report differences in myoblast proliferation in regenerating *mdx*

...sus control muscle. However, it has been suggested ...t growth factor-induced cell proliferation *in vitro* ...peared to be greater in *mdx* myoblasts (satellite-de-...ed cells) than in *mdx* fibroblasts or myoblasts of ...er strains [15]. Therefore, the present experiments ...ted the hypothesis that proliferation is greater in ...*x* than control myoblasts and is differentially af-...ted by T3 in the two strains. Control and *mdx* myo-...sts and fibroblasts were cultured together, subse-...ntly arrested, and then stimulated to determine the ...imal interval for detecting initial changes in S phase ...er a stimulus. Further experiments were done to ...arate myoblasts and fibroblasts using Percoll den-...y centrifugation and flow cytometry. The incorpora-...n of [³H]thymidine into DNA in S-phase cells (as an ...icator of cell proliferation) and the cell cycle phase ...tribution of cultures (analyzed by propidium iodide ...ining and flow cytometry) from control and *mdx*, ...reated, and T3-treated myoblast and fibroblast cell ...ulations were compared. These same populations ...re compared to myoblasts and fibroblasts recom-...ed in a 1:1 ratio to test whether cell–cell interplay ...motes proliferation.

MATERIALS AND METHODS

...imals and cell culture. Adult (7- to 10-week-old) control ...7BL10/ScSn) and *mdx* dystrophic mice were used in this study. ...Day 0, 4 mice from each strain and for each experiment were ...sthetized (ethyl ether) and sacrificed by cervical dislocation (ac-...ling to Canadian Council on Animal Care guidelines). Muscles ...e dissected from the hindlimb, forelimb, and back using aseptic ...nique. Muscle pieces were further dissected to remove tendons ...fat and chopped into a sludge using a sterile razor blade. The ...ige was placed into 25-cm² (50-ml) flasks (Falcon, Lincoln Park, ...with warm minimal essential medium (MEM) (Gibco BRL, ...nd Island, NY) supplemented with 15% horse serum (HS) ...clone Laboratories, Inc., Logan, Utah) and 2% chick embryo ex-...t (CEE) (containing <0.3 nmol/liter T3 by commercial assay) ...co) and incubated at 37°C in 5% O_2 and 95% CO_2 for 72 h. This ...nique increases cell yield by maximal activation of quiescent ...llite cells in nondystrophic (control) muscle, and homogeneously ...vates satellite cells in dystrophic (*mdx*) muscle.

...rcoll density centrifugation. After 3 days, the flask contents ...e emptied into 50-ml centrifuge tubes (Falcon), vortexed for 1 ..., and filtered 2× through gauze (Nitex) to remove larger pieces ...ebris. Filtered contents were centrifuged at 1200 rpm for 10 min ...°C (Heraeus Sepatech Varifuge RF, Baxter, Inc.), resuspended ...ml of warm MEM (supplemented with 15% carbon-stripped HS), ...pooled by strain (usually two samples). The final sample (brought ...ml) was layered onto 25 ml of 20% Percoll (Pharmacia, Uppsala, ...den) on a cushion of 5 ml of 60% Percoll, centrifuged at 10,000

To determine the length of time required for cells to pass through the cell cycle, semiconfluent control and *mdx* cells were subcultured and plated at equal densities. After 2–3 days, cells were arrested in metaphase using colchicine alkaloid (0.1 µg/ml) (Inland Alkaloid, Inc., Tipton, IN) in MEM supplemented with 15% carbon-stripped HS. After 42 h, cells were stimulated with MEM supplemented with 15% carbon-stripped HS and 4% CEE and were incubated with [³H]-thymidine (2 µCi/ml, sp act 92.0 Ci/mmol) (Amersham Life Science). Duplicate samples of cells from both strains were taken over 36 h as follows: every 2 h for 12 h, then every hour for 12 h, then every 2 h for the final 12 h of the experiment. Cells were removed from culture dishes by treatment with warmed 0.05% trypsin–EDTA (Gibco) (1–3 min) and enzyme action was halted with 2× the amount of HS. Cells were counted, centrifuged as above, and resuspended in 5 ml of 100% methanol to precipitate DNA. Following 24 h in metha-nol at 4°C, DNA was pelleted (6000 rpm at 4°C) and resolubilized in 1 ml of 2% Triton X-100 (J. T. Baker Chemical Co., Phillipsburg, NJ) and 2% lauryl sulfate (SDS) (Sigma Chemical Co., St. Louis, MO) overnight at 4°C [17]. Aliquots of soluble DNA were placed in 5-ml scintillation vials (Kimble Glass, Vineland, NJ) followed by addition of 5 ml of scintillation cocktail (Ready Safe, Beckman Instruments, Inc., Fullerton, CA). Vials were counted for 5 min on a Beckman LS 6500 scintillation counter (Beckman Instruments). DPM were corrected for cold thymidine in the carbon-stripped HS (unstripped HS contained <0.43 µM cold thymidine and carbon-stripping re-moved 80% of radioactive thymidine in a triplicate test experiment).

Serum was carbon-stripped [modified after 18]. Briefly, to 75 ml of HS was added 6.0 g of activated carbon (Fisher Scientific, Nepean, Ontario). This mixture was stirred at 4°C for 22 h and then centri-fuged at 10,000 rpm for 90 min at 4°C. The supernatant was passed through a 0.20 µM filter unit (Nalge Sybron Co., Rochester, NY) and then added to MEM and stored at 4°C prior to use. This treatment removes thyroid hormones, cortisol, and a number of other steroid hormones, yet the serum appears to retain growth promoting proper-ties [18]. In the present experiments, carbon-stripping of HS removed 75% of T3 (as analyzed by a commercial T3 assay).

Flow cytometry. Semiconfluent cells were removed from culture dishes by treatment with warmed 0.05% trypsin–EDTA (Gibco) (1–3 min) and enzyme action was halted with equal amounts of HS. Cells were pelleted and resuspended in 2 ml of Hepes-buffered MEM (no serum) and analyzed by a fluorescence-activated cell sorter (Model 753 Epics, Coulter Electronics, Inc.) equipped with an argon-ion laser operating at 500 mW (488 nm). Forward angle scatter (lin-ear) was first gated to remove debris and dead cells. Ninety-degree light scatter (also linear) was used to gate cells based on their cyto-plasmic granularity [19]. The cell suspension was sorted (in sterile phosphate-buffered saline) based on "low" and "high" cytoplasmic granularity. Cells were collected into 2 ml of sterile Hepes-buffered MEM and plated into 100× 20-mm Primaria culture dishes (approxi-mate plating density (per cm²) of *mdx* low cells = 9.0×10^4, *mdx* high cells = 9.7×10^4, control low cells = 13.9×10^4, and control high cells = 12.6×10^4) with MEM supplemented with 15% HS and 2% CEE and were allowed to proliferate until semiconfluent.

Populations were further subcultured into five 100× 20-mm Pri-maria dishes each and then 2–3 days later were subcultured into six 100× 20-mm dishes (six low and six high for each strain) with

began to differentiate, were fixed for 5 min at room temperature in methanol/acetone (1:1), and then rinsed in 0.01 M PBS twice. Cells were blocked for 1 h with 10% horse serum (HS) and 1% bovine serum albumin (BSA) in PBS. Following a 60-min incubation at 37°C with rabbit anti-skeletal muscle myosin (Sigma Chemical Co.) monoclonal antibody (diluted 1:100 in PBS plus 10% HS and 1% BSA), coverslips were rinsed twice in PBS and incubated for 1 h at 37°C with an anti-rabbit Ig, Texas red-linked whole antibody (Amersham, Inc., Mississauga, Ontario) (diluted 1/200). Coverslips were rinsed, incubated in 1 μM bisbenzimide in PBS for 4 min at room temperature to stain nuclei, rinsed, and mounted with Immumount (Lipshaw Immunon, Pittsburgh, PA). Cells were photographed with black and white film (TMAX400, Kodak) on a BHT-2 Olympus photomicroscope equipped with epifluoresence optics.

T3 treatment and propidium iodide staining for flow cytometry. After 3 days in MEM supplemented with 15% HS and 2% CEE, cells were switched to MEM containing 15% carbon-stripped HS and 4% CEE and allowed to adapt for 24 h. Cells were once again fed with the above MEM and supplements. At this time, T3 (Sigma Chemical Co.) (10^{-9} M in 0.05 M NaOH vehicle) was added to three of the six plates in each group (control and *mdx*; low, high, and mixed cells). Nineteen hours later, 1 h before sampling, [³H]thymidine (2 μCi/ml, sp act 92.0 Ci/mmol) was added to two of the six plates (one T3-treated plate and one untreated plate from each group) for 1 h. These cells were collected and cell DNA was prepared for scintillation counting using the method described above [17]. Data were collected as [³H]thymidine uptake per cell for *mdx* and control strains, and low, high, and mixed cells, with T3 or without T3. At the same time that these cells were collected, the remaining four plates of cells from each group were dealt with by trypsin–EDTA treatment as above (the two T3-treated plates were pooled and the two untreated plates were pooled from each group), centrifuged at 1200 rpm for 10 min at 4°C, resuspended in 3 ml 0.05 M PBS, counted, centrifuged at 1200 rpm for 7 min at 4°C, and resuspended in 500 μl of sterile 0.9% NaCl on ice. Cells from each group were then added to 5 ml of ice-cold 70% EtOH while vortexing and incubated on ice for 30 min. Cells were centrifuged as above, resuspended in 0.05 M PBS, centrifuged again, and resuspended (in the dark) in 500 μl of 10 μg/ml propidium iodide (PI) (Molecular Probes, Inc., Eugene, OR) and 50 μg/ml RNAse (ICN Biochemicals, Inc., Cleaveland, OH) solution. The samples were analyzed using a flow cytometer set up for detection of PI fluorescence of nuclear DNA (2N and 4N amounts of DNA). Forward and side scatter gates, as well as doublet discrimination gates, based on integrated peak and integrated fluorescence signals were used to identify single cells from debris and cellular aggregates. An algorithm was applied to the histograms to calculate proportions of cells in G_0/G_1, S and G_2/M phases of the cell cycle (PARA1 DNA Analysis Program, Coulter Electronics, Inc., Hialeah, FL).

Statistics. Data (means ± SEM) were tested using a three-way ANOVA to compare different cell types (low and high light scatter), T3 treatment effects, strain differences, and interactions (NWA Statpak, NW Analytical, Inc., Portland, OR). A probability of $P < 0.05$ was used to accept a difference as significant. χ^2 contingency tests were used to analyze the frequency distributions of cells in different phases of the cell cycle, comparing cell populations and treatment effects (Stats Plus, Human Systems Dynamics, Northridge, CA).

RESULTS

Isolation and Characterization of Myoblasts and Fibroblasts by Percoll Density Centrifugation, Flow Cytometry, and Immunocytochemistry

The use of Percoll density centrifugation (PDC) allowed cells of interest to be separated from larger debris and erythrocytes. Many cells were present in the

low density (20%) Percoll fraction in all control and *mdx* experiments and were harvested from the gradient for culture. Within 6 days, cells were abundant enough to collect for analysis and sorting using flow cytometry. The use of flow cytometry allowed a mixed population of cells to be separated (from both strains) into two populations based on forward-angle light scatter (size) and side scatter (cytoplasmic granularity). A gate of between 10 and 60 units (arbitrary) was selected for the cells of interest (modified after [19]). Cells that had a cytoplasm with very little or no granularity were sorted into the low light scatter category, and cells that had a very high cytoplasmic granularity were sorted into the high light scatter category (Fig. 1). Similar contour plots of cell size versus granularity were revealed in the sorts for *mdx* and control cells, which also yielded the same cell populations by identical low and high gatings.

The low and high populations were characterized using antibodies to skeletal muscle myosin. Cultures of *mdx* low cells (Fig. 2) allowed to differentiate for a short period (1–2 days) contained many cells which expressed small amounts of skeletal muscle myosin (Fig. 2B), indicating that the low cultures contained a large majority of myoblasts. In contrast, cultures of *mdx* high cells contained very few myosin-positive cells (Fig. 2D). Control and *mdx* low and high cell isolates had very similar proportions of cells with myosin staining.

Determination of Cell Cycle Length in Control and mdx Unsorted Cells

After release from cell cycle arrest by stimulation (time 0 in Fig. 3), both control and *mdx* cells showed an extended lag period approximately 6–10 h in length between stimulation and the initial observation of cytokinesis. After this, cells proceeded through the remaining phases of mitosis and moved into G_1 (at about 12 h, judging by the general end of cytokinesis). This phase lasted for approximately 8–10 h for both strains. Cells then proceeded through the G_1 checkpoint into S phase, as indicated by the rise in [³H]thymidine uptake per cell by cells of both strains (beginning at 19–20 h). The [³H]thymidine incorporation continued for the remaining hours of the experiment prior to mitosis. Thus, eliminating the initial lag period for the release from the arrested state (6–10 h), the optimal interval for detecting changes in DNA replication during S phase in cycling cells begins between 19 and 20 h after stimulation. Although cells in this experiment did not complete the G_2/M phase (which would be observed as a drop in [³H]thymidine incorporation per cell), data suggest that the approximate length of the cell cycle for unsorted cells is 26–28 h.
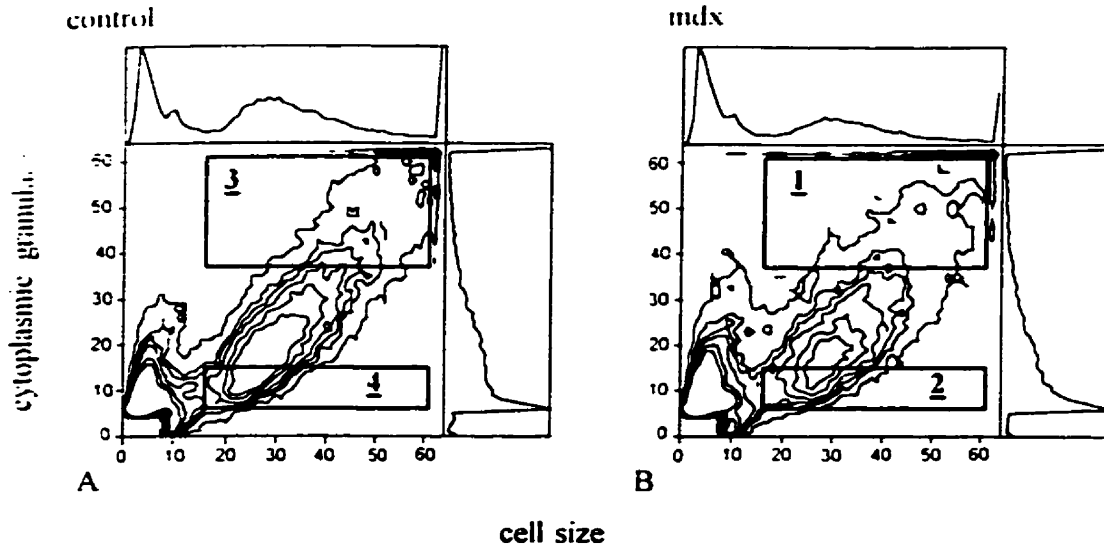
control   mdx

A   B

cell size

FIG. 1. Contour plots of bivariate forward-angle scatter (cell size) data versus 90° light scatter (cytoplasmic granularity). Channel numbers are in arbitrary units. Matching linear histograms are also shown above each plot. (A) Control. (B) *mdx*. Boxes indicate gates used for sorting. Box 1, *mdx* high cells; Box 2, *mdx* low cells; Box 3, control high cells; and Box 4, control low cells.

Analysis of [³H]Thymidine Uptake into DNA in Control and *mdx* Sorted Cells

As an estimation of cell proliferation, the uptake of [³H]thymidine (during the hour before sampling) by sorted low and high cells and mixed cell populations was examined after 24 h adaptation to MEM supplemented with 15% carbon-stripped HS and 4% CEE, plus an additional 20 h with or without T3 treatment. Figure 4 represents the mean uptake per cell (±SEM)

of duplicate samples (two DPM readings for each strain, cell type, and treatment group). Analysis of variance determined a significant effect of strain on proliferation ($P < 0.0001$), since overall *mdx* cells had greater uptake per cell than control cell populations. There were significant differences in uptake by low, high, and mixed populations ($P < 0.0001$) and significant interaction between strain and cell type populations ($P < 0.0001$). Those two effects are observed as a lower uptake per cell in control high cells compared
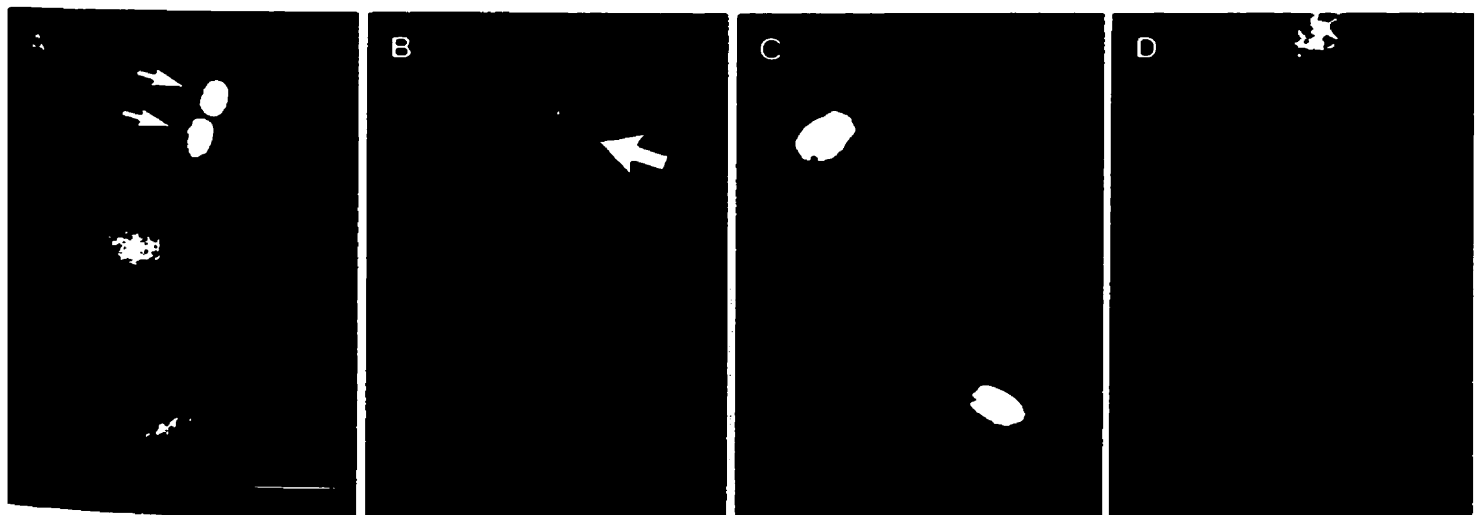

FIG. 3. Photomicrographs of immunocytochemistry for skeletal muscle myosin and bisbenzimide staining for nuclei in sorted *mdx* low (A and B) and *mdx* high (C and D). (A) Nuclear staining of a field of *mdx* low cells. Note the two nuclei in the small myotube (arrows). (B) The same small myotube as in A is positive for anti-skeletal muscle myosin immunostaining (arrow). (C) Nuclear staining of a field of *mdx* high cells. (D) In the same field as C, the majority of cells do not show anti-skeletal muscle myosin fluorescence. Bar, 55 μm. 220×.
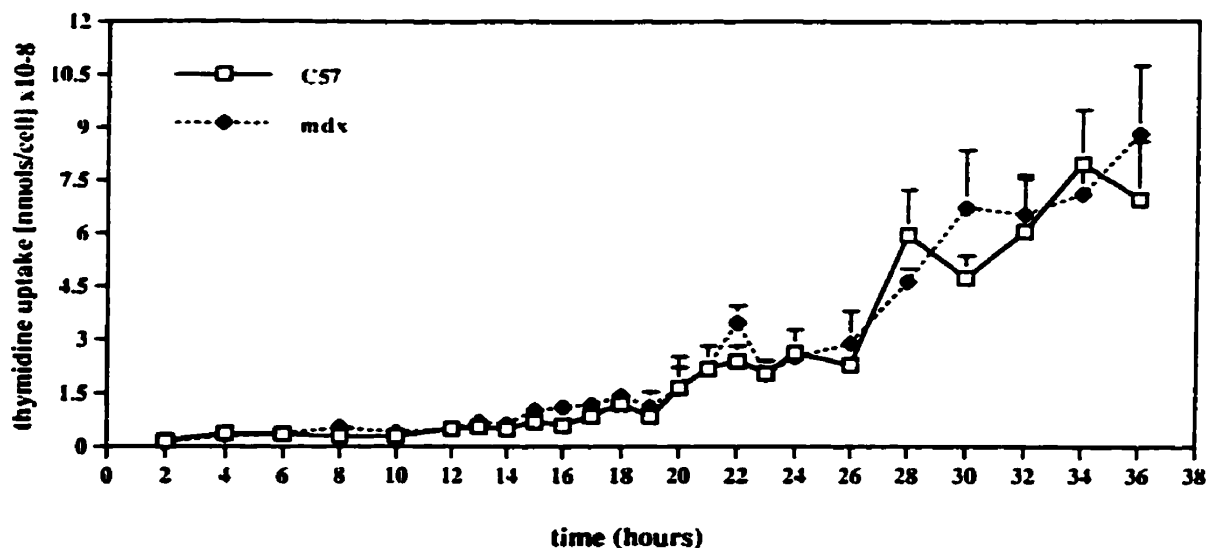
FIG. 3. Line graph comparing [³H]thymidine uptake (nmol per cell) in control (C57, open squares) and *mdx* (solid diamonds) unsorted cells after stimulation out of colchicine arrest in metaphase. Values are expressed as means ± SE of duplicate samples. Where standard error bars are not shown they were too small to be resolved on the graph.

to control low or mixed cells, while uptake by *mdx* mixed cells was greater than in *mdx* low or high populations.

While there was no significant general effect of T3 treatment on uptake per cell ($P = 0.63$), T3 treatment had differential effects on cell proliferation, observed as significant interaction between strain and T3 treat-

ment ($P < 0.05$) and between cell type and T3 treatment ($P < 0.0001$). The interactions are observed in low cells, where T3 decreased uptake per cell in both control and *mdx* populations. T3 treatment affected only the *mdx* high cells (not controls), increasing their uptake per cell. Mixed control cell populations showed increased uptake after T3 (approximating an additive
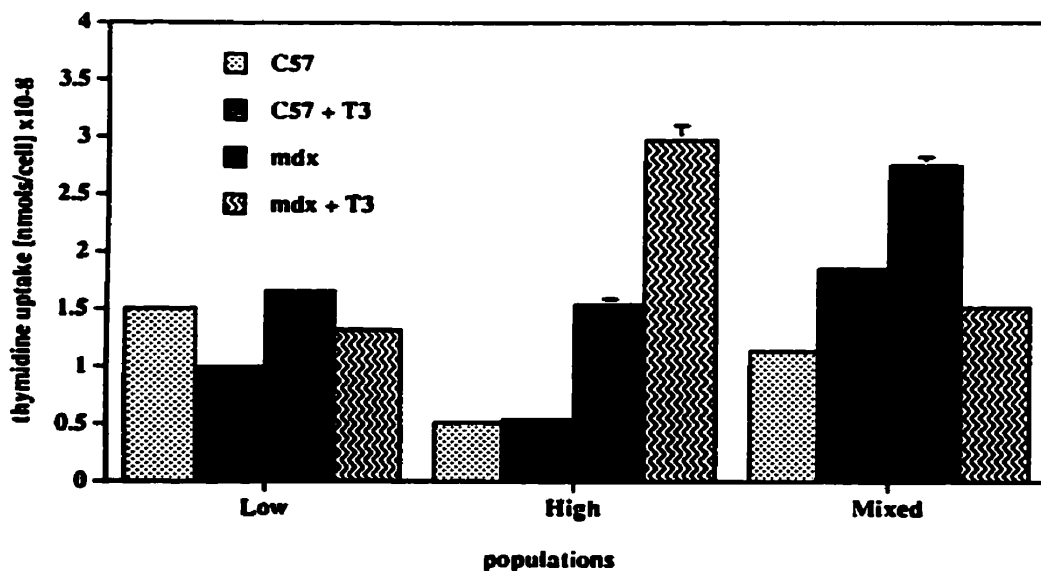

FIG. 4. Bar graph comparing [³H]thymidine uptake (nmol per cell) in control (C57) and *mdx* cells grouped into low, high, and remixed populations and grown in MEM supplemented with 15% carbon-stripped HS and 4% CEE, with T3 and without T3 treatment. Bars represent duplicate DPM readings from a single sample. Values are expressed as means ± SE. Missing standard error bars were too small to be resolved on the graph. Comparison of strains and cell populations each showed significant differences, and each interacted with T3.

effect of the uptake by separated low and high T3-treated cells). *Mdx* mixed cells showed additive uptake in untreated conditions, but a significant decrease in uptake per cell was observed after T3 treatment. These results suggest that the *mdx* low cells are stimulated to proliferate by the presence of the high cells (i.e., in the untreated *mdx* mixed group) and that *mdx* low cell uptake is inhibited by T3 in the presence of high cells in the mixed population. In this experiment, the variation in uptake within groups was low, likely since the low, high, and mixed populations were all derived from the same animals and were processed together. Therefore, data show there were significant interaction effects of T3 treatment with strain and cell types which support the possibility of differential effects of T3 on control and *mdx* myoblast populations.

Analysis of Proliferation in Control and mdx Sorted Cells by Propidium Iodide

The precise origin of the changes in uptake per cell in the above analysis (Fig. 4) are not certain, since the estimation of proliferation by [^{3}H]thymidine uptake per cell over 1 h is only a rough indicator of population dynamics. In order to examine more closely the proliferative phase in cycling cells, the frequency distribution of cells in the cell cycle was determined by PI staining and flow cytometric analysis. Figure 5 shows the plotted histograms of DNA content (2N in G_0/G_1 phase, 2N to 4N in S phase, and 4N in G_2/M phase) versus cell number from each of the 12 populations (control and *mdx*; untreated and T3-treated; and low, high, and mixed cells). The proportion of cell populations in G_0/G_1, S, and G_2/M phases are indicated, as calculated by the algorithm. The proportions of cells in each phase were converted to frequencies and were used in a χ^2 statistical comparison of populations by cell type (differences down the columns of Fig. 5), by treatment group (differences across the rows of Fig. 5), or by phase (testing G_0/G_1, S, and G_2/M phases separately). The separate comparisons allowed for the origin of the significant differences in χ^2 to be determined.

In comparing distributions within each cell type (columns), there were significant differences between treatment distributions only in the low cell category ($\chi^2 = 34.9, P < 0.001, df = 6$), most of which originated in the proportions in G_0/G_1 (partitioned $\chi^2 = 17$, or approximately 50%), with smaller contributions from changes in the distribution in S phase (partitioned $\chi^2 = 9.5$, or approximately 27%).

The comparison between cell types for each treatment group (rows) showed significant differences between the frequency distribution of cell type populations for untreated controls ($\chi^2 = 14.9, P = 0.005, df = 4$), T3-treated controls ($\chi^2 = 9.3, P = 0.05, df = 4$), and untreated *mdx* cells ($\chi^2 = 10.4, P = 0.03, df = 4$).

Again, the G_0/G_1 phase contributed significantly to the differences (20–30% of χ^2), with S phase contributing in control untreated and T3-treated groups (50 and 55% of χ^2, respectively). The G_2/M phase contributed 50% of χ^2 changes from expected frequencies only in untreated *mdx* cells.

In comparing within phases as a confirmation of the comparisons by cell type or treatment, χ^2 tests were significant only in G_0/G_1 phase ($\chi^2 = 15.6, P = 0.02, df = 6$), with contributions by untreated low cells (35% of χ^2) and T3-treated high cells (25% of χ^2).

Therefore, the three χ^2 partitioning studies (of the same data) suggest that there are consistent differences in how the different populations cycle. Those differences originate from G_0/G_1 in three categories: (a) in untreated low cells, with more *mdx* low cells in G_0/G_1 than control low cells, (b) in *mdx* T3-treated high cells, with fewer in G_0/G_1 than *mdx* low cells (untreated and T3-treated), and (c) in control T3-treated high cells, with more in G_0/G_1 than in control low cells (untreated and T3-treated). S phase contributed to significant changes in χ^2 in control untreated low cells (more in S phase than in *mdx* untreated or T3-treated low cells) and in *mdx* T3-treated low populations (fewer in S phase than in *mdx* untreated low cells).

Note that data reported in Figs. 4 and 5 are from one large experiment. One plate per group was used to estimate proliferative populations by recording radioisotope uptake per cell, while two other plates per group were used to study cell cycle phase distributions by PI staining and flow cytometry.

DISCUSSION

The results of the present experiments show that control and *mdx* dystrophic muscle cells demonstrate different changes in proliferation and cell cycling when treated with T3. Those differences are also specific to certain cell types (myoblasts, fibroblasts, or mixed myoblast and fibroblast populations). There were significant differences between treatment groups, cell types, and strains in G_0/G_1 and S as analyzed by flow cytometry and PI staining. The results also show a differential response to T3 between control and *mdx* myoblasts (low cells stained by anti-skeletal muscle myosin) by significant interactions between T3 treatment, cell type, and strain. Results thus confirm and extend earlier work *in vivo* on the effects of hyperthyroidism and hypothyroidism on muscle regeneration [12, 13, Pernitsky *et al.*, 1996, in press]. The results suggest that the regenerative capability of *mdx* myoblasts may be a result of differential regulation of cell cycling. That differential may involve distinct muscle regulatory gene sensitivity to T3 and endogenous production of basic fibroblast growth factor (bFGF) [20] or expression of bFGF
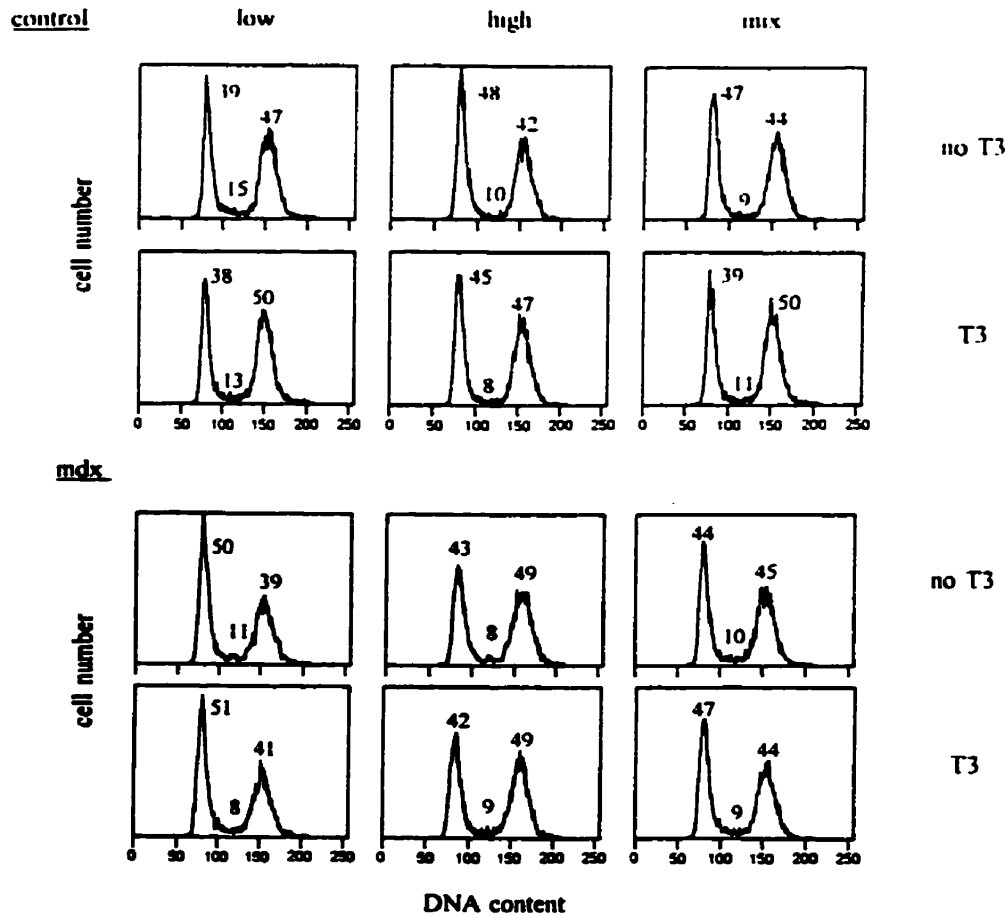
FIG. 5. Histograms of flow cytometric analysis of control and *mdx* low (left column), high (middle column), and mixed cells (right column) and displayed by treatment (with T3 and without T3) by propidium iodide staining of DNA. Data represent the proportion of cells in G_0/G_1 phase (first peak = 2N amount of DNA), S phase (middle = between 2N and 4N amounts of DNA), and G_2/M phase (second peak = 4N amount of DNA). Five thousand cells were analyzed from each population. Significant differences were determined by χ^2. Significant differences were observed between control and *mdx* low cell types, particularly in G_0/G_1 and S phases affected by T3.

or T3 receptors and their signal transduction pathways controlling the cell cycle.

It was previously shown that *mdx* muscle contains more bFGF, a potent mitogen, than normal mouse muscle [21], Duchenne muscular dystrophy, or other human biopsy samples [22]. Since myoblasts produce bFGF during repair [20], it is possible that the *mdx* myoblasts and fibroblasts may express more of that mitogen than the control myoblasts and fibroblasts *in vitro*. This would subsequently lead to a greater early proliferation or more sustained proliferation in *mdx* cultures. While the experiment made to time the initiation of DNA synthesis after stimulation does not suggest a difference in proliferation rate compared to control populations, the idea requires further testing. However, there were some multinucleated cells observed in these cultures, possibly withdrawn from the cell cycle due to the earlier arrest with colchicine, and their numbers may have differed between control and *mdx* cultures.

MyoD is a MRF that constitutes a focal point for positive and negative control of myogenesis. MyoD expression initiates myogenic differentiation and induces inhibition during the G_1 phase of the cell cycle [23]. The control of myogenesis by MyoD is complex. For example, in experiments on MyoD knockout mice [24], muscles *in vivo* showed dramatically less effective regeneration than wildtype mice and significantly decreased proliferation by myogenic cells labeled by myogenin expression and [3H]thymidine uptake. In the *in vitro* studies, however, myogenic cell numbers were not reduced, but elevated. Those results suggested that self-renewal by early stem cells, rather than myogenic differentiation, occurs in the absence of MyoD. Growth factors may repress MyoD function by stimulating expression of very early response genes which repress MyoD transactivation [25, 26]. Negative regulation of MyoD function by growth signals (such as bFGF) occurs in proliferating myoblasts, while withdrawal of exogenous growth factors triggers MyoD's action to arrest

cell cycling and activate the myogenic program [23]. It is not known if control and *mdx* myoblasts express different levels of bFGF or how myoblasts and fibroblasts might differ in that regard, although a report of ... sensitivity to exogenous bFGF by *mdx* versus ... myoblast cultures [15] might be explained, in part, by a differential expression of the mitogen [20].

The high level of proliferation shown by untreated *mdx* mixed cells, in comparison to either low or high *mdx* cells alone, suggests that myoblasts and fibroblasts interact positively to promote mitogenesis, possibly by the addition of bFGF and/or other factors contributed by the fibroblasts or through direct cell-to-cell contact. However, mixing control myoblasts and fibroblasts in the same untreated conditions does not appear to have an additive effect on proliferation. The difference between the two strains regarding separate versus mixed populations may also relate to differences in mitogen production, receptor expression, or interaction with MyoD and other MRFs.

Other important findings in this study confirm that sorting mixed myoblast and fibroblast cell populations according to 90° light scatter (cytoplasmic granularity) permits the distinction of low (myoblast) and high (fibroblast) light scatter populations in *mdx* and control cultures as reported [19]. The sorted cells were further separated from cells with intermediate scatter which are an uncharacterized mixed population of cells. The expression of anti-skeletal muscle myosin in early differentiated control and *mdx* low cells further confirms that the low population contains a very large majority of myoblasts that are separated from a mixed population by flow cytometry and that the population sorted as high contains a large majority of skeletal muscle myosin-negative fibroblasts.

The observed increase in [³H]thymidine uptake per cell in the *mdx* fibroblast population after T3 treatment is puzzling, particularly since both myoblast and mixed populations of *mdx* cells in the same experiment showed decreased uptake per cell with T3 treatment. In the same experiment, there were significant effects on cell cycling attributable to a low frequency of *mdx* T3-treated fibroblasts in G_0/G_1. However, the change was small (only 15% of the total significant χ^2 value for the differences in G_0/G_1), and the distribution was the lowest in frequency among the other fibroblast cultures. However, S phase for fibroblasts did not contribute to significant χ^2 changes with T3 treatment. Thus, there is a difference between S phase estimation by PI staining and flow cytometry and estimates of proliferation in a population based on [³H]thymidine uptake per cell, even in a single experiment. The latter method estimates DNA synthesis over a 1-h pulsed exposure in a population presumed to be moving through various phases of the cell cycle in a continuous sequence. The cells replicating their DNA are only observed in a very

restricted window in S phase itself. The histograms in Fig. 5 show a small proportion of cells in S phase, and [³H]thymidine uptake analysis will only identify small numbers of cells that may be at the begining, the middle, or at the end of S phase and which cannot be distinquished from one another. Thus, in view of the flow cytometry findings, observations of increased [³H]-thymidine uptake per cell in *mdx* T3-treated fibroblasts indicate that additional experiments are needed to follow particular cells (S phase cells, for example) through a cycle by bromodeoxyuridine (Brdu) and PI double labeling. Those experiments would determine three aspects of a differential effect of T3 on cell cycling: (a) if the cells in the [³H]thymidine uptake experiments are present as a group just entering S phase from G_0/G_1 or just about to leave S phase and enter G_2/M, (b) if that cell population is more synchronized in activity in response to T3 treatment than untreated populations, and (c) if that T3-treated population is synchronized more due to endogenous regulation of proliferation or myogenesis.

The interesting aspect of the uptake by *mdx* fibroblasts (comparison between untreated and T3-treated cells) is that fibroblasts also appear to show a differential effect of T3 treatment. That observation suggests that fibroblasts deserve renewed study for their role in the possible endocrine mediation of muscle repair processes such as remodeling of the extracellular matrix and the dynamics of cell recruitment during wound repair. There clearly are strain-specific effects of T3 on cell cycling that differ between myoblasts and fibroblasts and that appear to be modified by cell-to-cell interactions.

REFERENCES

1. Baldwin, K. M., Hooker, A. M., Campbell, P. J., and Lewis, R. E. (1978) *Am. J. Physiol.* **235**(3), C97–C102.

2. Simonides, W. S., and Van Hardeveld, C. (1989) *Endocrinol.* **124**(3), 1145–1153.

3. Samuels, H. H., and Tsai, J. S. (1973) *Proc. Natl. Acad. Sci. USA* **70**, 3488–3492.

4. Carnac, G., Albagli-Curiel, O., Vandromme, M., Pinset, C., Montarras, D., Lauet, V., and Bonnieu, A. (1992) *Mol. Endocrinol.* **6**(8), 1185–1194.

5. Hughes, S. M., Taylor, J. M., Tapscott, S. J., Gurley, C. M., Carter, W. J., and Peterson, C. A. (1993) *Development* **118**, 1137–1147.

6. Muscatt, G. E. O., Mynett-Johnson, L., Dowhan, D., Downes, M., and Griggs, R. (1994) *Nucleic Acids Res.* **22**(4), 583–591.

7. Izumo, S., Nadal-Ginard, B., and Mahdavi, V. (1986) *Science* 231, 597–600.

8. Bulfield, G., Siller, W. G. F., Wight, P. A. L., and Moore, K. J. (1984) *Proc. Natl. Acad. Sci. USA* 81, 1189–1192.

9. Koenig, M., Hoffman, E. P., Bertelson, C. J., Monaco, A. P., Feener, C., and Kunkel, L. M. (1987) *Cell* 50, 509–517.

10. Anderson, J. E., Ovalle, W. K., and Bressler, B. H. (1987) *Anat. Rec.* 219, 243–257.

11. Anderson, J. E., Bressler, B. H., and Ovalle, W. K. (1988) *J. Muscle Res. Cell Motil.* 9, 499–516.

12. McIntosh, L. M., Pernitsky, A. N., and Anderson, J. E. (1994) *Muscle Nerve* 17, 444–453.

13. McIntosh, L. M., and Anderson, J. E. (1995) *Biochem. Cell Biol.* 73, 181–190.

14. Anderson, J. E., Liu, L., Kardami, E., and Murphy, L. J. (1994) *J. Neurol. Sci.* 123, 80–87.

15. DiMario, J., and Strohman, R. C. (1988) *Differentiation* 39, 42–49.

16. Yablonka-Reuveni, Z., and Nameroff, M. (1987) *Histochemistry* 87, 27–38.

17. Smith, B. T., Galaugher, W., and Thurlbeck, W. M. (1980) *Am. Rev. Respir. Dis.* 121, 701–707.

18. Tanswell, A. K., Joneja, M. G., Lindsay, J., and Vreeken, E. (1983) *Exp. Lung Res.* 5, 37–48.

19. Yablonka-Reuveni, Z. (1988) *Cytometry* 9, 121–125.

20. Garrett, K. L., and Anderson, J. E. (1995) *Dev. Biol.* 169, 596–608.

21. Anderson, J. E., Liu, L., and Kardami, E. (1991) *Dev. Biol.* 147, 96–109.

22. Anderson, J. E., Kakulas, B. A., Jacobsen, P. F., Kornegay, R. D., and Grounds, M. D. (1993) *Growth Factors* 9, 107–121.

23. Martelli, F., Cenciarelli, C., Santarelli, G., Polikar, B., Felsani, A., and Caruso, M. (1994) *Oncogene* 9, 3579–3590.

24. Megeney, L. A., Kablar, B., Garrett, K., Anderson, J. E., and Rudnicki, M. A. (1996) *Genes Dev.* 10, 1173–1183.

25. Li, L., Chambard, J. C., Karin, M., and Olson, E. N. (1992) *Genes Dev.* 6, 676–689.

26. Bengal, E., Ransone, L., Scharfmann, R., Dwarki, V. J., Tapscott, S. J., Weintraub, H., and Verma, I. M. (1992) *Cell* 68, 507–519.